

INFORMATION TO USERS

This manuscript has been reproduced from the microfilm master. UMI films the text directly from the original or copy submitted. Thus, some thesis and dissertation copies are in typewriter face, while others may be from any type of computer printer.

The quality of this reproduction is dependent upon the quality of the copy submitted. Broken or indistinct print, colored or poor quality illustrations and photographs, print bleedthrough, substandard margins, and improper alignment can adversely affect reproduction.

In the unlikely event that the author did not send UMI a complete manuscript and there are missing pages, these will be noted. Also, if unauthorized copyright material had to be removed, a note will indicate the deletion.

Oversize materials (e.g., maps, drawings, charts) are reproduced by sectioning the original, beginning at the upper left-hand corner and continuing from left to right in equal sections with small overlaps. Each original is also photographed in one exposure and is included in reduced form at the back of the book.

Photographs included in the original manuscript have been reproduced xerographically in this copy. Higher quality 6" x 9" black and white photographic prints are available for any photographs or illustrations appearing in this copy for an additional charge. Contact UMI directly to order.

UMI

A Bell & Howell Information Company
300 North Zeeb Road, Ann Arbor MI 48106-1346 USA
313/761-4700 800/521-0600

RICE UNIVERSITY

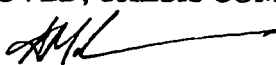
**BONE FORMATION BY THREE-DIMENSIONAL
OSTEOBLAST CULTURE IN BIODEGRADABLE
POLY(α -HYDROXY ESTER) SCAFFOLDS**

by

SUSAN L. ISHAUG-RILEY

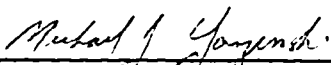
A THESIS SUBMITTED
IN PARTIAL FULFILLMENT OF THE
REQUIREMENTS FOR THE DEGREE
DOCTOR OF PHILOSOPHY

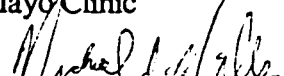
APPROVED, THESIS COMMITTEE


Antonios G. Mikos, T.N. Law Associate
Professor of Chemical Engineering and
Bioengineering


Larry V. McIntire, E.D. Butcher Professor of
Chemical Engineering and Biomedical
Engineering


Frederick B. Rudolph, Professor
Biochemistry and Cell Biology


Michael J. Yaszemski, M.D., Ph.D.
Department of Orthopaedic Surgery
Mayo Clinic


Michael J. Miller, M.D.
Associate Professor Plastic and
Reconstructive Surgery
University of Texas M.D. Anderson Cancer
Center

Houston, Texas

May, 1997

UMI Number: 9727567

**UMI Microform 9727567
Copyright 1997, by UMI Company. All rights reserved.**

**This microform edition is protected against unauthorized
copying under Title 17, United States Code.**

UMI
300 North Zeeb Road
Ann Arbor, MI 48103

ABSTRACT

BONE FORMATION BY THREE-DIMENSIONAL OSTEOBLAST CULTURE IN BIODEGRADABLE POLY(α -HYDROXY ESTER) SCAFFOLDS

by

Susan Lynn Ishaug-Riley

The feasibility of culturing osteoblasts on biodegradable poly(α -hydroxy esters) to form new bone was investigated through a series of five studies. The first study demonstrated that rat calvarial osteoblasts attached, proliferated, and functioned equally well on all the biodegradable polymer substrates studied [poly(L-lactic acid) (PLLA), 75:25 poly(DL-lactic-co-glycolic acid) (PLGA), 50:50 PLGA, and poly(glycolic acid) (PGA)] throughout the 14 day study, even though the polymer films were continuously degrading.

The second study showed that osteoblast migration occurred as a monolayer of individual osteoblasts and not a calcified tissue front on poly(α -hydroxy ester) films. Copolymer ratio in the polymer films did not affect the rate of increase in culture area covered by the growing cell colony; however, the rate of increase in culture area was lower for cell colonies formed with a lower osteoblast seeding density. The proliferation rate for the osteoblasts arising from bone chips was lower than either of the isolated cell colonies.

Bone formation *in vitro* was investigated in the third and fourth study by culturing stromal osteoblasts or rat calvarial osteoblasts in three-dimensional (3-D), biodegradable 75:25 PLGA foams. The polymer foams supported the growth of seeded osteoblasts as well as their differentiated function. Cell number, alkaline phosphatase activity, and mineralized tissue deposition increased significantly over time for all the polymer foams. Osteoblasts seeded at a lower cell density proliferated more rapidly, reaching comparable cell numbers at later culture times, but pore size over the range tested did not affect cell proliferation or function.

In the final study, porous biodegradable poly(DL-lactic-co-glycolic acid) foams were seeded with rat stromal osteoblasts and implanted into the rat mesentery for up to 49 days to investigate *in vivo* bone formation using this osteoblast transplantation method. An organized and mineralized bone-like tissue was formed in all the constructs as early as 7 days post-implantation. Foam pore size did not affect the penetration depth of mineralized tissue or mineralized tissue volume per surface area found within the constructs at any time during the study.

ACKNOWLEDGEMENTS

A majority of graduate students would probably say that the road to a Ph.D. feels endless. If I say that I never had a long endless day or never felt frustrated by certain aspects of the process I would be lying. I would say, however, that my experience was very rewarding and much more interesting and fun than I could have expected. I attribute this to a variety of factors, such as my thesis topic, and especially my coworkers.

I could not have asked for a better thesis topic. I had always thought I would like to work with artificial organs, but soon realized that organ regeneration has the potential of becoming a better alternative for the treatment of organ failure. The exciting thing about this research is that it has clinical applications and that my work may some day help someone in need of new engineered bone. My advisor, Dr. Antonios Mikos, is responsible for bringing this important research to Rice University and to my attention and therefore deserves a lot of the credit.

I was so fortunate that Tony Mikos decided to come to Rice when I began my graduate studies so that I would have the opportunity to work with him. He was so enthusiastic about the research that it was an inspiration for a graduate student, such as myself. His willingness and availability for questions and discussions made it easier to get past stumbling stones and move along with the research. At times I became frustrated with some of the deadlines he imposed on me, but soon realized that I owe a lot of my accomplishments to his persistence and persuasion. Thank you Tony.

Genevieve Crane was my biggest asset in the lab. She took so much time out of her busy undergraduate schedule to come into the lab and help with the three-dimensional *in vitro* and *in vivo* studies. Not only did she help with the grunt work of the experiments, she got involved in the interpretation and analysis of the data. I hope she knows how much I appreciate all her dedicated help and the smile she brought with her to the lab.

I would also like to thank my other committee members, Drs. Larry McIntire, Frederick Rudolph, Michael Yaszemski, and Michael Miller. I understand that they are all very busy and I very much appreciate the time and effort they took in reading and critiquing this thesis.

In particular, I would like to thank Dr. Michael Yaszemski. He has been like a second advisor to me. His willingness to share his clinical perspective and knowledge with me has greatly helped in the completion of this work. Despite his unforgiving and relentless schedule, he was so generous with his precious time. His continued support in my future endeavors is also greatly appreciated.

I was fortunate to have the opportunity to work with another clinician, Dr. Michael Miller. He contributed to the three-dimensional studies, not only by performing the surgery, but by participating in the discussions of the project and looking toward future directions of the work. He gave me the opportunity to experience and understand the importance of our work by watching critical bone transplantation surgeries. His cheery face and the effort he made to laugh at my jokes are well received.

Dr. Alan Yasko has also been a welcomed contributor to this work. His great insight and continued enthusiasm in the project have been very helpful. He has great ideas and I got a lot out of our long talks about possible future directions of the project.

I would also like to thank Dr. Rena Bizios. She was a great asset throughout my graduate years. She helped me to get started, helped in the interpretation of our results, and gave very constructive comments on our manuscripts.

Kay Dee deserves a big thanks from me too. Not only did I learn the rat calvarial osteoblast isolation procedure from her skillful hands, but I benefited from her wisdom of rat osteoblast culture. Her humorous correspondences could really pick me up.

Ali Gurlek's assistance with the *in vivo* study is also appreciated. He was always willing to go out of his way to help with any aspect of the study without reservations.

Finally, I would like to let my labmates know how much I enjoyed working with them. It's because of them that I had such a great time in Houston!

Pete.....ditto.

TABLE OF CONTENTS

Abstract	ii
Acknowledgments	iv
Table of Contents	vii
List of Figures	x
List of Tables	xv
List of Abbreviations	xvi
Chapter 1 Introduction	1
1.1 Significance and Existing Bone Replacement Therapies	1
1.2 New Methods for Bone Regeneration	4
1.2.a Osteoblast Transplantation	4
1.2.b Bone Induction	7
1.2.c Prefabrication of Bone Flaps	8
Chapter 2 Background	10
2.1 Bone Anatomy and Biology	10
2.1.a Gross Structure	10
2.1.b Macroscopic Structure	11
2.1.c Microscopic Structure	13
2.1.d Molecular Composition	13
2.1.d.1 Bone Matrix	13
2.1.d.2 Bone Cells	15
2.1.d.2.a Mesenchymal Cells	15
2.1.d.2.b Osteoblasts	15
2.1.d.2.c Osteocytes	15
2.1.d.2.d Osteoclasts	17

2.1.d.2.e	Bone-Lining Cells	17
2.1.e	Bone Formation, Modeling, Remodeling, and Repair	18
2.2	Poly(α -hydroxy esters)	20
2.2.a	Poly(glycolic acid)	22
2.2.b	Poly(lactic acid)	22
2.2.c	Poly(lactic-co-glycolic acid)	23
2.3	Osteoblast Isolation, Culture, and Development	24
Chapter 3	Objectives	27
Chapter 4	Rat Calvarial Osteoblast Attachment, Proliferation, and Function on Two-Dimensional Poly(α -hydroxy ester) Films	29
4.1	Introduction	29
4.2	Materials and Methods	29
4.3	Results	35
4.4	Discussion	49
Chapter 5	Rat Calvarial Osteoblast Migration on Two-Dimensional Poly(α -hydroxy ester) Films	52
5.1	Introduction	52
5.2	Materials and Methods	53
5.3	Results	58
5.4	Discussion	68
Chapter 6	Rat Marrow Osteoblast Culture in Three-Dimensional Poly(α -hydroxy ester) Foams	75
6.1	Introduction	75
6.2	Materials and Methods	76
6.3	Results	82
6.4	Discussion	102

Chapter 7	Rat Calvarial Osteoblast Culture in Three-Dimensional Poly(α -hydroxy ester) Foams	108
7.1	Introduction	108
7.2	Materials and Methods	108
7.3	Results	111
7.4	Discussion	119
Chapter 8	Ectopic Bone Formation by Implantation of Osteoblast-Seeded Poly(α -hydroxy ester) Foams into the Rat Mesentery	124
8.1	Introduction	124
8.2	Materials and Methods	124
8.3	Results	129
8.4	Discussion	137
Chapter 9	Conclusions	143
References	145
Appendix	159
Vitae	161

LISTS OF FIGURES

1-1.	Fibula flap excision procedure	2
1-2.	Bone regeneration methodology	6
2-1.	Section of mature long bone	12
2-2.	Origins of bone cells	16
2-3a.	Chemical structure of poly(glycolic acid)	21
2-3b.	Chemical structure of poly(lactic acid)	21
2-3c.	Degradation of poly(lactic-co-glycolic acid)	21
2-4.	Proliferation and differentiation in the development of rat osteoblasts in culture ..	26
4-1.	Percent attached osteoblasts to polymer films over time	36
4-2.	Percent attached osteoblasts to polymer films after 8 hours in culture	38
4-3.	Proliferation kinetics for osteoblasts cultured on polymer films	39
4-4.	SEM micrographs of osteoblasts attached to a 50:50 PLGA film after 4 hours	40
4-5.	SEM micrographs of osteoblasts cultured on 50:50 PLGA films for (a) 1 day and (b) 4 days	41
4-6.	SEM micrograph of osteoblasts cultured on a 75:25 PLGA film after 1 day in culture	42
4-7.	Light stereomicrograph of osteoblasts cultured on a 50:50 PLGA film after 7 days in culture	43
4-8.	ALP activity expressed by osteoblasts cultured on polymer films	45
4-9.	Collagen synthesized by osteoblasts cultured on polymer films	46
4-10.	Percent collagen synthesized by osteoblasts cultured on polymer films	47
4-11.	Molecular weight of polymer films over time	48
5-1.	Light micrograph of circular osteoblast culture at day 0 on a 75:25 PLGA film ...	59
5-2.	Light micrograph of an osteoblast culture allowed to migrate for 14 days on a 75:25 PLGA film	61

5-3.	Digitized image of osteoblast migration for 14 days on a 75:25 PLGA films from a bone chip	62
5-4	Confocal depth coding micrograph of a high density seeded osteoblast culture on a 75:25 PLGA film after 6 days of migration	64
5-5.	Confocal depth coding micrograph of an osteoblast culture migrated from a bone chip onto a 75:25 PLGA film for 6 days	64
5-6.	Light micrograph of osteoblasts migrated from a bone chip onto 75:25 PLGA film for 14 days	65
5-7.	Fractional increase in osteoblast population culture surface area on various polymer substrates over time	66
5-8.	Fractional increase in osteoblast population culture surface area on 75:25 PLGA films over time for various osteoblast cultures	67
5-9.	Osteoblast proliferation on 75:25 PLGA films over time for various osteoblast cultures	69
5-10.	Cell densities on 75:25 PLGA films over time for or various osteoblast cultures ..	70
6-1a.	Scanning electron micrographs of a 90% porous 75:25 PLGA foam having pores size 150-300 μm	83
6-1b.	Scanning electron micrographs of a 90% porous 75:25 PLGA foam having pores size 300-500 μm	84
6-1c.	Scanning electron micrographs of a 90% porous 75:25 PLGA foam having pores size 500-710 μm	85
6-1d.	Scanning electron micrographs after 1 day in culture for a 90% porous 75:25 PLGA foam having pores size 150-300 μm and initially seeded with a low cell density ..	87
6-2a.	Confocal micrographs of a 300-500 μm polymer foam initially seeded with a low cell density and cultured for 1 day	88

6-2b. Confocal micrographs of a 300-500 μm polymer foam initially seeded with a high cell density and cultured for 1 day	88
6-2c. Confocal micrographs of osteoblasts seeded with a low cell density in 300-500 μm foams after 4 days in culture	89
6-2d. Confocal micrographs of osteoblasts seeded with a low cell density in 300-500 μm foams after 7 days in culture	89
6-3a. Number of cells/cm ² in foams over time for osteoblast/foam constructs with pore size 300-500 μm and seeded with either a low or high cell density	90
6-3b. Number of cells/cm ² in foams with various pores sizes over time initially seeded with a high cell seeding density	91
6-4a. Alkaline phosphatase activity in the osteoblast/foam constructs over time for foams with pore size 300-500 μm and seeded with either a high or low cell seeding density	93
6-4b. Alkaline phosphatase activity in the osteoblast/foam constructs over time for foams of various pore sizes seeded with a high cell seeding density	94
6-5a. Light micrograph of a H & E stained horizontal cross sections of a 300-500 μm pore size polymer foam initially seeded with 22.1×10^5 cells/cm ² and cultured for 56 days	95
6-5b. Light micrographs of a parallel cross section to that in figure 6-5a but stained using Von Kossa's staining method	96
6-6a. Light micrograph of a H & E stained vertical cross sections of a 300-500 μm pore size foam initially seeded with 22.1×10^5 cells/cm ² and cultured for 56 days	97
6-6b. Light micrographs of a parallel cross section to that in figure 6-6a but stained using von Kossa's staining method	98
6-7a. Average maximum depth below the polymer surface that mineralized tissue was deposited in the rat marrow osteoblast/foam constructs over culture time	100

6-7b.	Total mineralized volume/surface area in the rat marrow osteoblast/foam constructs over culture time	101
6-8.	Weight average molecular weights of the 75:25 PLGA polymer foams, initially seeded with a high cell density over time	103
7-1.	Confocal depth projection micrograph after 3 days in culture of a 1.9 mm thick foam having 150-300 μm pores and seeded with a high cell density	112
7-2a.	Number of cells/cm ² in foams over time for rat calvarial osteoblast/foam constructs with pore size 150-300 μm and seeded with either a low or high cell density	114
7-2b.	Number of cells/cm ² in foams with various pores sizes and thicknesses over time initially seeded with a high rat calvarial osteoblast seeding density	115
7-3a.	Alkaline phosphatase activity in rat calvarial osteoblast/foam constructs over time for foams with pore size 150-300 μm and seeded with either a high or low cell seeding density	116
7-3b.	Alkaline phosphatase (ALPase) activity in rat calvarial osteoblast/foam constructs over time for foams of various pore sizes seeded with a high cell seeding density	117
7-4a.	Light micrographs of a H & E vertical cross-sections of a 500-710 μm pore size polymer foam of thickness 1.9 mm initially seeded with a high rat calvarial osteoblast density and cultured for 14 days	118
7-4b.	Light micrographs of H & E stained vertical cross-sections of a 150-300 μm pore size polymer foam of thickness 3.2 mm initially seeded with a high rat calvarial osteoblasts density and cultured for 14 days	118
7-5.	Light micrographs of von Kossa stained vertical cross sections of a 500-710 μm pore size foam initially seeded with a high rat calvarial osteoblast density and cultured for 56 days	120

7-6a.	Average penetration depth of mineralized tissue after 56 days in culture for constructs with different pore sizes, thickness, and initial rat calvarial osteoblast seeding densities	121
7-6b.	Mineralized tissue volume/surface area in the osteoblast/foam constructs after 56 days in culture for constructs with different pore sizes, thickness, and initial rat calvarial osteoblast seeding densities	122
8-1.	Histological cross-section of a osteoblast-seeded polymer foam having pore size 150-300 μm explanted from the rat mesentery after 7 days <i>in vivo</i> (H & E)	130
8-2.	Histological cross-section of a osteoblast-seeded polymer foam having pore size 500-710 μm explanted from the rat mesentery after 7 days <i>in vivo</i> . (von Kossa).131	
8-3a.	Histological cross-section of a osteoblast-seeded polymer foam having pore size 150-300 μm explanted from the rat mesentery after 49 days <i>in vivo</i> . (H & E) ...132	
8-3b.	Magnified view of the histological section in figure 8-3a	133
8-4.	Penetration depth of mineralized tissue at different implantation time points and for foams with two different pore sizes	134
8-5.	Mineralized tissue volume per surface area over time for foams of different pore sizes explanted from the rat mesentery	135
8-6.	Total bone tissue volume per surface area over time for foams of different pore sizes explanted from the rat mesentery	136
8-7	Percent of mineralized tissue volume found in the foam volume penetrated by bone-like tissue	138
8-8	Molecular weight of explanted polymer foams over time	139

LIST OF TABLES

Table 1-1.	Bone matrix composition	14
Table 5-1.	Surface area of migrating osteoblast cultures on polymer films	60

LIST OF ABBREVIATIONS

2-D	Two-dimensional
3-D	Three-dimensional
ALPase	Alkaline phosphatase activity
BMP-2	Bone morphogenetic protein-2
FBS	Fetal Bovine Serum
GPC	Gel Permeation Chromatography
GS	Gentamicin sulfate
PBS	Phosphate buffered saline
PGA	Poly(glycolic acid)
PLGA	Poly(lactic-co-glycolic acid)
PLLA	Poly(L-lactic-co-glycolic acid)
PMMA	Poly(methyl methacrylate)
TGF-β	Transforming growth factor-beta

CHAPTER I

INTRODUCTION

1.1 Significance and Existing Bone Replacement Therapies

Over one million surgical procedures or new cases of skeletal deficiencies are reported each year [Langer and Vacanti, 1993]. These may result from tumors, diseases and infections, trauma, biochemical disorders, or abnormal skeletal development. Surgical intervention is required in a majority of these cases demanding a variety of therapies and graft materials depending on the type and size of the defect. The current graft materials include autografts, allografts, bone cements or polymers, metals, and ceramics. Although bone grafts have been used to fill defects in bone for over 100 years [DeBoer, 1988] and synthetic materials have had more recent success, they all have their associated problems.

Autografts and autologous flaps are the best bone replacements currently available because they avoid the complications of immune rejection while providing cells and bioactive molecules that can immediately begin the regenerative process. Vascular pedicles of autologous bone flaps can be attached to a vascular supply near the defect site to enhance the chances of bone cell survival in the flap and thus enhance bone tissue survival. The limited supply of autologous bone is probably the main problem with this procedure. Only a small quantity of bone can be harvested from a site within the patient to be transplanted into the defect site without major bone loss at the donor site. Donor site morbidity is thus another problem. The harvesting procedure often is very invasive and leaves massive scars (see Figure 1-1). Necrosis and resorption of the grafts due to lack of blood supply, especially in autografts, is another disadvantage of this procedure [Bajpai, 1983; Shaffer et al., 1985].

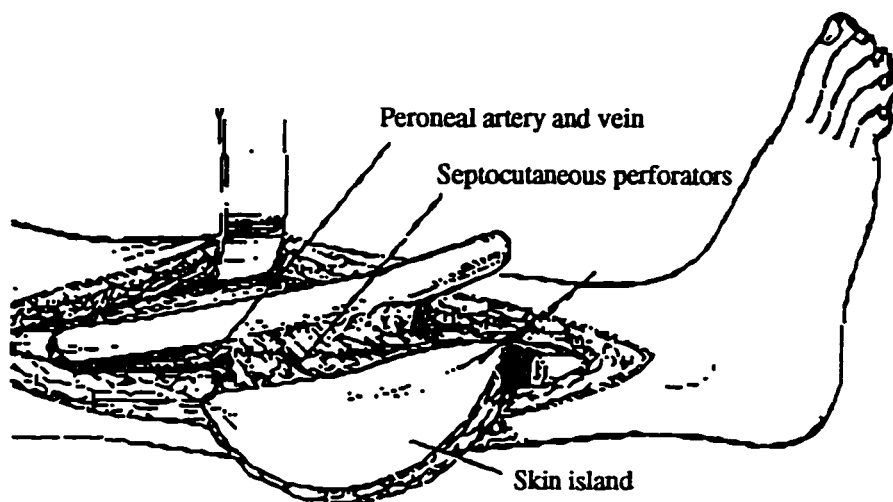


Figure 1-1. A typical surgical excision procedure used to obtain autologous bone for transplantation, illustrating the invasive nature of such a procedure. The patient's fibula is removed along with a vascular supply, shaped to fit, and transplanted into the defect site. The blood vessel and vein are surgically attached to an adjacent artery and vein to support the metabolic needs of the flap tissue.

Allografts may be used for larger skeletal defects. This bone graft material is obtained from bone banks and thereby avoids problems with limited supply. This procedure also does not require a second operation to obtain the graft material, so avoids donor site morbidity and pain. The main problem with this graft material is the potential for disease transmission to the patient and immune rejection of the implant. Fresh allografts elicit a vigorous inflammatory and specific immune response in addition to massive resorption of the graft [Friedlaender, 1987]. Even though processing techniques, such as deep-freezing, freeze-drying, demineralization, and irradiation have been used to reduce this immune response, the processing techniques can drastically change the mechanical properties of the material [Friedlaender, 1987] and the potential for disease transmission still exists. Difficulty in shaping these grafts to replace irregular skeletal defects, resorption and fracture of the graft, and nonunion of the graft-recipient bone interface are other possible complications [Shaffer et al., 1985].

Synthetic materials can be easily made into the desired shapes for filling any shaped defect, yet they lack important physiologic and some of the physical properties of natural bone. Metal, poly(methyl methacrylate) (PMMA) bone cements or other polymers, and ceramic prostheses are meant to be permanent, however the eventual removal of the implants may be necessary due to infection, fatigue damage or problems with the material/bone interface, such as implant loosening [Petty et al., 1985; Petty et al., 1988]. Most metals are too stiff and can cause stress shielding and resorption of the surrounding bone [Bajpai, 1983; Bobyn et al., 1992]. The exothermic reaction of poly(methyl methacrylate) can also cause local tissue necrosis. Wear debris from long-term PMMA and polyethylene implants or fatigue failure may call for their removal or replacement with new implants. The infection threshold of the patient is also reduced with permanent implants [Petty et al., 1985; Petty et al., 1988]. Synthetic or coralline hydroxyapatite ceramics are more recent biomaterials with their clinical use beginning in the last decade [Holmes et al.,

1988; Roux et al., 1988; Oonishi, 1991]. Although these ceramic materials have been shown to be biocompatible and osteoconductive [Kent et al., 1983], their mechanical strength is low [Light and Kanat, 1991] requiring the use of bone plates to stabilize grafts implanted in weight bearing locations [Guillemin et al., 1987; Light Kanat, 1991]. Synthetic hydroxyapatite bonds well with bone [Oonishi, 1991] but it has been shown to be nonresorbable [Jarcho et al., 1976] which limits its use. The pore size and porosity of natural coral hydroxyapatite is also limited by what can be found in the environment.

1.2 New Methods of Bone Regeneration

The inadequacies of the existing bone replacement methods have led us and others to search for alternative approaches to bone repair and regeneration. These new methods to engineer bone have focused on the use of synthetic materials as scaffolds for cell transplantation or as conduits to guide new bone growth. The work contained in this thesis focuses on the cell transplantation method, however, the results may also prove to be useful in the design of the other bone regeneration methods.

1.2.a Osteoblast Transplantation

Recent developments in cell transplantation offer new hope in finding a better way to repair bone defects. This novel approach involves the transplantation of isolated cells into a scaffold in order to regenerate a tissue and/or restore its function. This technique could possibly be used to regenerate bone considering that the regeneration of cartilage [Freed et al., 1993], urothelium [Atala et al., 1992], and intestine [Organ et al., 1992] has already been demonstrated in animal models by transplanting primary cell cultures in porous biodegradable polymers. In the case of bone regeneration, osteoblasts can be

harvested from bone marrow, culture expanded *in vitro*, and seeded onto an appropriate biodegradable scaffold. Then the osteoblast/scaffold construct can be implanted into the defect site (Fig. 1-2). The scaffold serves to organize the osteoblast much like the extracellular matrix of bone. Osteoblasts should populate the constructs by proliferation of the transplanted cells and the migration of cells into the construct from the surrounding tissue while the polymer scaffold gradually degrades. Eventually the construct should be filled with a calcified extracellular matrix secreted by the osteoblasts which can be remodeled, as natural bone does, based on the external loads experienced by the new bone.

The scaffolding material used in this approach must allow for the attachment of osteoblasts because they are anchorage-dependent cells which require a supportive matrix in order to survive. The material must also provide an appropriate environment for the proliferation and function of osteoblasts and allow for the ingrowth of vascular tissue to ensure the survival of the transplanted cells. It should be biodegradable with a controllable degradation rate into molecules that can be easily metabolized or excreted. Finally, it should be easily processed into irregular 3-D shapes and provide the structural strength until new bone can assume the structural role. Poly(α -hydroxy esters) satisfy many if not all these material requirements and will be discussed in detail in section 2.2.

Three-dimensional osteoblast cultures have been attempted in a variety of other scaffolds. Three-dimensional resorbable collagen matrices [Casser-Bette et al., 1990; Schoeters et al., 1992] or collagen gels [Sudo et al., 1986] have hosted osteoblast cultures. Even though collagen appeared to be a good substrate for osteoblast growth, collagen matrices do not exhibit sufficient strength to carry the load encountered in most defect sites [Bajpai, 1983]. In addition, collagen use is problematic as it may also invoke an immune response due to its antigenicity. Osteoblasts have also been grown on porous calcium phosphate ceramics [Cheung and Haak, 1989] or in polyphosphazene polymer matrices [Laurencin et al., 1996]. Both materials possess some positive qualities as a bone

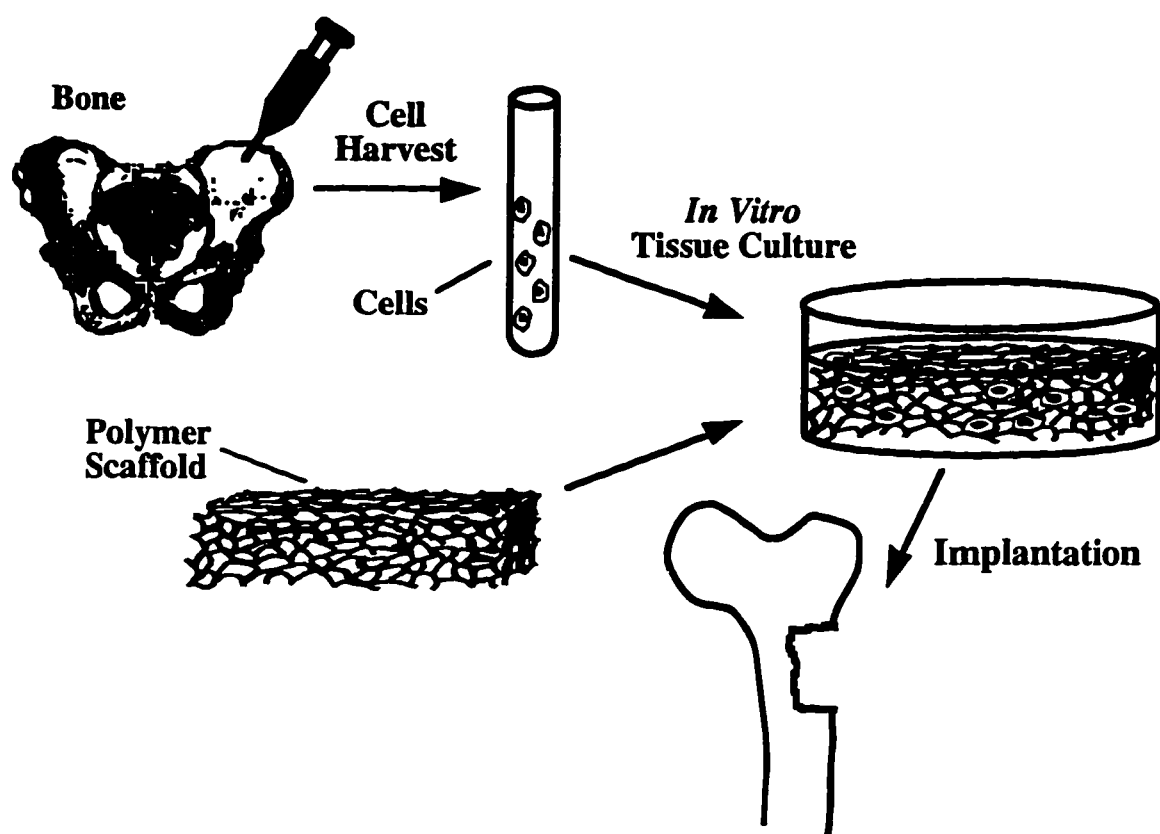


Figure 1-2. Schematic representation of bone regeneration methodology by osteoblast transplantation using biodegradable polymer scaffolds.

regeneration scaffold, however, the non-degradable or slowly degradable characteristics of calcium phosphate ceramics limit their remodeling potential and the biocompatibility of polyphosphazenes still needs to be tested.

Osteoblast culture has previously been attempted on one type of poly(α -hydroxy ester). Poly(glycolic acid) meshes of 100 μm thickness served as a substrate for osteoblast culture, demonstrating that the cells will proliferate and function on polymer fibers. When these meshes were implanted *in vivo*, cartilage formed during the first six weeks after implantation and was gradually replaced by bone after 20 weeks. The small thickness and low mechanical strength of the polymer scaffold in this mesh form may make replacing large skeletal defect in load bearing sites very challenging.

1.2.b Bone Induction

Alternative approaches to regenerate bone rely on the induction of bone into biomaterials. When the conduit material is implanted adjacent to bone tissue, cells from the tissue begin to invade and populate the material, lay down new matrix, and eventually form new bone. Synthetic polymers on their own usually lack the factors required to make the material osteoinductive but may be used as templates to enhance bone growth for fracture healing. Poly(propylene fumarate) has been developed as a biodegradable bone cement that can be easily polymerized and injected into irregularly shaped osseous defects [Yaszemski et al., 1995]. The polymer was mixed with a leachable salt component and tested in a rat proximal tibia defect model. Bone grew next to and within the polymer material demonstrating the potential of this material for use in orthopedic applications.

In addition, synthetic and natural conduit materials can be made osteoinductive by combining them with bioactive molecules such as bone morphogenetic proteins or transforming growth factor- β . It has been demonstrated that recombinant human bone

morphogenetic protein-2 (rBMP-2) in a demineralized bone matrix carrier will induce the formation of endochondral bone when placed in rat femoral defects [Yasko et al., 1992]. Bone formation occurred in a dose-dependent manner, and the experiment demonstrated the feasibility of using recombinant growth factors in orthopedic sites to obtain successful union. Successful results have also been obtained when rBMP-2 was implanted in a PLGA carrier into large segmental defect created in rat femurs [Lee, 1994].

1.2.c Prefabrication of Bone Flaps

Some complex osseous defects, such as those created in tumor surgery where the mandible or other facial bones are removed, require grafting bone in a hostile environment where tissue induction will not occur. In order for the implanted bone to survive and function, the graft must have a discreet vascular supply that can be attached via microsurgery to existing vessels near the defect site. Vascularized autogenous bone is usually obtained from the patient's iliac crest or fibula for transplantation in to craniofacial defects. This procedure leaves something to be desired because of the limitations in supply of graft material, the difficulty in shaping the transplanted bone and the significant morbidity at the donor site.

A novel approach of obtaining such autogenous vascularized grafts without the existing limitations or complications is currently being investigated [Miller et al., 1996]. The idea is that new bone of a predetermined shape could be formed by implanting a mold containing an osteoinductive scaffold onto a periosteal site remote from the defect. Over a period of weeks, the scaffold would be replaced with new bone, which could then be transplanted along with its vascular supply to fill the defect. When poly(methyl methacrylate) chambers of 0.5 to 1 cm in thickness were filled with chopped corticocancellous bone and implanted onto sheep rib periosteum, vascularized bone was

formed after 6 weeks with evidence of remodeling after 13 weeks. Full bone penetration was achieved in the 5 mm thickness chambers, 88 percent penetration was achieved in the 10 mm thickness chambers by six weeks, and bone failed to grow in empty chambers. This study demonstrated the feasibility of producing clinically significant pieces of bone by implanting osteoinductive scaffolds onto periosteal surfaces.

CHAPTER 2

BACKGROUND

2.1 Bone Anatomy and Biology

Bone is a complex organ which is constantly changing in response to mechanical and hormonal stimuli and has the capability of repairing or regenerating itself as long as suitable conditions exist. It performs two main functions: structural support and reservoir for ions such as calcium and phosphorus. It also serves to protect other organs such as the brain, serves as attachment sites for muscles and thereby is essential for movement, and is a storage site for the bone marrow. Successful advances in the treatment of skeletal defects relies on the understanding of the complex structure and function of bone, as well as the mechanical and hormonal stimuli which affect the growth and remodeling of bone.

2.1.a Gross Structure (long, short, and flat bones)

Three types of bones, based on shape, are apparent by gross observation: long, short, and flat bones. Long bones, such as the femur, tibia, humerus, and metatarsals, have a long middle section called the diaphysis and get wider toward each end at the metaphysis and finally end with the epiphysis. Short bones are approximately as long and they are wide and include such bones as the tarsals, carpals, and vertebrae. Flat bones are shaped at their name suggests and include the cranium, scapula, ilium, and others. The external surfaces of bones are covered by a membranous tissue called the periosteum which contains blood vessels that run into the bone and immature bone forming cells in its cambium layer. The central region of mature bones is filled with marrow.

2.1.b Macroscopic Structure (cortical and trabecular bone)

Each bone is made up of both cortical (compact) and trabecular (cancellous or spongy) bone (Fig. 2-1). Cortical bone makes up about 80 percent of the human skeleton [Recker, 1992] and forms the entire diaphysis of long bones and the outer shell of all bones. It is very dense ($1800\text{-}2000 \text{ kg/m}^3$ when wet) and has a compressive strength of 193 MPa and a tensile strength of 148 MPa [Gibson and Ashby, 1988]. A system of canals runs through cortical bone which houses the blood vessels and lymphatic vessels necessary to support the metabolic needs of the cells. Haversian canals run longitudinally through the bone, while Volkmann canals run from the periosteal surface to the endosteal (or central core) surface connecting with the haversian canals to create an elaborate network of canals. The haversian canals are surrounded by cylindrical depositions of bone called osteons, typically $200 \mu\text{m}$ in diameter and 1-2 centimeters long [Cowin et al., 1991]. Most of the collagen fibers and osteons run longitudinally to the axis of long bones giving cortical bone an anisotropic mechanical characteristic.

Trabecular bone is found in the core regions of flat and short bones and in the epiphyseal ends of long bones. It is much less dense ($310\text{-}560 \text{ kg/m}^3$) [Gibson Ashby, 1988] than cortical bone owing to its high porosity which ranges from 50 to 90 percent [Buckwalter et al., 1995]. The high porosity of trabecular bone is responsible for its lower compressive strength (5-15 MPa) and tensile strength (approximately 8 MPa) compared to cortical bone [Gibson Ashby, 1988]. The spicules of bone in trabecular bone are called trabeculae and are connected to each other giving the bone a spongy appearance. The orientation of trabeculae is along lines of principal stress making trabecular bone anisotropic as well.

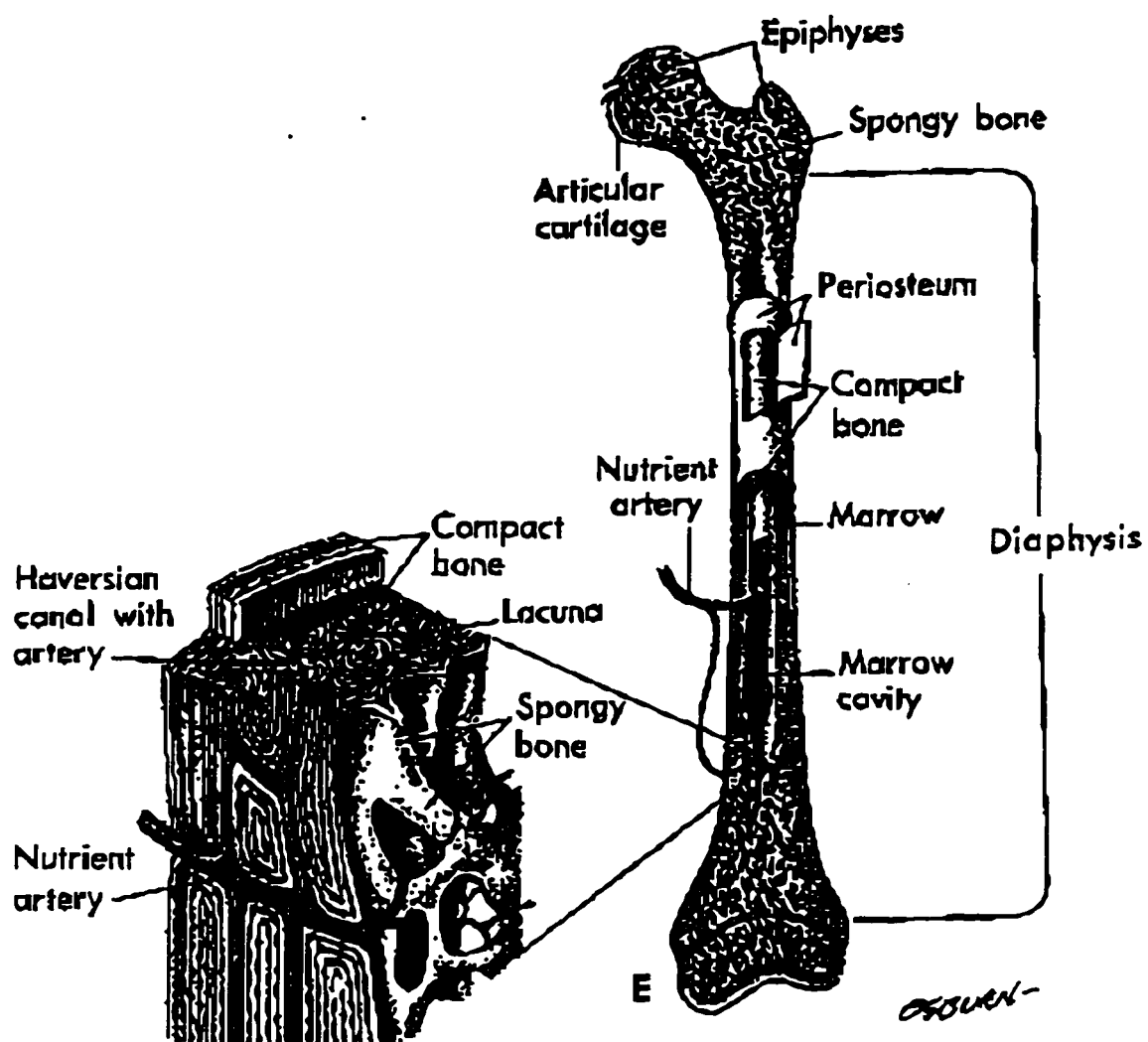


Figure 2-1. Section of mature long bone.

2.1.c Microscopic Structure (woven and lamellar bone)

A more magnified view of cortical and cancellous bone reveals two types of bone tissue, woven (fiber or primary) or lamellar (secondary) bone. Woven bone is an immature bone which is eventually resorbed and replaced by lamellar bone. It is found in children under the age of five and in the initial stages of fracture calluses in adults. It is laid down fairly rapidly thereby resulting in the irregular organization of collagen fibers and four times as many osteocytes per unit volume compared to lamellar bone [Buckwalter et al., 1995]. In contrast, the slower deposition of lamellar bone allows for organization of collagen fibers into parallel sheets referred to as lamellae. The lamellae are formed around the Haversian and Volkmann canals and appear as circular rings, much like a cross-section of a tree trunk. Minerals are also deposited more uniformly in lamellar bone than in woven bone. The uniform orientation of collagen fibers in lamellar bone results in its anisotropic behavior under mechanical load, whereas the mechanical properties of woven bone are similar in all directions.

2.1.d Molecular Composition

2.1.d.1 Bone Matrix

Bone consists of both an organic and an inorganic phase. The organic phase is mostly collagen fibers which resist the tensile forces, while the inorganic phase is solid calcium phosphate particles (or hydroxyapatite crystals) which resist compressive forces. More than 90% of the volume of lamellar bone is made up of bone matrix, with the remainder including cells and blood vessels [Triffit, 1980]. The organic portion of bone is mostly collagen type I, making up approximately 90% of the organic matrix. Other

proteins and growth factors found in bone matrix are listed in Table 2-1. Water and growth factors make up the remaining 15% of the total wet weight of bone. The inorganic portion of the matrix contains approximately 99 % of the body's calcium, 85% of the phosphorous, and between 40 and 60% of the body's sodium and magnesium [Buckwalter et al., 1995]. The majority of the calcium phosphate is found as hydroxyapatite crystals.

BONE MATRIX	
Organic (20% wet wt.)	Inorganic (65% wet wt.)
Collagen Type I (90%)	Hydroxyapatite ($\text{Ca}_{10}(\text{PO}_4)_6(\text{OH})_2$)
Collagen V & XII	Whitlockite ($(\text{Ca},\text{Mg})_3(\text{PO}_4)_2$)
Glycoproteins	Amorphous Ca_xPO_4 ($\text{Ca}_9(\text{PO}_4)_6$ (variable))
Proteoglycans	Octacalcium phosphate ($\text{Ca}_8\text{H}_2(\text{PO}_4)\cdot 5\text{H}_2\text{O}$)
Osteocalcin	Brushite ($\text{CaHPO}_4 \cdot 2\text{H}_2\text{O}$)
Osteonectin	
Bone sialoprotein (osteopontin)	
Bone phosphoprotein	
	Growth Factors
	Transforming growth factor-beta family (TGF- β)
	Insulin-like growth factor (IGF-1 and IGF-2)
	Bone morphogenic proteins (BMP)
	Platelet-derived growth factors (PDGF)
	Interleukins (IL-1 and IL-6)
	Colony-stimulating factors (CSF)

Table 2-1. Molecular components of bone.

2.1.d.2 Bone Cells

2.1.d.2.a Mesenchymal Cells

Pluripotential or undifferentiated mesenchymal cells are immature cells that have the potential to become osteoblasts if stimulated to do so. They reside in the bone canals, endosteum, periosteum and marrow. They may also be stimulated to migrate to bone from surrounding tissues or from the blood stream. While they are in their undifferentiated state, they have an irregular form with few organelles and minimum cytoplasm.

2.1.d.2.b Osteoblasts

Osteoblasts originate from a mesenchymal lineage and are responsible for laying down new bone matrix (Fig. 2-2). They are polyhedral cells with an eccentrically placed nucleus and cover 3-12% of the cancellous bone surfaces. When they are actively synthesizing new bone matrix, they contain abundant rough endoplasmic reticulum (RER), free ribosomes, and mitochondria. Their well developed golgi area produces vesicles containing pre-collagen units. Osteoblasts make contact with each other and osteoclasts through cytoplasmic processes.

2.1.d.2.c Osteocytes

When osteoblasts become embedded in their own secretions of mineralized matrix they are referred to as osteocytes. They are much less active than osteoblasts; therefore are smaller and have few RER, free ribosomes, and mitochondria. Osteocytes occupy a small

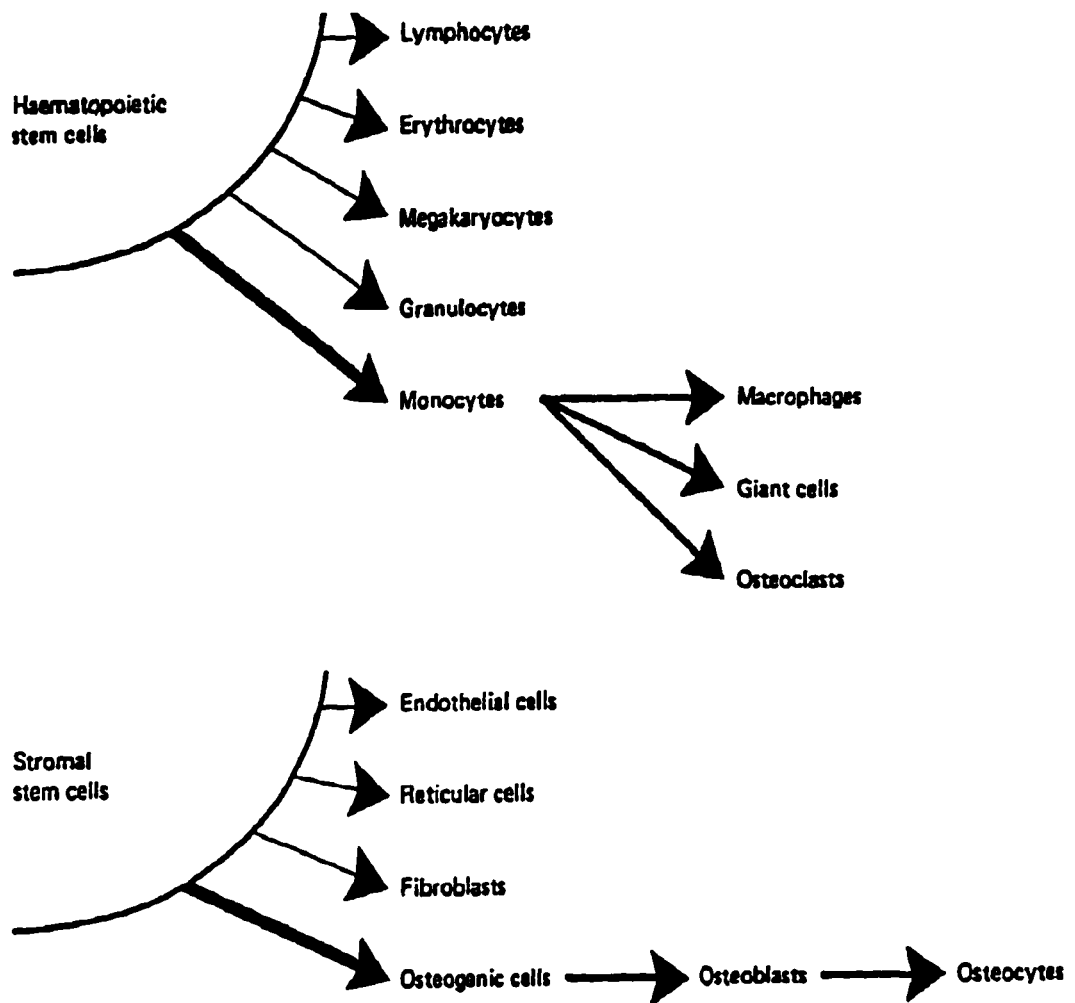


Figure 2-2. Origins of bone cells

cavity or lacuna and make contact (or form gap junctions) with adjacent osteocytes through their cytoplasmic processes which run through tiny channels called canaliculi.

2.1.d.2.d Osteoclasts

Osteoclasts are large multinucleated cells originating from hematopoietic stem cells in the bone marrow (Fig. 2-2). Osteoclast precursors are monocytic or mononuclear cells from the marrow or bloodstream which fuse to form multinucleated osteoclasts when stimulated. The mature osteoclast typically has three to twenty nuclei and functions to resorb bone. Their most distinctive feature is their ruffled or brush border at the bone contact surface. They contain plentiful mitochondria to supply the energy needed to resorb bone and lysosomes to export the acid phosphatases and proteases to the resorbing bone surface. The mechanism by which these cells resorb bone matrix begins with their binding to the contact surface, creating a sealed space between their exterior membrane and the bone surface. They decrease the pH in the sealed space from 7 to 4 by filling it with protons through the membrane-bound proton pumps, which solubilizes the minerals [Buckwalter et al., 1995]. Acid proteases are then released into the space to digest the organic matrix.

2.1.d.2.e Bone Lining Cells

Bone-lining cells (also referred to as resting osteoblasts or surface osteocytes) lie directly on the bone matrix surface. They have a flattened form with less cytoplasm and fewer organelles than osteoblasts. Their cytoplasmic extensions penetrate the bone matrix and come in contact with the cytoplasmic extension of osteocytes. The mechanical forces experienced by osteocytes may be relayed to the lining cells via these connections which in

turn may play a role in attracting osteoclasts to specific sites to resorb bone or be responsible for stimulating lining cells to become active and deposit new bone.

2.1.e Bone Formation, Modeling, Remodeling, and Repair

Bones develop by either endochondral or intramembranous ossification. Endochondral ossification occurs in the formation and growth of long bones, fracture repair, and the incorporation of bone grafts. It involves the replacement of a cartilage intermediate by new bone. Chondrocytes in the cartilage template enlarge, then die, and leave large empty cavities which are invaded by blood vessels, osteoclasts, and osteoprogenitor cells. The osteoprogenitor cells differentiate into osteoblasts and mineralize the cartilage matrix and form new bone matrix. In long bones, the region where the transformation from cartilage to bone occurs is called the growth plate. Osteoclasts then resorb the mixture of calcified cartilage matrix and immature bone while osteoblasts replace it with mature lamellar bone. Intramembranous ossification, which leads primarily to the formation of flat bone, involves the deposition of woven bone directly from layers of mesenchymal cells and loose organic matrix. Appositional formation is the laying down of new bone on an existing surface and occurs during periosteal enlargement (or widening) of bones and during bone modeling and remodeling.

Bones model themselves in response to the mechanical loads they experience. This relationship between bone structure and function was first observed by Wolff in the 1890's and is referred to as Wolff's law [Wolff, 1892]. Bone matrix is deposited in regions of high load making bones denser and stronger, while bone resorption exceeds bone formation in low stress regions resulting in decreased bone density. The modeling process generally refers to alterations in the shape of the bones, whereas remodeling refers to bone turnover that does not alter overall bone shape. The sequence of events in bone remodeling

includes osteoclast activation, resorption of bone, osteoblast activation, and formation of new bone at the resorption site. In osteonal remodeling, osteoclasts cut tunnels through the bone making way for blood vessel penetration. Osteoblasts then form layers along the resorption cavity surface to deposit successive lamellae of new bone matrix. The remodeling of bone is thought to serve two purposes. It may be a method to prevent the accumulation of fatigue damage which in turn prevents fractures due to propagation of fatigue cracks. It may also be responsible for the maintenance of mineral homeostasis.

Fracture repair occurs in three stages: inflammation, callus formation, and remodeling. The formation of a hematoma, or blood clot, is the first event to occur following a fracture. Acute inflammatory cells arrive to remove necrotic debris along with polymorphonuclear leukocytes and macrophages. The callus formation and remodeling stages of fracture repair are similar to that of endochondral ossification. Formation of a fracture callus proceeds by the recruitment and proliferation of mesenchymal cells as well as their differentiation into osteoblasts. The cells synthesize a cartilaginous matrix and ossify this matrix to form woven bone. Remodeling of the fracture callus is the third and final stage of fracture repair, eventually replacing the callus with the more organized lamellar bone.

These modeling and remodeling processes play an important role in new bone formation and thus can be seen to occur in grafts following transplantation. As was described earlier, part of the remodeling process involves replacing the old extracellular matrix with new tissue. In osteoblast transplantation, the polymeric scaffolding material is meant to temporarily mimic the natural extracellular matrix of the bone and to support the osteoblasts until sufficient extracellular matrix is produced by the transplanted cells to replace the degrading material and assume the supportive role.

2.2 Poly(α -hydroxy esters)

Poly(α -hydroxy esters) are a family of linear aliphatic polymers. Two of the most common polymers in this family, poly(glycolic acid) (PGA) (Fig. 2-3a) and poly(lactic acid) (PLA) (Fig. 2-3b), as well as their copolymers, poly(lactic-co-glycolic acids) (PLGA) (Fig. 2-3c), have had recent successes in orthopedics. PGA, PLA, and their copolymers are all biocompatible, degrading by hydrolysis, and to a lesser extent enzymatic degradation *in vivo*, [Holland et al., 1986] to products which can be eliminated from the body either through metabolic pathways (tricarboxylic acid cycle) or by direct renal excretion [Hollinger and Battistone, 1986]. They can be easily manufactured into irregular shapes needed for filling bone defects and have the distinct advantage of being capable of degrading from a period of weeks to years depending on the copolymer ratios [Tamada and Langer, 1993]. Acidic and basic environments catalyze hydrolysis and thus can dramatically decrease the degradation rates [Chu, 1982] so implant location can also affect degradation rates. Since PLA, PLGA, and PLGA are among the few synthetic degradable polymers approved by the Food and Drug Administration (FDA) for human clinical use, less testing should be required to get approval to use these polymer in new applications, such as a scaffolding material for osteoblast transplantation.

Poly(α -hydroxy esters) fulfill many of the material requirements necessary for osteoblast transplantation. These include biocompatibility, biodegradability, and osteoconductivity. The range of degradation rates that can be achieved by the copolymers suggests that it may be possible to fabricate a polymeric scaffold to degrade at a rate which would allow for osteoblast proliferation and sufficient bone matrix secretion to withstand local stresses. The high strength of many of these polymers is also advantageous since a polymer scaffold must have sufficient strength to be implanted in bone defect sites and maintain its strength throughout the degradation process, until new bone is formed. They

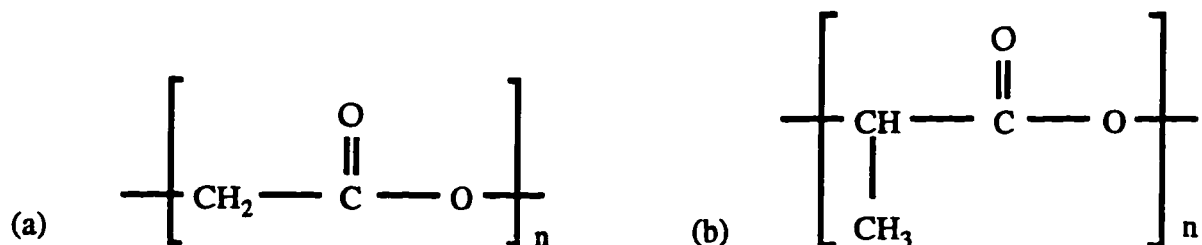


Figure 2-3. Chemical structures of (a) poly(glycolic acid) and (b) poly(lactic acid).

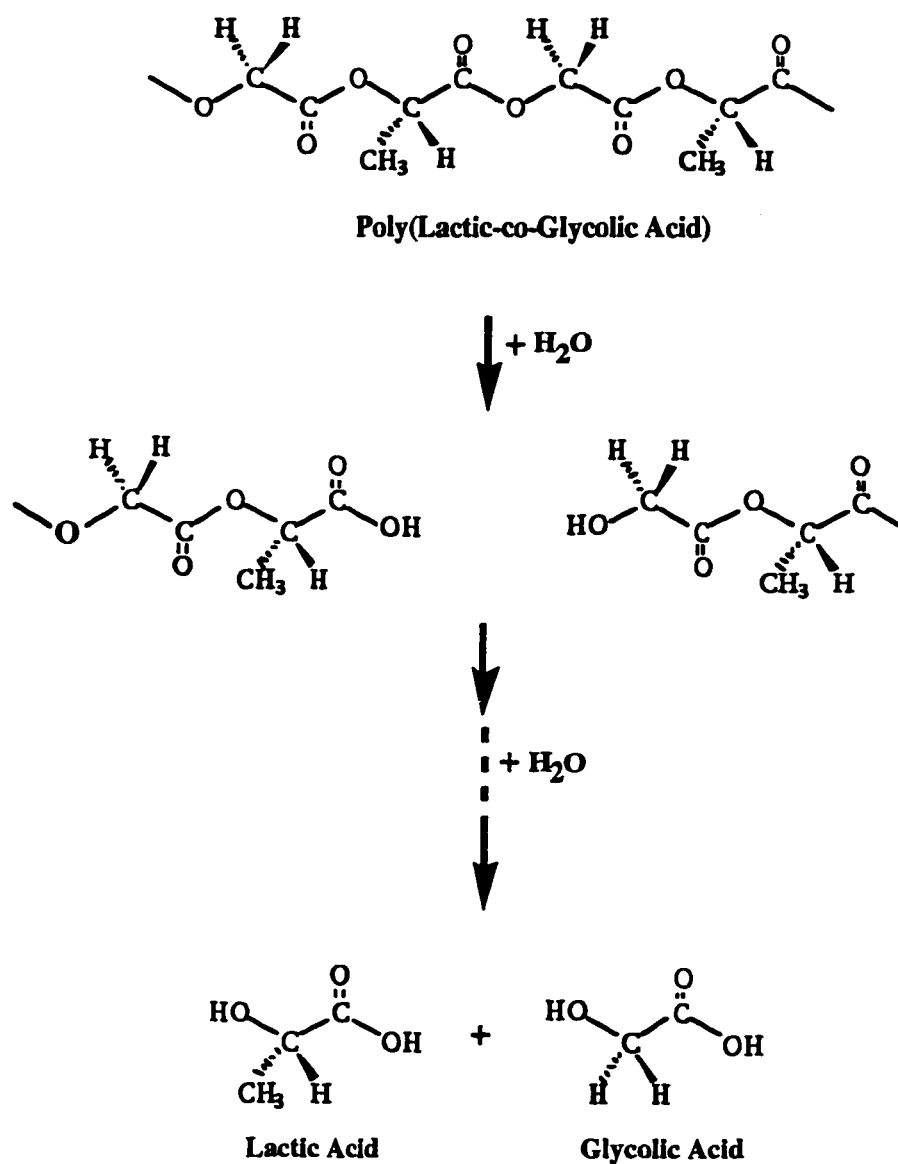


Figure 2-3c. Hydrolytic degradation reaction of poly(lactic-co-glycolic acids) into their monomer units lactic acid and glycolic acid.

are also easily sterilizable and can be fabricated into foams with high porosity for maximal cell loading.

2.2.a. Poly(glycolic acid) (PGA)

PGA is the simplest linear, aliphatic polyester. Its high crystallinity (between 46-52%) [Reed and Gilding, 1981] and hydrophilicity gives rise to a high melting point and relatively low solubility in most common organic solvents. It degrades essentially by bulk erosion in a matter of weeks to months depending on the initial molecular weight and crystallinity of the starting material. PGA has been available as degradable sutures under the trademark "Dexon" since 1970. One of the highest strengths reported was of self-reinforced cylindrical rods of PGA which had a flexural strength of 370 MPa [Vainiopää et al., 1987].

2.2.b Poly(lactic acid) (PLA)

PLA is less crystalline (37% for PLLA) [Gilding and Reed, 1979] but is more hydrophobic than PGA and therefore degrades at a slower rate (up to 4 years). The presence of the methyl group sterically hinders ester bond cleavage and imparts its hydrophobic character, as well as increases its solubility in organic solvents. PLA is also a chiral molecule due to the extra methyl group and thus exists in two stereoisomeric forms (D and L). Besides the two stereoregular polymers D-PLA and L-PLA, a racemic polymer (D,L-PLA) obtained by mixing D and L lactic acid or a meso-PLA can be synthesized from D,L-lactide. L-PLA or PLLA, as it is also called, is the most widely used stereoisomer of the polymer since its hydrolysis yields L(+) lactic acid which is the naturally occurring form of the molecule. PLLA is one of the strongest biodegradable polymers having a

tensile modulus of 3 GPa and tensile strength of 50 MPa when unoriented [Engelberg and Kohn, 1991]. It has been used in the form of screws and plates for internal bone fixation [Vert et al., 1984; Bos et al., 1987]. They are also osteoconductive [Vert et al., 1981; Hollinger, 1983; Hollinger Battistone, 1986] and are replaced by new bone tissue when implanted into bone sites. No acute inflammatory reaction was observed when PLLA samples were implanted subcutaneously in rats, [Bos et al., 1991] however, foreign-body inflammatory reactions and bone resorption have been observed following long term degradation of the polymer [Böstman, 1991; Suganuma and Alexander, 1993]. This delayed inflammatory reaction represents the most serious complication, but may be overcome by controlling the release of the acidic degradation products by possibly starting with a polydispersed polymer (in other words a polymer composed of a broad range of molecular weight chains) [von Recum et al., 1995].

2.2.c Poly(lactic-co-glycolic acids) (PLGA)

Copolymerizing the precursor ring molecules, lactide and glycolide, increases the range of physical and mechanical properties that can be achieved in poly(α -hydroxy esters). Crystallinity is rapidly lost in the copolymers, resulting in higher degradation rates compared to the homopolymers. These rates continue to increase as the copolymers get closer to an equimolar ratio, however, the relationship between molar ratio of the corresponding copolymers and the physicomechanical properties is not linear [Miller et al., 1977]. PLGA copolymers are presently approved by the Federal Drug Administration (FDA) for use as degradable sutures; two of which are known as "Vicryl" and "Polyglactin 910."

2.3 Osteoblast Isolation, Culture, and Development

Not only is the choice of polymer material important for the overall success of bone formation by osteoblast transplantation, but the method by which the osteoblasts are obtained can affect the desirability of the new procedure and its outcome. Methods have been developed and perfected to isolate and culture osteoblasts originating from rats, [Peck et al., 1964; Rao et al., 1977; Yagiela and Woodbury, 1977; Nijweide et al., 1981; Boonekamp et al., 1984] mice, [Wong and Cohn, 1975; Ecarot-Charrier et al., 1983] chicks, [Nijweide, 1975; Tenenbaum and Heersche, 1982] rabbits, [Tibone and Bernard, 1982; Howlett et al., 1986] and humans, [Beresford et al., 1983; Beresford et al., 1984; Gehron Robey and Termine, 1985; Luria et al., 1987] either enzymatically or by migratory techniques. Fetal rat calvarial osteoblasts are ideal for *in vitro* studies because these cells are well characterized, readily obtainable, and are easy to isolate. However, the most desirable method for transplantation would be to obtain osteoblasts percutaneously from the patient's bone marrow. This would avoid the need for open surgery with its possible donor-site complications of pain, infection, and damage to nerves and blood vessels. In addition, because the cells would be of autologous origin, there would be no risk of immune rejection and little chance of pathogen transfer. Several studies have demonstrated the feasibility of obtaining bone forming cells from human, rabbit, and rat bone marrow [Howlett et al., 1986; Maniatopoulos et al., 1988; Haynesworth et al., 1992]. These techniques involve *in vitro* expansion of the mesenchymal stem cells present in the marrow by the addition of the appropriate factors to culture media to enhance osteoblast differentiation and function.

The detailed series of developmental events leading from pluripotential mesenchymal stem cells to differentiated mineral producing osteoblasts and osteocytes are very complex and are not fully understood. It is known, however, that three distinct

developmental phases are observed *in vitro* and *in vivo*: growth phase, matrix developmental phase, and mineralization phase (Fig. 2-4). Immature osteoblasts or osteoprogenitor cells express a variety of genes, enzymes, and proteins during each phase. Fetal rat and clonal murine calvarial osteoblasts express high levels of collagen type I genes, fibronectin, and TGF- β in addition to proliferative-related genes (eg. c-fos, c-myc, and H4 histone) during their proliferative phase [Owen et al., 1990; Lian and Stein, 1992; Pockwinse et al., 1992; Quarles et al., 1992]. A similar pattern of high expression of TGF- β with collagen type I is found during endochondral bone formation *in vivo* [Bortell et al., 1990]. When cellular proliferation begins to slow-down the second developmental phase begins to take over. Alkaline phosphatase activity increases ten-fold during this phase [Lian Stein, 1992] along with additional matrix deposition and reorganization. With the onset of the mineralization phase the genes for osteocalcin, osteopontin, and related genes are upregulated while the matrix is being mineralized.

Growth factors, such as transforming growth factor-beta (TGF- β), bone morphogenetic protein-2 (BMP-2), or vitamin D3, can influence the progression of the cells during various phases. Dexamethasone, which is a glucocorticoid hormone, has been shown to stimulate the proliferative capacity of osteoprogenitor cells [Aubin et al., 1992]. Ascorbic acid and β -glycerol phosphate have also been shown to be important for collagen deposition and mineralization in cultured osteoblast systems.

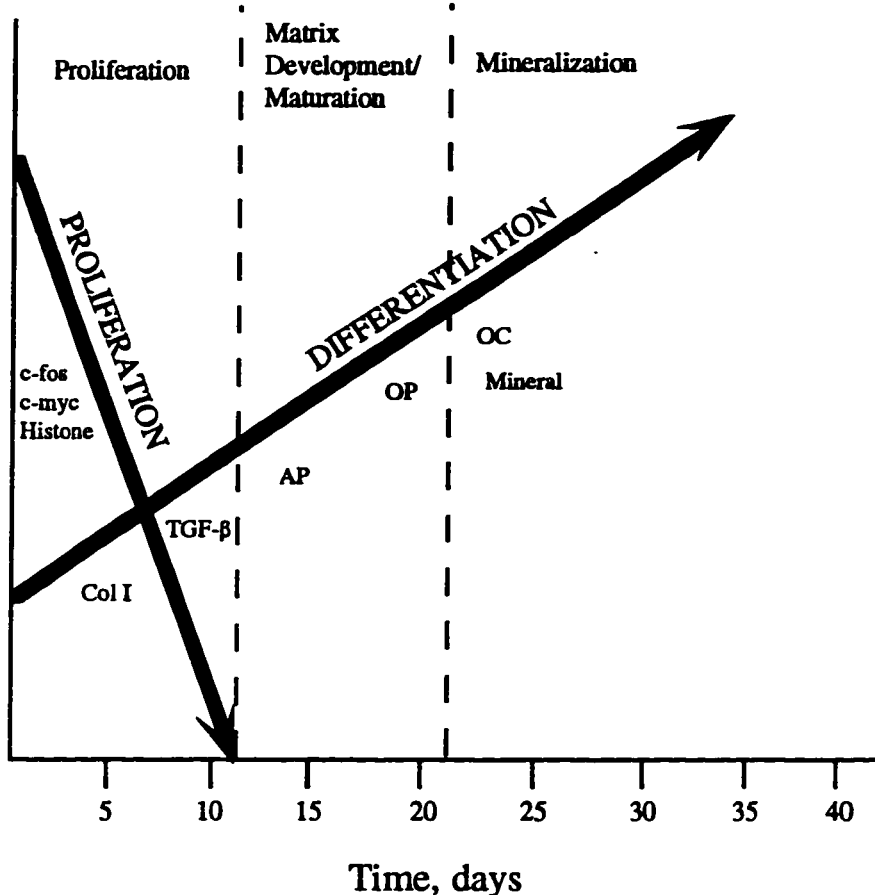


Figure 2-4. Illustration depicting the time scale and reciprocal relationship between proliferation and differentiation in the development of rat osteoblasts in culture. The three developmental phases are designated by dashed lines and the principal developmental genes and growth factors which are expressed during each period are listed: Proliferation-related genes (c-fos, c-myc, and histone); TGF- β , transforming growth factor-beta; Col I, collagen type I; AP, alkaline phosphatase; OP, osteopontin; OC, osteocalcin; Mineral, total accumulated calcium.

CHAPTER 3

OBJECTIVES

The intention of the work contained within this thesis was to demonstrate whether poly(α -hydroxy esters) are a suitable scaffolding material for bone regeneration by osteoblast transplantation. Osteoblasts are anchorage dependent cells and need to attach to an appropriate substrate in order to survive. The first study, Rat Calvarial Osteoblast Proliferation and Function on Two-Dimensional Poly(α -hydroxy ester) Films, was carried out to determine if these biodegradable polymers would allow for the attachment, proliferation, and function of osteoblasts. The success of the polymers to provide a suitable surface for osteoblast attachment was critical for the continuation of the project. The first study also investigated which of the four poly(α -hydroxy esters), PLLA, 75:25 PLGA, 50:50 PLGA, or PGA, would allow for the best attachment, proliferation and function of the osteoblasts.

Once the attachment kinetics, proliferation kinetics, and osteoblast function on the polymer substrates were determined in the first study, we proceeded to investigate the migratory characteristics of osteoblasts on the polymers. The migration of osteoblasts may play a key role in the incorporation of osteoblasts into the polymer scaffolds and the stabilization of osteoblast/polymer constructs into defect sites. One of the aims of the Rat Calvarial Osteoblast Migration on Two-Dimensional Poly(α -hydroxy ester) Films study was to establish whether osteoblasts migrated as a monolayer or as a tissue front. We were also interested to learn if there was a difference in the migration kinetics of osteoblasts from isolated cell cultures or from bone tissue.

The important parameters in the function and migration of osteoblasts on these polymers were investigated on two-dimensional polymer films because this was the most straight-forward and reliable way to achieve those results. Bone, however, is a three-

dimensional organ and thus requires a three-dimensional implantable material in order for regeneration to occur in large critical size defects. Therefore, the ability to culture osteoblasts in three-dimensions in foams of poly(α -hydroxy esters) had to be demonstrated. Two studies were performed to investigate some potentially important parameters for this three-dimensional culture system. We were especially interested in the possible effect of foam pore size on osteoblast proliferation and function because an optimum pore size has been observed for the bone ingrowth in ceramic materials. Rat marrow osteoblasts were cultured in poly(α -hydroxy ester) foams in one study to determine the effect of osteoblast seeding density and foam pore size on cellular proliferation and function. In the other study, we utilized neonatal rat calvarial osteoblasts for three-dimensional cultures in foams with different pore sizes, thicknesses, and cell seeding densities to confirm the results found in the previous study as well investigate the additional parameter of foam thickness.

Finally, the three-dimensional osteoblast seeded polymer foams were implanted into an *in vivo* site to ascertain whether the transplanted osteoblasts could survive. The survival of osteoblasts is dependent on whether their metabolic needs are met. The implant site chosen was the rat mesentery because this well-vascularized site has already been shown to provide an abundant source of blood vessels to polymer foam constructs. The pore size of the osteoblast/foam constructs was varied because this parameter had previously been shown to affect the rate of fibrovascular tissue ingrowth and could potentially affect the success of the implant.

CHAPTER 4

RAT CALVARIAL OSTEOBLAST ATTACHMENT, PROLIFERATION AND FUNCTION ON TWO-DIMENSIONAL POLY(α -HYDROXY ESTER) FILMS

4.1 Introduction

The success of the osteoblast transplantation approach for new bone formation depends heavily on the ability of osteoblasts to attach to the scaffolding material since osteoblasts are anchorage-dependent cells; whereby they must attach to a substrate in order to survive. The cells must also be able to grow and function as osteoblasts when cultured on the transplantation scaffold so that they may produce a mineralized matrix. Thus, early passaged rat calvarial osteoblasts were cultured on four poly(α -hydroxy esters): PLLA, 75:25 PLGA, 50:50 PLGA, and PGA to determine if the osteoblasts would attach, proliferate, and function on the various polymer substrates and if copolymer composition had any effect on the measured parameters.

4.2 Materials and Methods

Materials

The biodegradable polymers used in the experiments were PLLA (Polysciences, Warrington, PA), 75:25 PLGA (Birmingham Polymers, Birmingham, AL), 50:50 PLGA (Medisorb, Cincinnati, OH), and PGA (Birmingham). The ratios 75:25 and 50:50 designate the copolymer ratios of lactic to glycolic acid. The PLLA and 50:50 PLGA came in a pellet form, while the 75:25 PLGA was a coarse powder, and the PGA came in small chunks. The weight average molecular weight of the supplied polymers were 95,800

(PI=1.52) for PLLA, 73,400 (PI=1.80) for 75:25 PLGA, and 51,600 (PI=1.88) for 50:50 PLGA, as measured by gel permeation chromatography (GPC). PI stands for the polydispersity index, and is equal to the ratio of weight average to number average molecular weight. The PGA is highly insoluble in most solvents so the molecular weight was not measured (inherent viscosity of PGA reported by Birmingham Polymers is 1.39 dL/g in hexafluoroisopropanol at 30°C).

Methods

Polymer Preparation

Polymer films 14 mm in diameter were made by a melt mold compression technique. Approximately 4 g of raw polymer were loaded into cylindrical Teflon molds of 14 mm internal diameter and placed in a mechanical convection oven with accuracy ± 1 °C (Blue M Electric, Blue Island, IL) at 195 °C for PLLA, 240 °C for PGA, and 80 °C for 75:25 PLGA and 50:50 PLGA. The molds were heated in the oven under compression (22 N) for 30 min and then cooled at room temperature for 15 min before removing the solid cylindrical polymer block.

Films of 0.5 mm in thickness were cut from the cylindrical blocks of polymer on a diamond saw (Isomet 11-1180, Buehler, Evanston, IL) with the exception of 75:25 PLGA films which were cut 1 mm thick (75:25 PLGA films cut 0.5 mm thick exhibited curling around the edges under cell culture conditions). The films were held to the bottom of 24-well tissue culture plates (Corning Science Products, Corning, NY) with a small amount of inert high temperature vacuum grease (Dow Corning, Midland, MI) which was previously determined to not affect the viability of osteoblasts [Puleo, 1991]. The adhered films were sterilized by exposure to UV light for 1 hr for each side.

Osteoblast Isolation and Culture

Osteoblasts were isolated from neonatal (less than 1 day old) Sprague Dawley rat calvaria by a enzymatic digestive process described by Puleo et al. [Puleo et al., 1991]. Briefly, calvaria of 10 rats were stripped of periosteum, minced, and stirred in a collagenase/trypsin solution consisting of 5 mL of a 0.33% collagenase solution (C-0130, Sigma Chemical, St. Louis, MO,) in Mg⁺⁺ and Ca⁺⁺ free Dulbecco's Phosphate Buffered Saline (PBS) containing 2.4% bovine serum albumin (Sigma) and 1 mL PET — a trypsin solution containing 0.0625% trypsin (T-8253, Sigma), 0.0125% ethylene glycol-bis(b-aminoethyl ether) N,N,N',N'-tetraacetic acid (EGTA) (Sigma), 0.625% polyvinylpyrrolidone (Sigma), and 26 mM N-(2-hydroxyethyl)piperazine-N'-(2-ethanesulfonic acid) (HEPES) (Sigma) in 1.125% NaCl — at 37 °C for three consecutive 20 min digestion periods. The third supernatant was collected and grown with Dulbecco's Modified Eagle Medium (DMEM) (Gibco, Grand Island, NY) supplemented with 10% Fetal Bovine Serum (FBS) (Gibco) and 25 µg/mL gentamicin sulfate (GS) (Sigma) in a 37 °C humidified atmosphere of 5% CO₂. When confluent monolayers were reached, the cells were passaged with the PET trypsin solution until 4-5 passages were reached. For experiments, the cells were cultured in complete media which consisted of DMEM supplemented with 10% FBS, 8 µg/mL GS, 10 mM Na β-glycerol phosphate (Sigma), and 50 µg/mL L-ascorbic acid (Sigma).

Attachment Studies

A confluent number of osteoblasts (approximately 53,000 cells/cm²) were plated on top of each polymer substrate and on the bottom of the tissue culture polystyrene (TCPS) wells which served as the controls. The cultures were placed in the incubator for 0.5, 1, 2,

4, 6, and 8 hrs and upon removal were washed with PBS and trypsinized. Aliquots of the resulting dissociated cell suspensions were counted on a Coulter counter multisizer (model 0646, Coulter Electronics, Hialeah, FL). Only counts between 8 and 32 μm in diameter were utilized.

Proliferation Studies

Osteoblasts (53,000 cells/cm²) were plated on the four polymer substrates and on the bottom of TCPS wells, left in the incubator for 8 hrs before an additional 1 mL of complete media was added to each well, and cultured under standard cell culture conditions. Media was changed daily in an effort to avoid potential toxic effects caused by high concentrations of the polymer degradation products (lactic and/or glycolic acid). Cell proliferation was determined by cell counts (performed as described in the attachment studies section) after 1, 4, 7, and 14 days in culture.

Alkaline Phosphatase Activity

Production of alkaline phosphatase (ALPase) was measured spectrophotically. Osteoblast cultures of 7 and 14 days were washed with PBS and then frozen. Upon thawing, the cells were scraped from the polymer films or well bottom using disposable cell scrapers (Fisher Scientific, Springfield, NJ) with 1 mL Tris buffer (pH 8.0) (Sigma) and sonicated (Ultrasonik 300, J.M. Ney, Bloomfield, CT) for 4 min at 110 watts (50/60 Hz) on ice. Aliquots of 20 μL were incubated with 1 mL of a p-nitrophenyl phosphate solution (16 mmole/L) (Diagnostic Kit 245, Sigma) at 30 °C for up to 5 min. The production of p-nitrophenol in the presence of ALPase was measured by monitoring light

absorbance by the solution at 405 nm, at 1 min increments. The slope of the absorbance versus time plot was used to calculate the ALPase activity.

Collagen Synthesis

The amount of total collagen produced by the osteoblasts over a 24 hr period was determined by radiolabeling all synthesized proteins with ^3H -proline and selectively digesting the collagenous proteins by collagenase [Puleo et al., 1991]. Proteins were radiolabeled by incubating cell cultures of 7 and 14 days with 3 $\mu\text{Ci}/\text{mL}$ L-[5- ^3H]-proline in complete media. After 24 hrs, the proteins were extracted with 1 M acetic acid (Sigma), containing 1 mg/mL pepsin (Sigma), for 4 hrs at room temperature. Aliquots of the protein extract solutions (0.2 mL) were added to 1.5 mL microcentrifuge tubes (Fisherbrand, Pittsburgh, PA) along with 0.1 mL Hepes buffer (60 μmole , pH 7.2) (Sigma) and 0.2 mL of a 0.02 N HCl solution containing 1.25 μmole N-ethylmaleimide (Sigma), 25 μg purified collagenase (Sigma) and 0.25 μmole CaCl_2 (Sigma). The tubes were incubated at 37 °C with shaking for 90 min. The reaction was stopped by adding an equal volume (0.5 mL) of a 10% trichloroacetic acid (TCA) (Spectrum, Gardena, CA) containing 0.5% tannic acid (TA) (Aldrich, Milwaukee, WI) solution. The tubes were placed in an ice bath for 15 min and were then centrifuged at 1500 g for 5 min at 4 °C. Each supernatant solution, which consisted of digested collagenous proteins, was transferred to counting vials containing 12 mL scintillation cocktail (Ecolume, ICN Biomedicals, Irvine, CA). The precipitates were resuspended with 0.5 mL of a 5% TCA solution with 0.25% TA and centrifuged under the same conditions. Each supernatant was added to the corresponding counting vials and the solutions were counted on a scintillation counter (Minaxi b Tricarb 4000 series, Packard Instruments, Laguna Hills, CA) for the presence of radioactive proline. The non-collagenous proteins remained in the precipitates which were resuspended in 1.5 mL of a

5% TCA solution with 0.25% TA, added to new counting vials, and counted. The amount of collagen was calculated by the following formula, where CP stands for the collagenous protein counts and NCP stands for the non-collagenous counts. The 5.2 correction factor takes into account that there is 5.2 times more proline and hydroxyproline in rat collagen than in the non-collagen proteins [Puleo et al., 1991].

$$\% \text{ collagen synthesized} = \left[\frac{\text{CP}}{\text{CP} + 5.2 \text{ NCP}} \right] \times 100 \quad (1)$$

Scanning Electron Microscopy (SEM)

Osteoblasts were fixed *in situ* with 2.5% glutaraldehyde (Sigma) in 0.1 M cacodylate buffer (pH 7.4) (Sigma) for 15 min and then rinsed with 0.1 M cacodylate buffer. The cells were stained (for contrast enhancement) with 1 mL of cold 1% osmium tetroxide (Polysciences), placed on ice for 30-40 min, were rinsed with distilled-deionized water, and stored in a deep freezer (-80 °C). Before SEM observation using a JEOL JSM-5300 system (Boston, MA), the fixed and stained cell samples were freeze-dried and sputter-coated with gold (approximately 40 nm thick).

Histology

Osteoblast cultures were prepared for histological evaluation by first rinsing with PBS and then fixing in 10% neutral buffered formalin (Sigma). All intracellular and extracellular proteins were stained with 0.1% (w/v) Coomassie Brilliant Blue (Sigma) in a solution of 10% acetic acid and 45% methanol for 10 min. After rinsing with water and air drying, the cell samples were viewed under a stereomicroscope (Nikon SMZ-U, Melville, NY).

Gel Permeation Chromatography (GPC)

The number and weight average molecular weights of PLLA, 75:25 PLGA, and 50:50 PLGA were determined by gel permeation chromatography (Waters, Milford, MA) equipped with a differential refractometer (Waters, Series 410) as previously reported [von Recum et al., 1995]. The cells were removed from the polymers by trypsinization and rinsing with distilled-deionized water. The polymer samples were dissolved in chloroform and filtered to remove any insoluble components. The solubilized samples were then eluted in a series configuration through a Phenogel guard column (model 494386, 50 x 7.8 mm, particles 5 mm, Phenomenex, Torrane, CA), a Waters Ultrastyragel (model 10573, 7.8 x 300 mm, 10⁴ Å particle diameter), and a Waters Ultrastyragel (model 10571, 7.8 x 300 mm, 500 Å particle diameter) at a flow rate of 1 mL/min.

Statistical Analysis

All measurements were collected in triplicates and expressed in means ± standard deviations. Single factor analysis of variance (ANOVA) was employed to assess statistical significance of results. Scheffé's method was used for multiple comparison tests at a significance level of 95%.

4.3 Results

Osteoblasts attached to 50:50 PLGA and tissue culture polystyrene (TCPS) with increasing numbers over an 8 hr period (Fig. 4-1). The number of attached osteoblasts began to level off with 66 (± 3) % of the plated cells remaining attached to the 50:50 PLGA

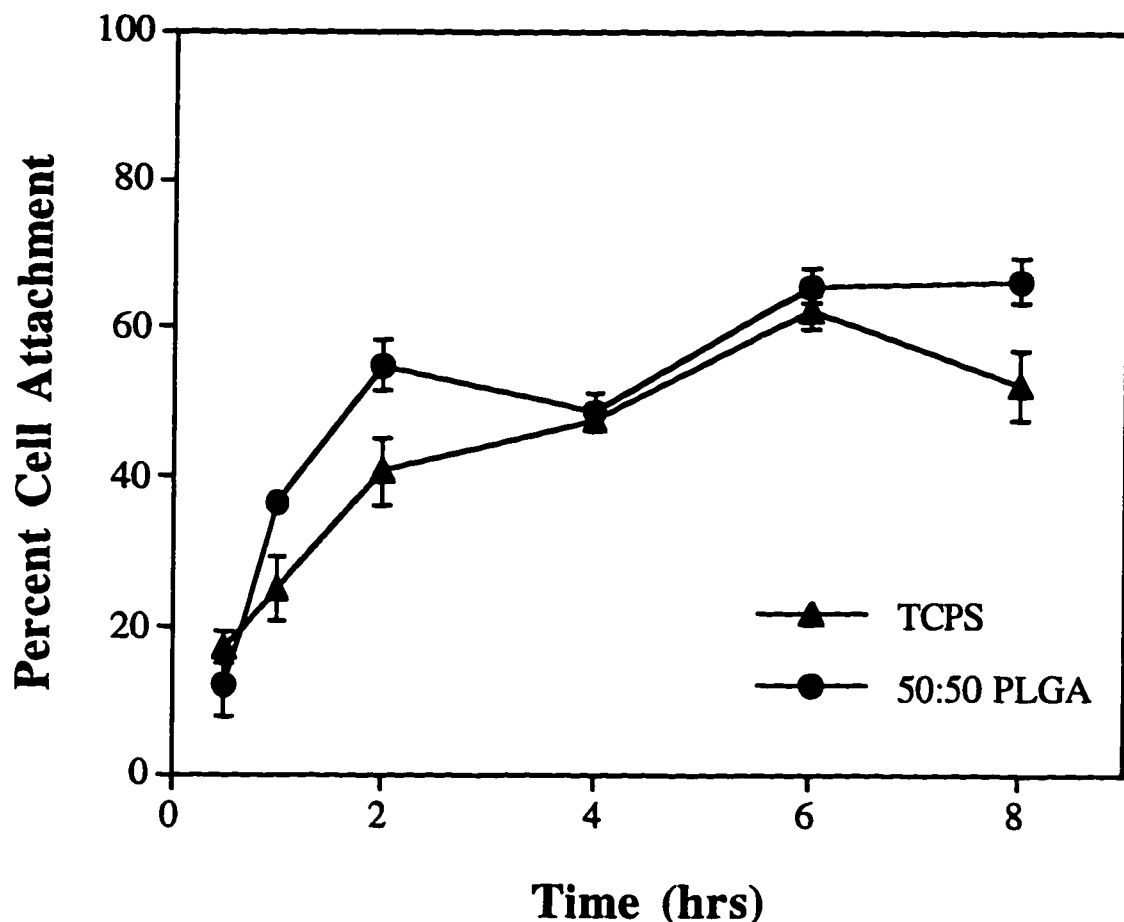


Figure 4-1. Percent of plated osteoblasts that attached to tissue culture polystyrene (TCPS) and 50:50 PLGA films as a function of time in culture (error bars designate means \pm s.d. for $n=3$).

and 52 (± 5) % for TCPS at 8 hrs. The results in Figure 4-2 depict cell attachments to all the substrates after 8 hrs in culture and are expressed as a percent attachment with respect to the number of cells attached to the TCPS control substrates at the same time. Osteoblasts attached equally well to all the polymer substrates as compared to the control TCPS (Fig. 4-2). Although fewer osteoblasts attached to PLLA as compared to 50:50 PLGA ($p < 0.05$) after 8 hrs in culture, there were still substantial numbers of the cells attached to the PLLA substrates.

Proliferation was measured for osteoblasts cultured on the substrates for 1, 4, 7, and 14 days. Compared to the TCPS controls, the cells grew equally well on all the polymer substrates after 1 day in culture (Fig. 4-3); however, when compared to the other polymer substrates, the number of osteoblasts that initially grew on the PLLA substrates was significantly less. By day 4, all the cultures had exceeded confluent numbers (53,000 cells/cm²). Beyond 4 days in culture, cell proliferation was similar for all the substrates.

During the first 4 hours in culture, osteoblasts retained a rounded morphology, as they attached to 50:50 PLGA (Fig. 4-4). Lamellipodia were observed extending toward adjacent cells. By 1 day in culture on 50:50 PLGA films, the osteoblasts were spread and formed a monolayer, consistent with cell counts (Fig. 4-5a). By 4 days in culture, cell counts were more than double confluence numbers confirming the multilayer pattern of growth which is characteristic of the cell line (Fig. 4-5b). A cell monolayer was also observed by SEM on a 75:25 PLGA film after 1 day in culture (Fig. 4-6). The approximate diameter of spread osteoblasts was on the order of 30 μm , and that for rounded cells was 10 μm .

Stained cultures grown on top of the opaque polymer substrates were examined with a stereomicroscope. A typical histological appearance of the cultures is shown in Figure 4-7 for osteoblasts cultured on a 75:25 PLGA film at day 7. Darker stained regions

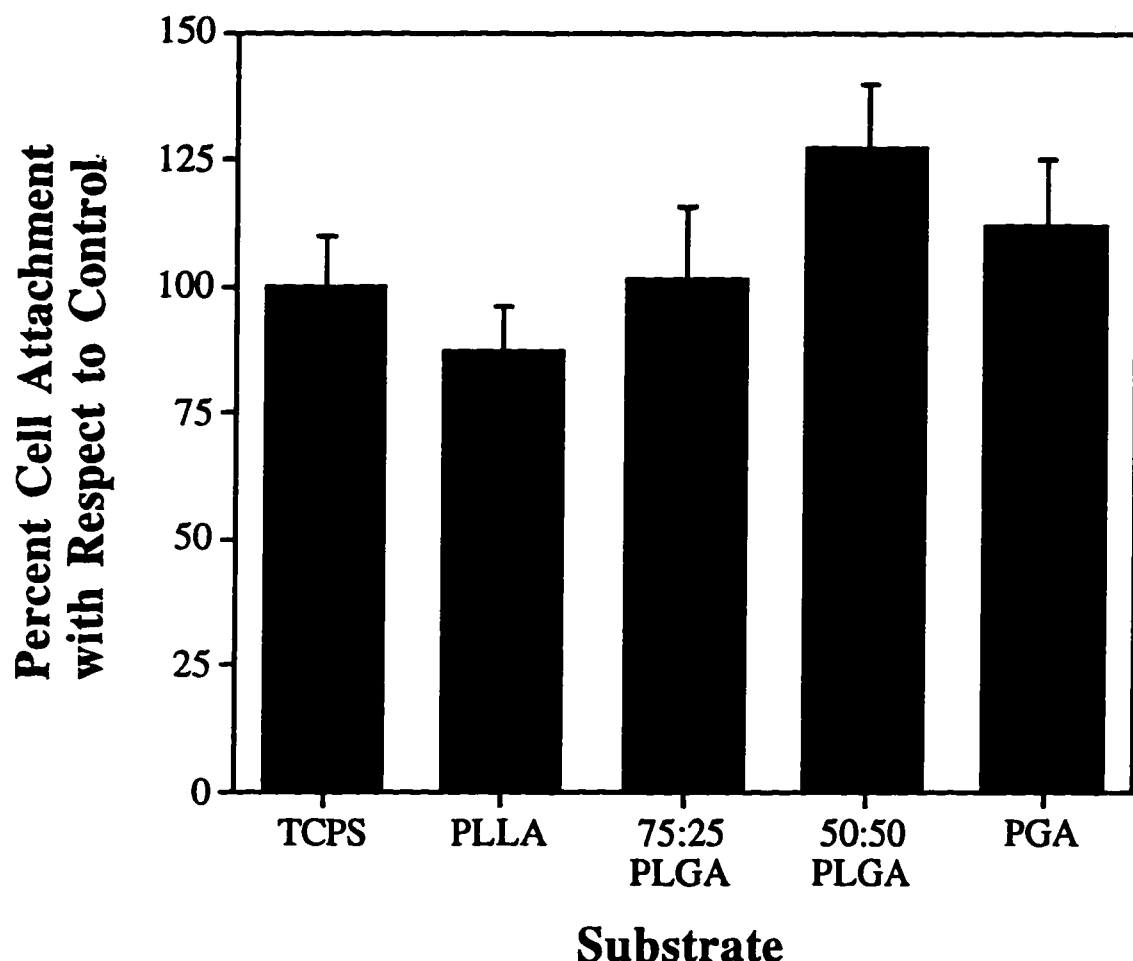


Figure 4-2. Number of osteoblasts attached to PLLA, 75:25 PLGA, 50:50 PLGA, and PGA expressed as a percent of the number of osteoblasts attached to the control TCPS after 8 hrs in culture (error bars designate means \pm s.d. for n=3).

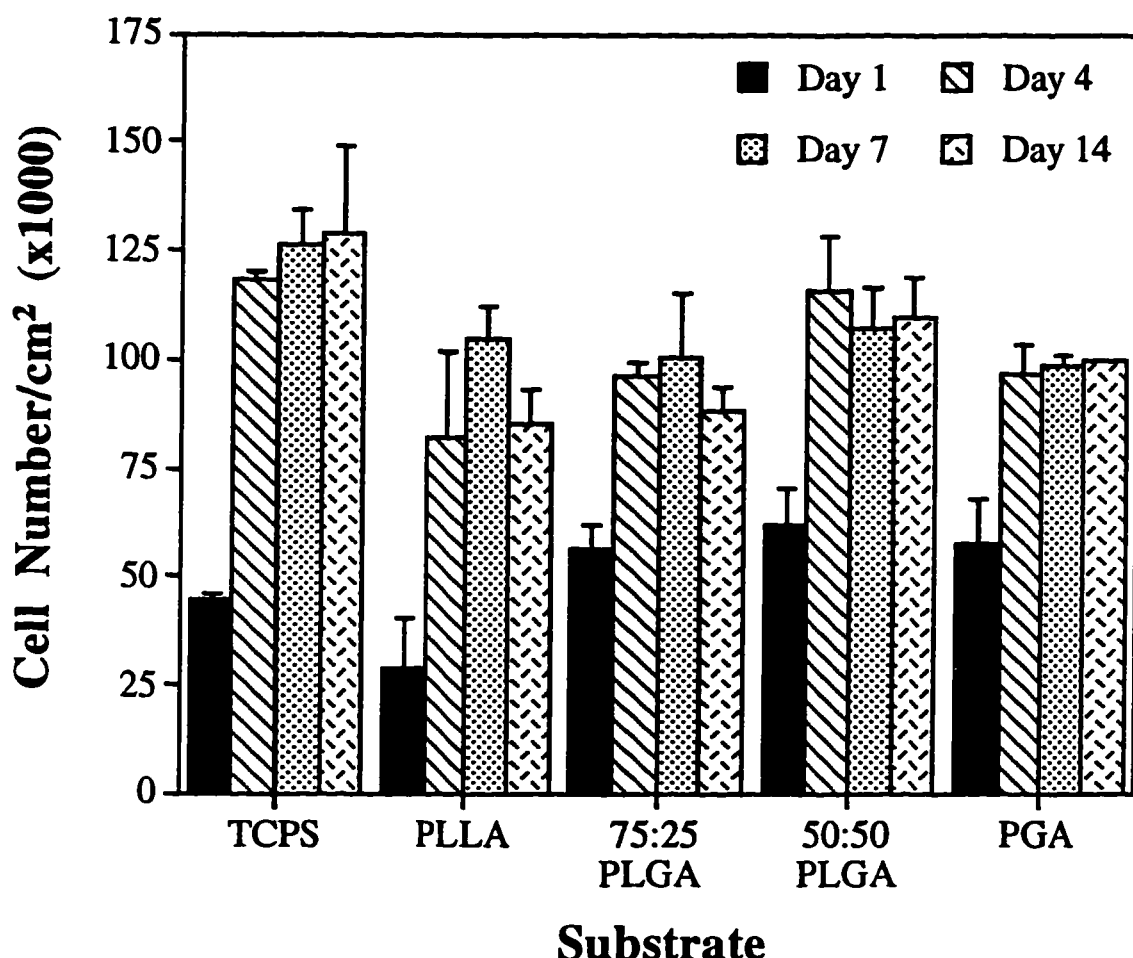
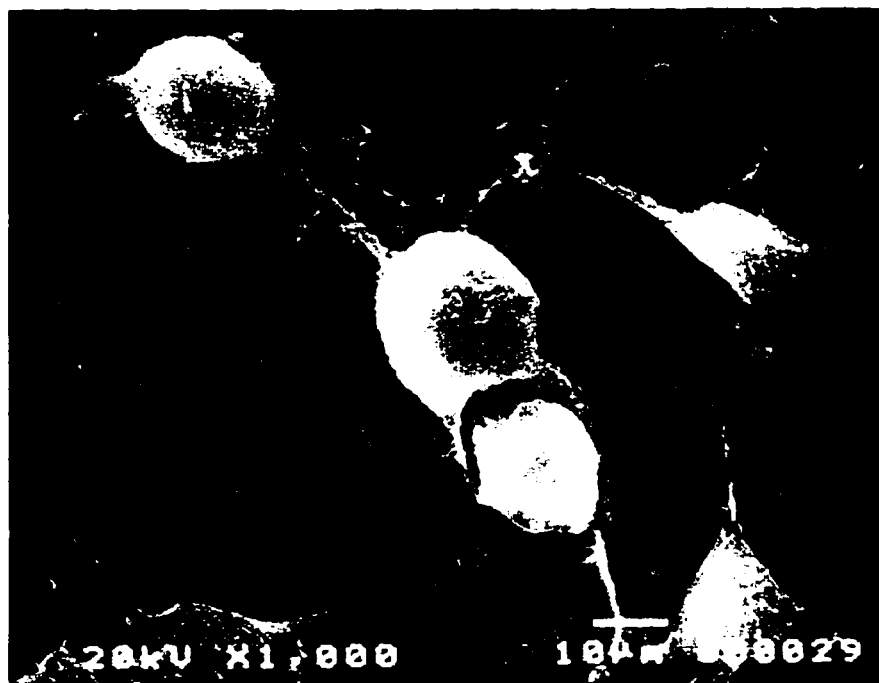
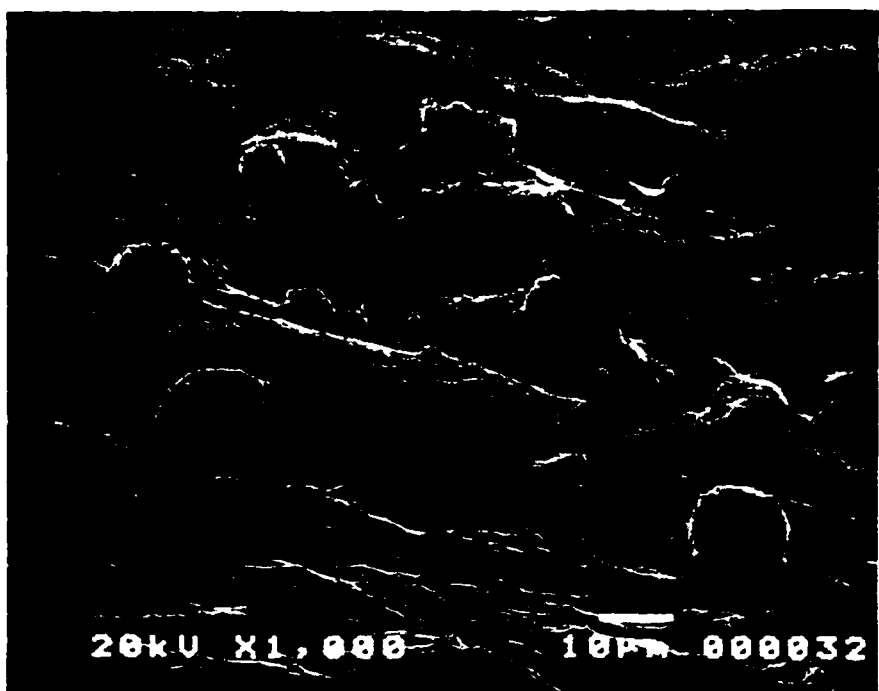


Figure 4-3. Proliferation kinetics for osteoblasts cultured on PLLA, 75:25 PLGA, 50:50 PLGA, PGA, and control TCPS (error bars designate means \pm s.d. for n=3).



(a)



(b)

Figure 4-4. SEM micrographs of osteoblasts attached to a 50:50 PLGA film after 4 hrs in culture viewed at (a) 0 ° and (b) 60 ° tilt.

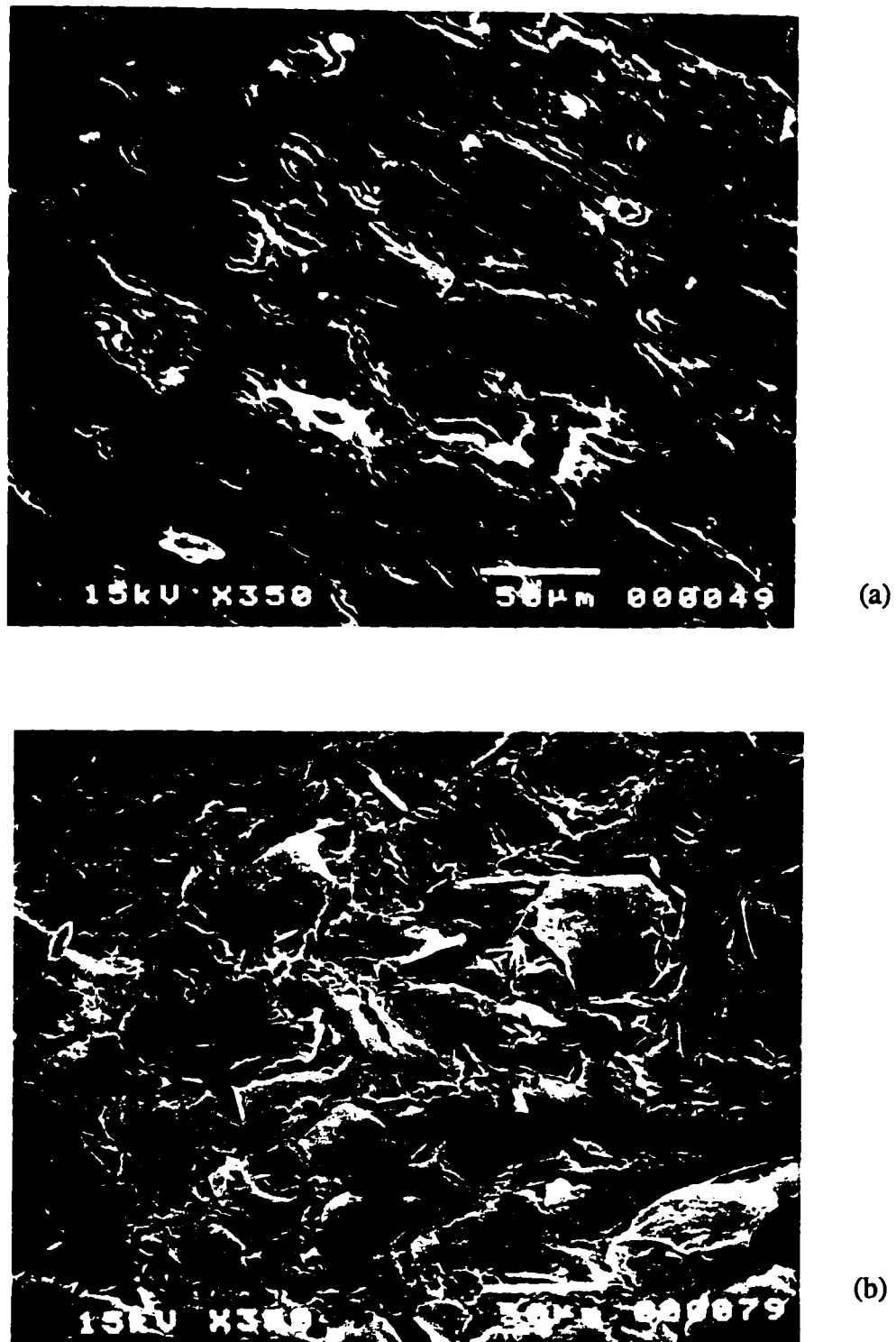


Figure 4-5. SEM micrographs of osteoblasts cultured on 50:50 PLGA films for (a) 1 day and (b) 4 days (samples were viewed at 45 ° tilt).

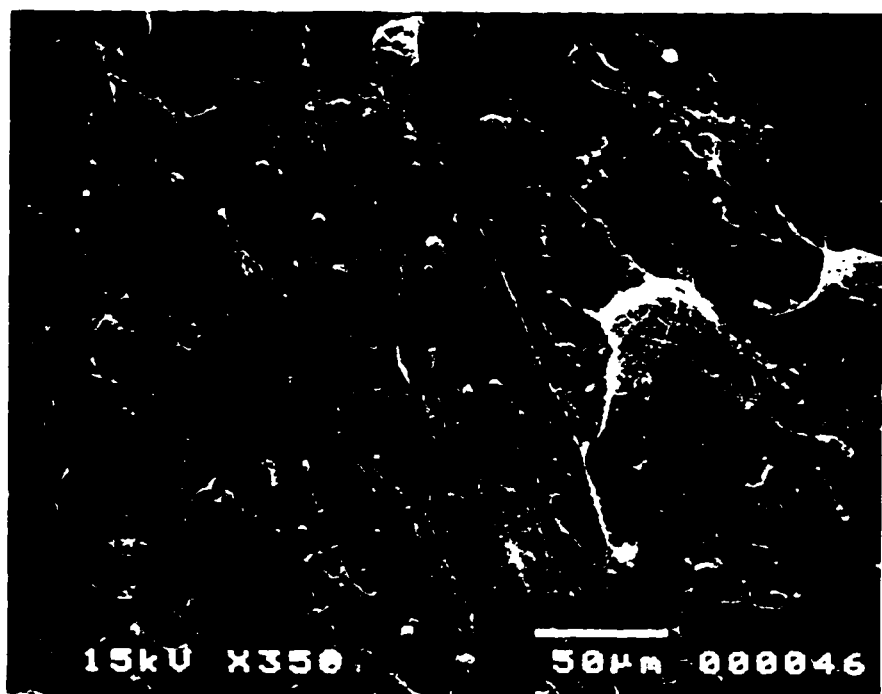


Figure 4-6. SEM micrograph of osteoblasts cultured on a 75:25 PLGA film after 1 day in culture (sample was viewed at 45° tilt).

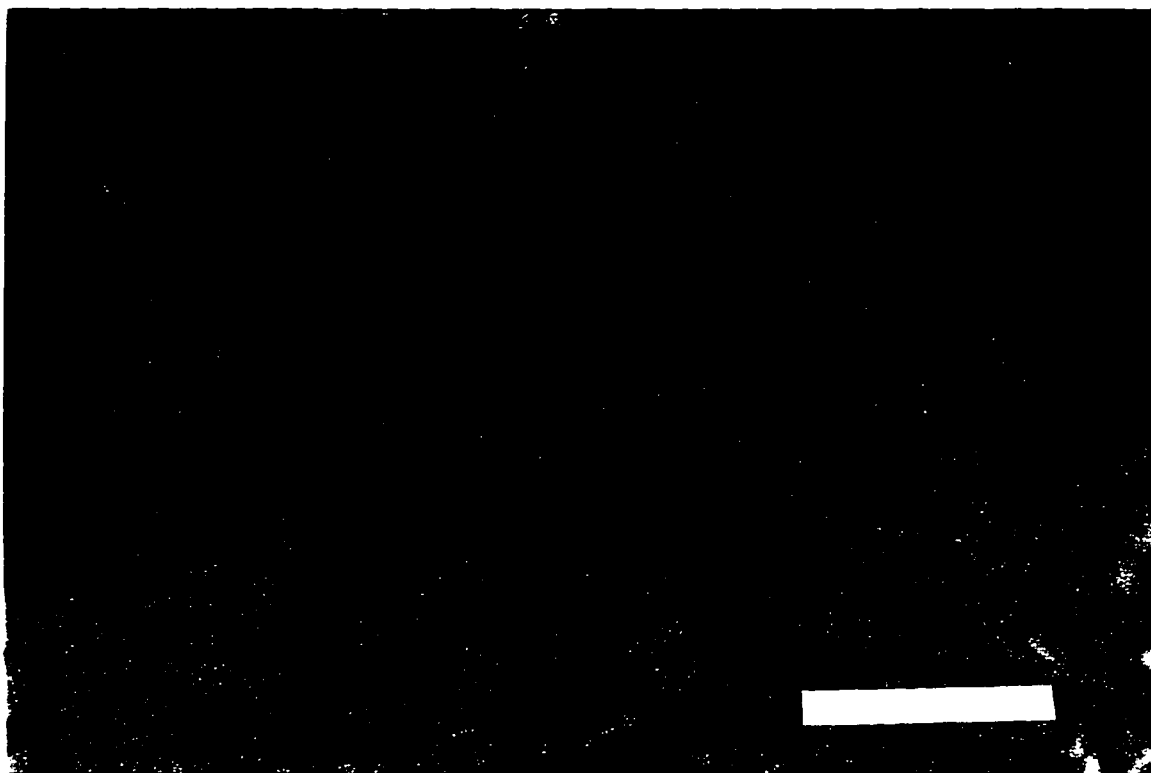


Figure 4-7. Light stereomicrograph of osteoblasts cultured on a 50:50 PLGA film after 7 days in culture. The picture was taken at the edge of the polymer substrate so that individual cells could be seen since the culture at the center of the film was too darkly stained to distinguish individual cells. The stain utilized was Coomassie Brilliant Blue. (Bar equals 500 μm .)

were also observed throughout the cultures at day 14 (pictures not shown) indicating that osteoblasts were piled up in those areas.

Osteoblasts grown on all the substrates tested in this study expressed high ALPase activity throughout the 14 days of the experiment (Fig. 4-8). Compared to TCPS, the 75:25 PLGA and PGA films were the only substrates which had similar ALPase activity results after 7 days in culture. The activities measured for osteoblasts cultured on PLLA and 50:50 PLGA films were significantly smaller ($p < 0.05$). There was a substantial increase ($p < 0.01$) in ALPase activity for osteoblasts cultured on 75:25 PLGA, which compared well to the value for TCPS by day 14. The ALPase activity for osteoblasts cultured on PLLA also increased with time ($p < 0.01$) but its value at day 14 was much lower than the corresponding value for 75:25 PLGA. The ALPase activity for the osteoblasts cultured on 50:50 PLGA and PGA films on day 14 was not different from that on day 7.

There was no significant difference in the amount of collagen synthesized or in the percent of collagen (relative to the total protein) synthesized by osteoblasts cultured on the different substrates (Figs. 4-9 and 4-10). However, the production of collagen by osteoblasts cultured on TCPS decreased ($p < 0.001$) from day 7 to day 14, whereas the amount of synthesized collagen increased ($p < 0.01$) for osteoblasts cultured on PLLA films (Fig. 4-9). Osteoblasts cultured on 75:25 PLGA, 50:50 PLGA, and PGA did not synthesize more collagen over the 14 day time period. The percent of collagen relative to the total protein synthesized by cells cultured on the polymer substrates did not vary with time (Fig. 4-10).

All the polymers degraded to varying degrees over the experimental period (Fig 4-11). PLLA did not degrade significantly over the 14 day period, whereas the weight average molecular weight of 75:25 PLGA significantly decreased ($p < 1 \times 10^{-5}$) from day 0

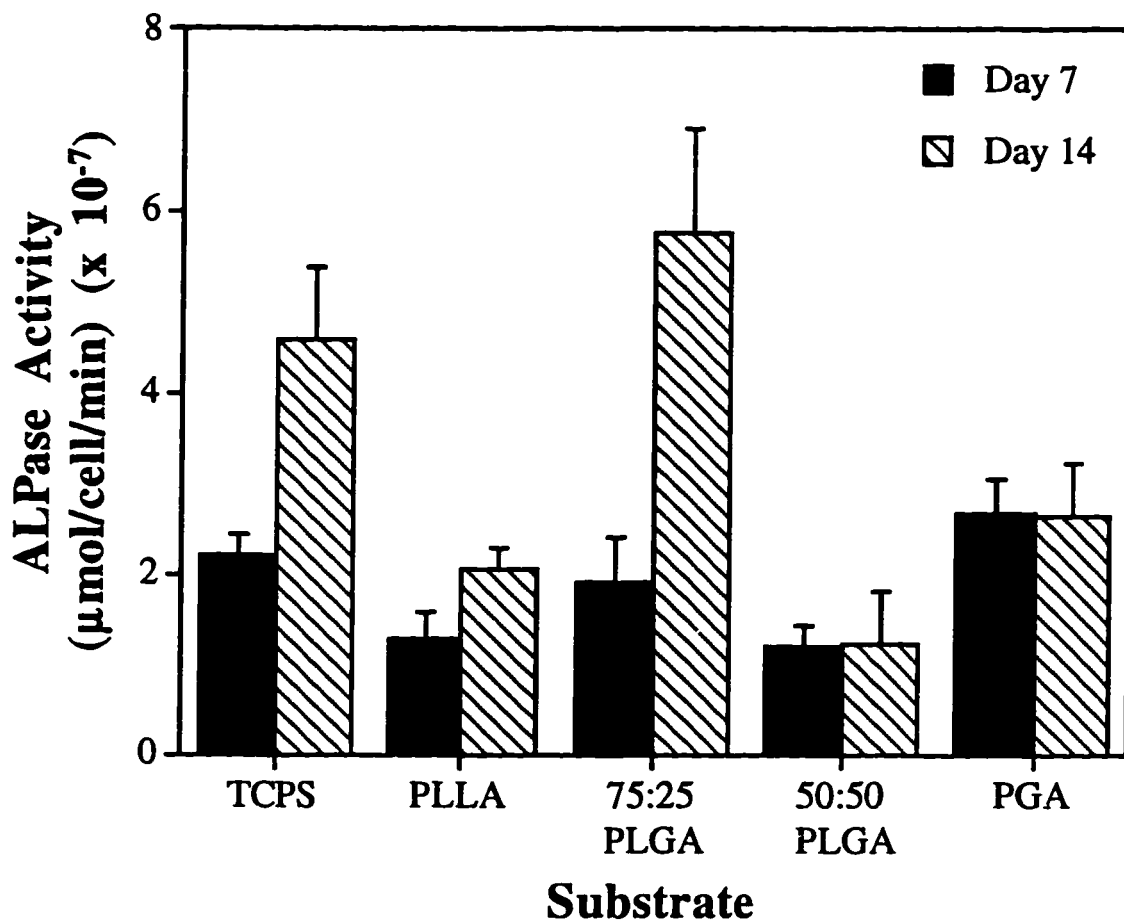


Figure 4-8. ALPase activity expressed by osteoblasts cultured on PLLA, 75:25 PLGA, 50:50 PLGA, PGA, and control TCPS after 7 and 14 days in culture (error bars designate means \pm s.d. for n=3).

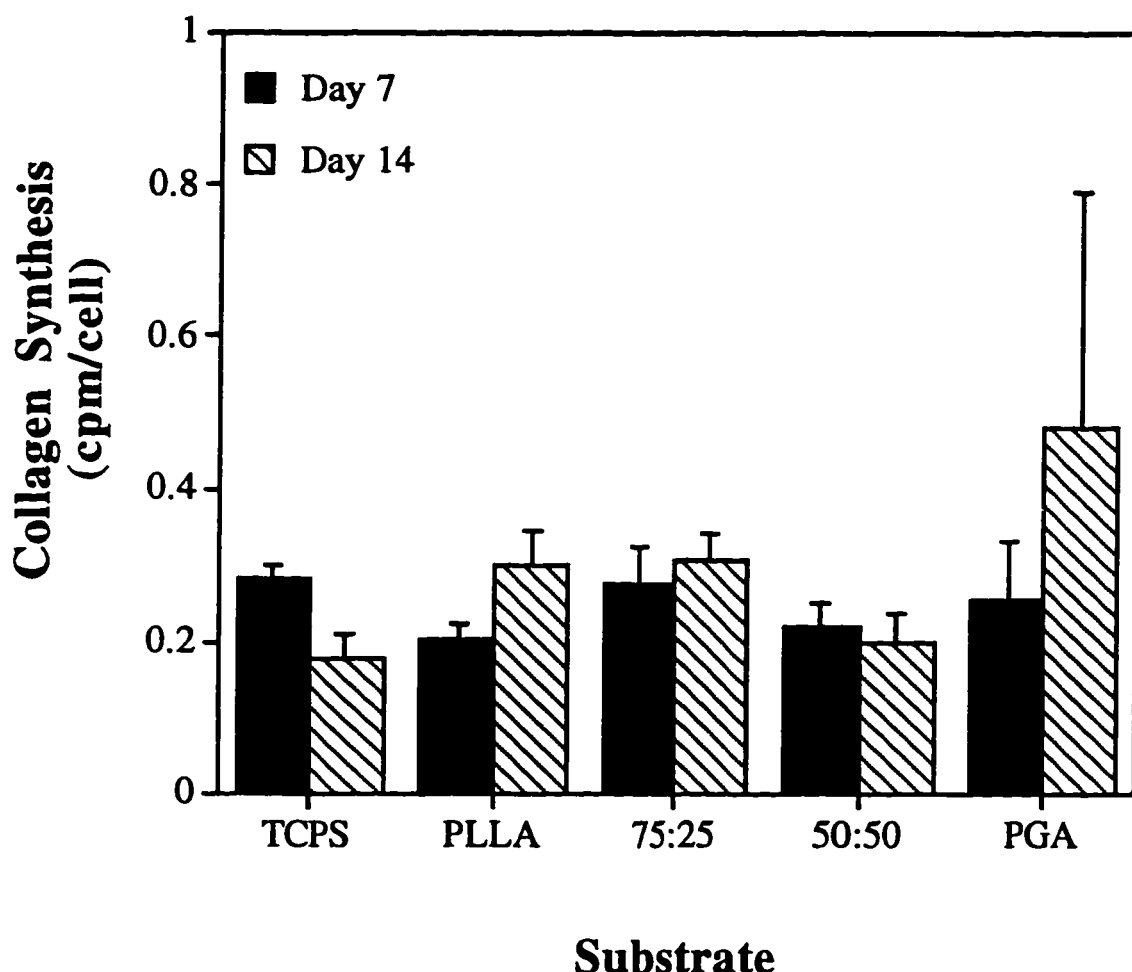


Figure 4-9. Collagen synthesized by osteoblasts cultured on PLLA, 75:25 PLGA, 50:50 PLGA, PGA, and control TCPS during the 24 hr period following 7 and 14 days in culture, expressed as counts per min per cell (error bars designate means \pm s.d. for n=3).

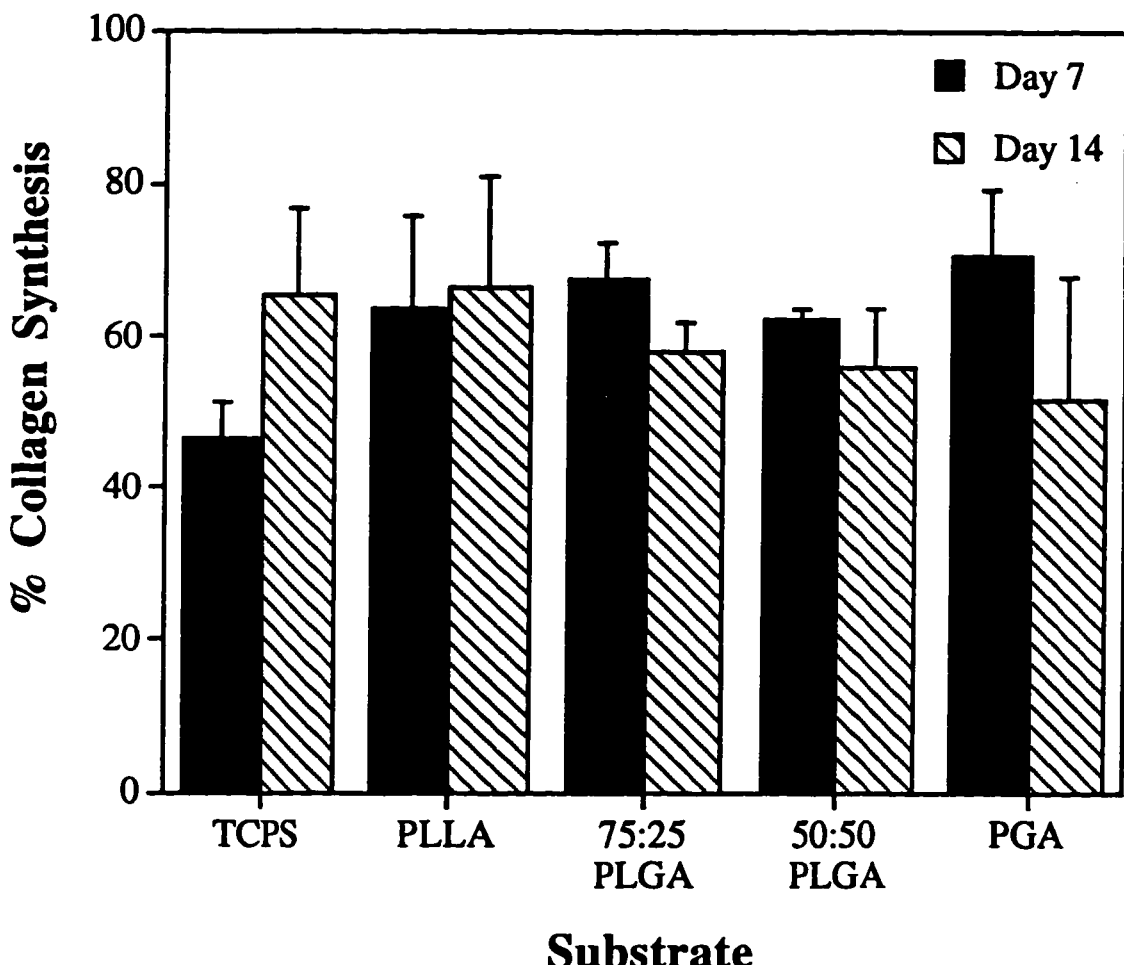


Figure 4-10. Collagen synthesis expressed as percent of total protein synthesized by osteoblasts cultured on PLLA, 75:25 PLGA, 50:50 PLGA, PGA, and control TCPS during the 24 hr period following 7 and 14 days in culture (error bars designate means \pm s.d. for n=3).

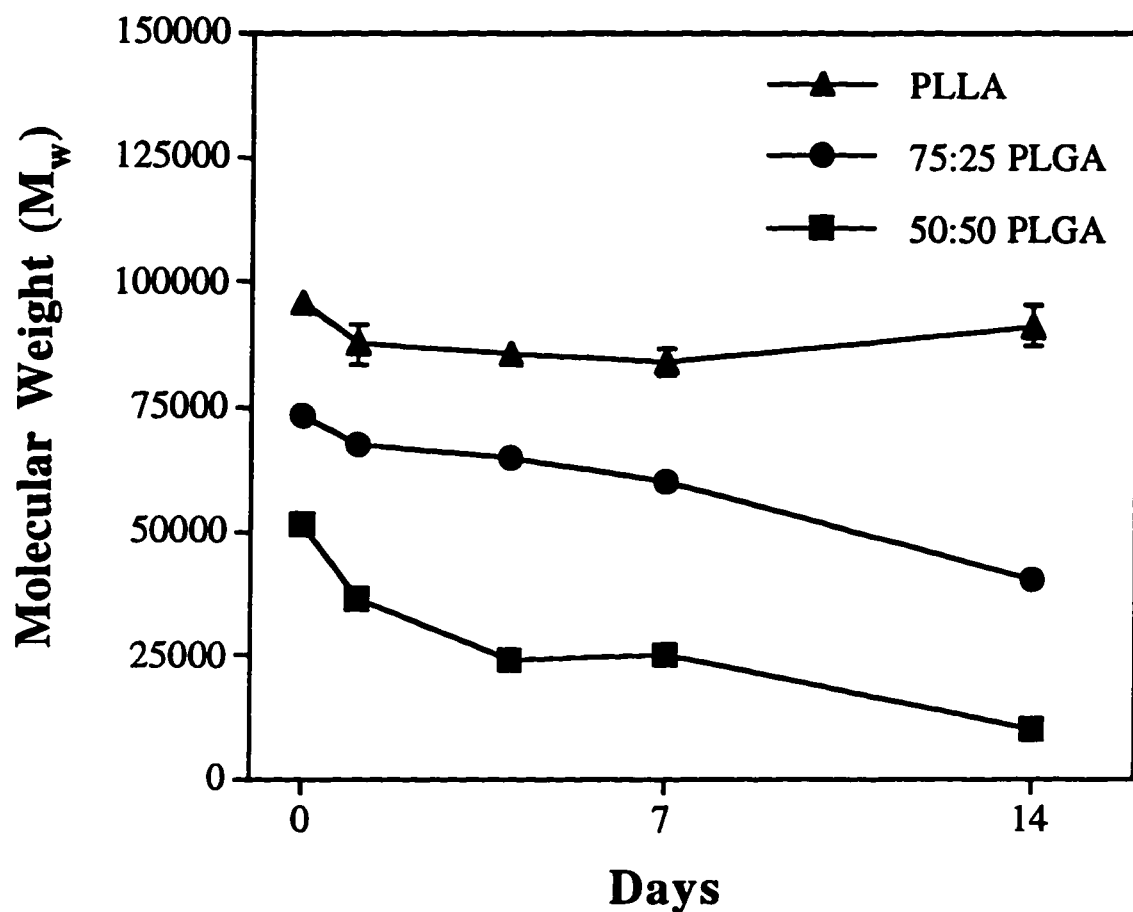


Figure 4-11. Variation in weight average molecular weight, M_w , of PLLA, 75:25 PLGA, and 50:50 PLGA with culture time (error bars designate means \pm s.d. for $n=3$).

to day 14 and the 50:50 PLGA polymer degraded to an even greater extent over the same time period.

4.4 Discussion

Osteoblasts have been cultured on orthopedic biomaterials to evaluate their biocompatibility and to assess the stability of bone-biomaterial interfaces [Puleo et al., 1991; Groessner-Schreiber and Tuan, 1992; Malik et al., 1992; Vrouwenvelder et al., 1992]. In our study, more than 100% attachment of osteoblasts was observed on 50:50 PLGA relative to TCPS after 2 hrs in culture, whereas osteoblasts seeded on orthopedic biomaterials such as poly(methyl methacrylate), stainless steel, a cobalt-chromium-molybdenum alloy, poly(2-hydroxyethyl methacrylate), and a titanium-aluminum-vanadium alloy [Puleo et al., 1991] showed 100% or less osteoblast attachment relative to TCPS after the same time period. Significantly lower percentages of cell attachment (50-60%) to hydroxyapatite and borosilicate glass coverslips have also been observed [Puleo et al., 1991]. Our comparative attachment study was performed after 8 hrs in culture instead of 2 hrs; at this time, we found 87-127% attachment to all the polymer substrates studied (PLLA, 75:25 PLGA, 50:50 PLGA, and PGA) relative to the number of cells attached to TCPS (control substrate).

Osteoblasts grew at the same rate on 50:50 PLGA and TCPS. Similar growth of osteoblast-like MC3T3-E1 cells on these two substrates was observed by other investigators, [Elgendi et al., 1993] although the absolute cell densities in that study were greater. We observed cell densities of $12.6 (\pm 7.8) \times 10^4$ for TCPS and $10.7 (\pm 9.2) \times 10^4$ cells/cm² for 50:50 PLGA after 7 days in culture, whereas cell densities for the osteoblast-like cells grown on TCPS and 50:50 PLGA were 70×10^4 and 60×10^4 cells/cm², respectively [Elgendi et al., 1993]. These differences in proliferation cell

densities are most likely due to the initial seeding density used in the experiments, which was 5.3×10^4 cells/cm² for our study and a much greater 1×10^5 cells/cm² for the study with osteoblast-like cells [Elgendi et al., 1993]. Compared to TCPS, significantly lower ALPase activity was obtained when osteoblasts were grown on 50:50 PLGA ($p < 0.05$) for day 7, whereas no significant differences in ALPase activity were observed for the osteoblast-like cells grown on TCPS and on 50:50 PLGA [Elgendi et al., 1993]. On the other hand, the ALPase activities for osteoblasts grown on 75:25 PLGA and PGA at day 7 were not statistically different in the present study.

Many cell types exhibit an inverse relationship between growth and differentiation *in vitro* [Mooney et al., 1992]. Investigations of osteoblast developmental stages [Arnow et al., 1990; Aubin et al., 1992; Quarles et al., 1992] indicated that as proliferation slowed down, production of ALPase increased. As well, proliferating osteoblasts demonstrated decreased expression of their typical phenotypic activities during periods of rapid growth. As cell replication slowed down, the cells began to produce more ALPase and other markers of osteoblastic phenotype. In our study, osteoblasts cultured on TCPS and 75:25 PLGA also exhibited an increase in ALPase activity simultaneously with a decrease in the rate of cell proliferation. We also measured ALPase activities for osteoblasts cultured on TCPS 30 times higher than that reported for transformed osteoblast cell lines [Quarles et al., 1992] after 2 weeks of culture. This extreme difference in ALPase activities could be due to the difference in the cell types used. Studies with osteoblast-like cells do not necessarily reflect events observed with primary or early passaged osteoblasts [Morey-Holton et al., 1993].

The amount of collagen synthesis per cell remained constant with time for osteoblasts cultured on the polymer substrates (present study), whereas collagen synthesis decreased with time for osteoblasts cultured on TCPS and on orthopedic biomaterials [Puleo et al., 1991]. The enhanced collagen synthesis on the poly(α -hydroxy esters) may

be due to release of degradation products, such as lactic acid and glycolic acid; lactic acid has been shown to stimulate collagen synthesis in wound healing [Clark and Henson, 1988]. Although osteoblasts cultured for 7 days on poly(α -hydroxy esters) displayed 60-70% collagen synthesis relative to total protein synthesis (present study) as compared to 50-55% for osteoblasts cultured on orthopedic biomaterials, [Puleo et al., 1991] the percent of collagen synthesis remained invariant with time for both studies.

A sequence of morphological changes in osteoblasts attached to orthopedic biomaterials over time was demonstrated by Malik et al. [Malik et al., 1992]. Our SEM studies showed similar changes from a rounded morphological shape for osteoblasts during initial (i.e., 4 hrs) attachment to 50:50 PLGA to a flatter and spread cell shape after longer term cultures (i.e., 1 day or longer). In addition, our histology studies verified the polygonal and spindle-like morphology typical of osteoblasts [Bellows et al., 1986; Puleo et al., 1991; Groessner-Schreiber Tuan, 1992; Malik et al., 1992; Vrouwenvelder et al., 1992; Elgendi et al., 1993].

The polymer substrates degraded to varying degrees throughout our study. The PLLA degraded the least because of its high crystallinity and hydrophobicity, [Pistner et al., 1993] but the 50:50 PLGA degraded very rapidly because it is amorphous and more hydrophilic than both PLLA and 75:25 PLGA [Reed Gilding, 1981]. The degradation of PGA was not studied because PGA is only soluble in hexafluoroisopropanol, an extremely toxic chemical. However, from published degradation studies [Chu, 1985] we expect that PGA also degraded substantially during the 14 days of our experiments.

CHAPTER 5

RAT CALVARIAL OSTEOBLAST MIGRATION ON TWO-DIMENSIONAL POLY(α -HYDROXY ESTER) FILMS

5.1 Introduction

Osteoblast migration, in addition to proliferation, is thought to play a key role in endochondral or intramembranous bone formation, bone remodeling, and repair of bone tissue. It is even believed that the first step in bone formation may be the migration of osteoprogenitor cells or osteoblasts to the site, usually in response to a chemotactic factor [Reddi et al., 1988; Rifas et al., 1989; Beck et al., 1991; Yee et al., 1993]. Osteoprogenitor cells and osteoblasts are known to migrate into the epiphyseal growth plate zone during endochondral ossification and eventually ossify the cartilage region [Reddi, 1981; Yaszemski et al., 1996]. In the remodeling of bone, osteoblasts migrate along the haversian canals or into osteoclast resorption bays and lay down new bone matrix [Rifas et al., 1989; Pfeilschifter et al., 1990; Tenenbaum, 1992]. Finally, osteoblasts migrate to injured skeletal sites and eventually ossify the fracture callus, similar to the mechanism which occurs during endochondral ossification [Marden et al., 1990; Sandberg et al., 1993].

Surgical approaches directed toward assisting the repair of bone defects are affected by both the repair and remodeling processes. Autogenous and allogenous bone grafts as well as demineralized bone matrix are all used as osteoinductive scaffolds for assisting bone repair and rely on the migration of osteoblasts to fill and remodel the graft material into host bone [Reddi et al., 1988]. As in natural or grafted bone repair and remodeling, the migration of osteoblasts from bone tissue surrounding the implant site into the polymeric scaffolds will be important for new bone formation and implant stabilization.

Knowledge of osteoblast migration behavior on these polymers *in vitro* will facilitate our understanding of osteoblast migration into the polymer scaffold *in vivo*.

In this study we used both a quantitative and qualitative approach to elucidate the migratory behavior of osteoblasts on biodegradable PLGA films to determine if copolymer composition, isolation procedure, or seeding density have an effect on osteoblast migration and proliferation rate. The migration and proliferation of osteoblasts on the copolymers 75:25 and 85:15 PLGA was investigated by culturing bone tissue or isolated osteoblast colonies of two different seeding densities on the polymer film surfaces.

5.2 Materials and Methods

Materials

The biodegradable polymers used in the experiments were 75:25 PLGA and 85:15 PLGA (Birmingham Polymers, Birmingham, AL). The weight average molecular weights of the polymer films were 75,600 (PI=2.07) for 75:25 PLGA, and 113,800 (PI=2.04) for 85:15 PLGA as measured by gel permeation chromatography (GPC). PI stands for the polydispersity index, and is equal to the ratio of weight average to number average molecular weight. Tissue culture polystyrene (TCPS) of 6-well tissue culture plates (Falcon, Becton Dickinson, NJ) was used as the reference substrate.

Methods

Polymer Preparation

Polymer films were solvent cast onto 1 x 1 inch² glass coverslips by coating them with 0.3 mL of 0.0167 g/mL polymer in chloroform solution. The films were allowed to dry overnight in a laminar flow hood and were subsequently placed under high vacuum (10 mm Hg) for 12 hours to remove any remaining traces of solvent. Uniformity of the films was established by peeling them off the coverslips after being soaked in water for several hours and by scanning electron micrographs that revealed a smooth polymer surface. The polymer coated coverslips were placed into 6-well tissue culture plates and sterilized by exposure to UV light for 1 hour per side.

Osteoblast Isolation and Culture

Osteoblasts were isolated from neonatal (less than 1 day old) Sprague Dawley rat calvaria by an enzymatic digestive process described in chapter 4. For experiments, osteoblasts were cultured in complete media which consisted of DMEM supplemented with 10% FBS, 8 mg/mL GS, 10 mM Na β -glycerol phosphate (Sigma), and 50 μ g/mL L-ascorbic acid (Sigma).

Bone Chip Isolation

Bone chips were isolated from the calvaria of neonatal Sprague Dawley rats. Periosteum- stripped calvaria were stirred in the same enzyme solution mentioned in the Osteoblast Isolation and Culture Section at 37°C for two 20 min digestion periods. The

bone chips were rinsed in phosphate buffered saline (PBS) and cut into circles of approximately $16.4 \pm 1.6 \text{ mm}^2$ ($n=12$) with surgical scissors and the aid of sterile digital calipers.

Cell Migration/Proliferation Assay

Osteoblasts were seeded at either $84,000 \text{ cells/cm}^2$ (high seeding density) or $42,000 \text{ cells/cm}^2$ (low seeding density) in the 3/16 inch diameter center circle of Teflon fences [Pratt et al., 1984] placed on top of the substrates in 6-well plates. The osteoblasts were allowed to attach and proliferate under standard culture conditions. After two days, the Teflon fence was removed, the culture was rinsed with PBS to remove any unattached cells, and fresh media was replaced in the well. The time at which the fence was removed is referred to as day 0. After the fence was removed, osteoblasts were allowed to migrate and proliferate radially from the 3/16 inch initial circular culture for 1, 4, 7, and 14 days. The media was changed every two days.

Bone chips were placed in the center of 75:25 PLGA films. Small steam-sterilized weights were placed on top of the bone chips to prevent them from floating in the media. The weights consisted of short Teflon rods (6 mm in diameter) with stainless steel nuts attached to the tops (total weight = $4.05 \pm 0.06 \text{ g}$, $n=12$). Only the bottom Teflon portion of the weights was in contact with the bone chips. The bone chips were cultured for 1, 4, 7, and 14 days with the weights in place for the entire culture period. During this time, osteoblasts could migrate from the bone tissue onto the polymer films.

Histomorphometric Analysis

At the specified days the cultures were rinsed with PBS, fixed with 10% neutral buffered formalin, and stained with toluidine blue-O (1% w/v) which stains cell nuclei blue. Histomorphometric analysis was utilized to determine the surface area covered by the migrating and proliferating osteoblasts. Digitized images of the stained cultures were taken using an SIT camera (Daje-MTI, Michigan City, IN) equipped with a zoom lens and interfaced to a computer equipped with NIH Image 1.54 analysis software. The cell culture region was manually selected by drawing a line along the migration front and the surface area was calculated by the calibrated software program.

Von Kossa Staining

Von Kossa's method was used to stain bone chip cultures to determine if the cell migration front consisted of calcified tissue. The osteoblast cultures were fixed in 10% neutral buffered formalin for 15 min and rinsed with distilled-deionized water. The fixed samples were then stained with filtered 5% silver nitrate while being exposed to bright daylight for 30 min, and counterstained with filtered 0.5% safranin-O for 30 s. As a result, calcium phosphate deposits stain black and cells pink.

Cell Proliferation

The number of cells that proliferated and migrated from the cell colonies and from the bone chips was determined at days 1, 4, 7, and 14 by the following method. The bone chips and weights were removed from the polymer surfaces prior to cell counting. All cultures were rinsed with PBS, the cells were enzymatically lifted from the surface of the

polymer films, and counted on a Coulter Counter Multisizer (model 0646, Coulter Electronics, Hialeah, FL) using counts between 8.2 and 32 μm .

Confocal Microscopy

The osteoblast cultures on the polymer films were fluorescently stained with 2', 7'-bis-(2-carboxyethyl)-5-(and-6)-carboxyfluorescein, acetoxyethyl ester (BCECF-AM) and cell population migration characteristics were examined using a confocal microscope (Zeiss LSM Axiovert, Carl Zeiss, Germany). Cultures were incubated with 5 mg/mL BCECF-AM in complete media for 1 hour. Following a rinse in PBS and replacement of fresh media, the cell cultures were ready for confocal microscopic viewing. Depth projection micrographs were constructed from 16 horizontal image sections through the cultures.

Gel Permeation Chromatography

The number and weight average molecular weights of 75:25 PLGA were determined over the course of the experiment by gel permeation chromatography (Waters, Milford, MA) equipped with a differential refractometer (Waters, Series 410). The cells were removed from the polymers by trypsinization and rinsed with distilled-deionized water. The area of the polymer films that was in contact with the cells and bone chips was cut out, dissolved in HPLC grade tetrahydrofuran, and filtered to remove any insoluble components. The solubilized samples were then eluted through a Phenogel 10 Linear column (series 26973, 300 x 7.8 mm, Phenomenex, Torrance, CA) at a flow rate of 1 mL/min. Polystyrene standards were used to construct a primary calibration curve.

Statistical Analysis

All experiments were run in triplicates and expressed as mean \pm standard deviation except for the bone chip area for day 0. The bone chip area for day 0 was calculated as the mean of the 12 bone chips used for the other time points since the bone chip sizes did not change over the course of the study. Single-factor analysis of variance (ANOVA) was employed to assess statistical significance of the results. Scheffé's method was used for multiple comparison tests at a significance level of $p < 0.05$.

5.3 Results

Sharply defined circular osteoblast colonies were achieved on all the substrates by seeding osteoblasts into the center of Teflon fences and culturing for 2 days before removal of the fences (Fig. 5-1). The initial substrate surface area covered by the cells for each sample type was reproducible when measured immediately after removal of the fence; however, this initial area did not always correspond exactly to the area (17.8 mm^2) of the center circle in the fence (Table 5-1). Following removal of the Teflon fences, osteoblasts migrated radially, as well as proliferated, to produce larger circular cultures over time. Figure 5-2 shows a representative stained high density ($84,000 \text{ cells/cm}^2$) seeded culture preparation after 14 days of culture. Osteoblasts also migrated directly from bone chips onto the polymer films (Fig. 5-3).

Observations of all the stained cultures as well as confocal micrographs (Fig. 5-4) revealed that the perimeter of the culture area, or migration front, consisted of a monolayer of osteoblasts. In contrast, osteoblasts piled up to form multilayers in the interior of the circular cultures. This resulted in the darker staining in the middle of the cultures, behind the cell migration front (Figs. 5-2 & 5-3). Confocal depth projection micrographs of



Figure 5-1. Light micrograph of isolated osteoblast culture on a 75:25 PLGA film for two days, immediately after removal of Teflon fence (day 0). Stain: Toluidine blue-O. Magnification: 4.48 X.

Substrate	Initial Seeding Density (cells/cm ²)	Surface Area * (mm ²)	Number of Experiments
TCPS	84,000	21.9 ± 2.4	3
85:15 PLGA	84,000	23.3 ± 2.9	3
75:25 PLGA	84,000	24.4 ± 1.2	3
75:25 PLGA	42,000	18.0 ± 2.2	3
75:25 PLGA	(Bone Chips)	16.4 ± 1.6	12

* mean ± s.d.

Table 5-1. Surface area of osteoblast cultures at the beginning of the migration/proliferation experiments following 2 days of culture within the restricted 17.8 mm² center circle of the Teflon fence for different seeding densities and substrates tested and including the area of the bone chips plated on the 75:25 PLGA films.



Figure 5-2. Light micrograph of isolated osteoblast culture on a 75:25 PLGA film cultured for 14 days post removal of the Teflon fence. Stain: Toluidine blue-O. Magnification: 4.48 X.

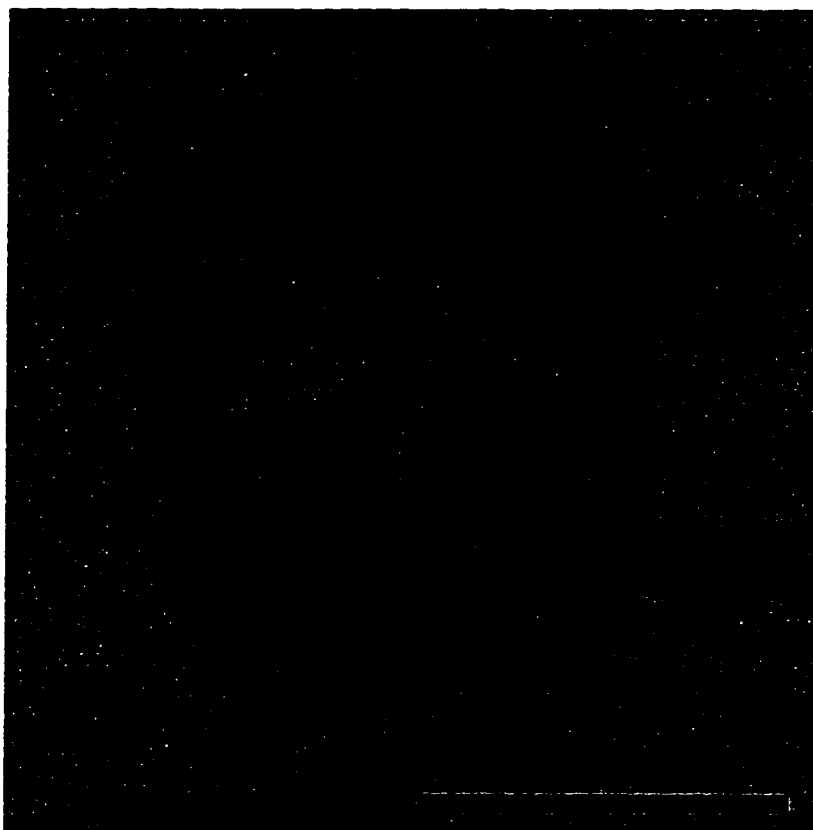


Figure 5-3. Osteoblast culture resulting from cell migration and proliferation from a bone chip placed on a 75:25 PLGA film. During the cell culture period the bone chip was in the center region area devoid of cells. While migrating the cells grew around the bone chip for 14 days. The darker stained regions suggest cell piling adjacent to the bone chip. Stain: Toluidine blue-O; Bar = 5 mm.

osteoblasts from bone chips also show that the cell migration front consisted of a monolayer of osteoblasts and that osteoblasts closer to the bone chip were multilayered (Fig. 5-5). Only the bone chips stained black with von Kossa stain, providing evidence that the migration took place by individual osteoblasts (stained pink with counter stain) and not as a calcified tissue migration front (Fig. 5-6).

Significant osteoblast migration was observed on all the substrates studied using the same initial high cell seeding density (Fig. 5-7). At the beginning of the experiment, osteoblasts seeded at a high density on 75:25 PLGA covered a surface area of $24.4 \pm 1.2 \text{ mm}^2$ (Table 5-1). After 14 days in culture, the surface area coverage had increased 8.9 ± 1.3 times (Fig. 5-7) to a surface area of $217.0 \pm 29.6 \text{ mm}^2$. This culture area at day 14 for 75:25 PLGA was similar to the area covered by osteoblasts grown on 85:15 PLGA, but was significantly ($p < 0.05$) greater than the area covered by osteoblast populations cultured on TCPS for the same time period. By 14 days, the cell culture area had increased 6.8 ± 0.8 times above its initial value for osteoblasts cultured on TCPS and 8.7 ± 1.2 times for the 85:15 PLGA substrate. This increase in culture area corresponds to a rate of $9.15 \pm 0.42 \text{ mm}^2/\text{day}$ for osteoblasts cultured on TCPS, $12.95 \pm 0.50 \text{ mm}^2/\text{day}$ for 85:15 PLGA films, and $14.13 \pm 0.71 \text{ mm}^2/\text{day}$ for 75:25 PLGA films, when a linear regression is fitted through the points in figure 5-7.

Initial osteoblast seeding density had an effect on the rate of cell migration and proliferation (Fig. 5-8). Osteoblast colonies formed by seeding a lower density ($42,000 \text{ cells/cm}^2$) of isolated osteoblasts resulted in cell cultures covering smaller ($p < 0.05$) surface areas at day 14 as compared to surface area results obtained with the higher density seeded cultures. This increase in area for lower seeding density cultures corresponded to a rate of $4.89 \pm 0.32 \text{ mm}^2/\text{day}$. The increase in surface area covered by osteoblasts that migrated from the bone chips onto 75:25 PLGA was similar to the results for the low cell density seeded cultures, resulting in a rate of $6.03 \pm 0.51 \text{ mm}^2/\text{day}$. By 14 days, surface

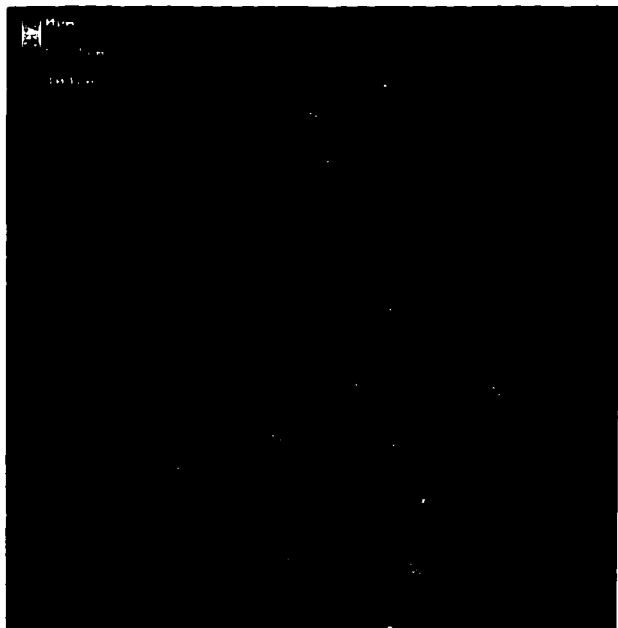


Figure 5-4. Confocal depth coding micrograph of the migration front of a high density (initially seeded with $84,000 \text{ cells/cm}^2$) osteoblast culture on a 75:25 PLGA film, cultured for 6 days post removal of the Teflon fence. The migration front consists of a monolayer of osteoblasts.

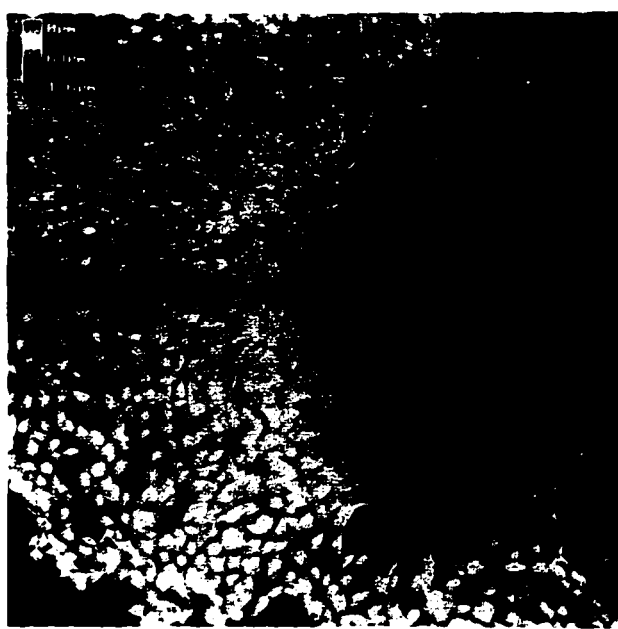


Figure 5-5. Confocal depth coding micrograph of osteoblasts that migrated from a bone chip cultured for 6 days on 75:25 PLGA film. The culture consists of a monolayer of osteoblasts at the migration front but becomes multilayered closer to the bone chip.



Figure 5-6. Light micrograph of osteoblasts that migrated from a bone chip cultured for 15 days on a 75:25 PLGA film. Stain: von Kossa. Magnification: 10 X.

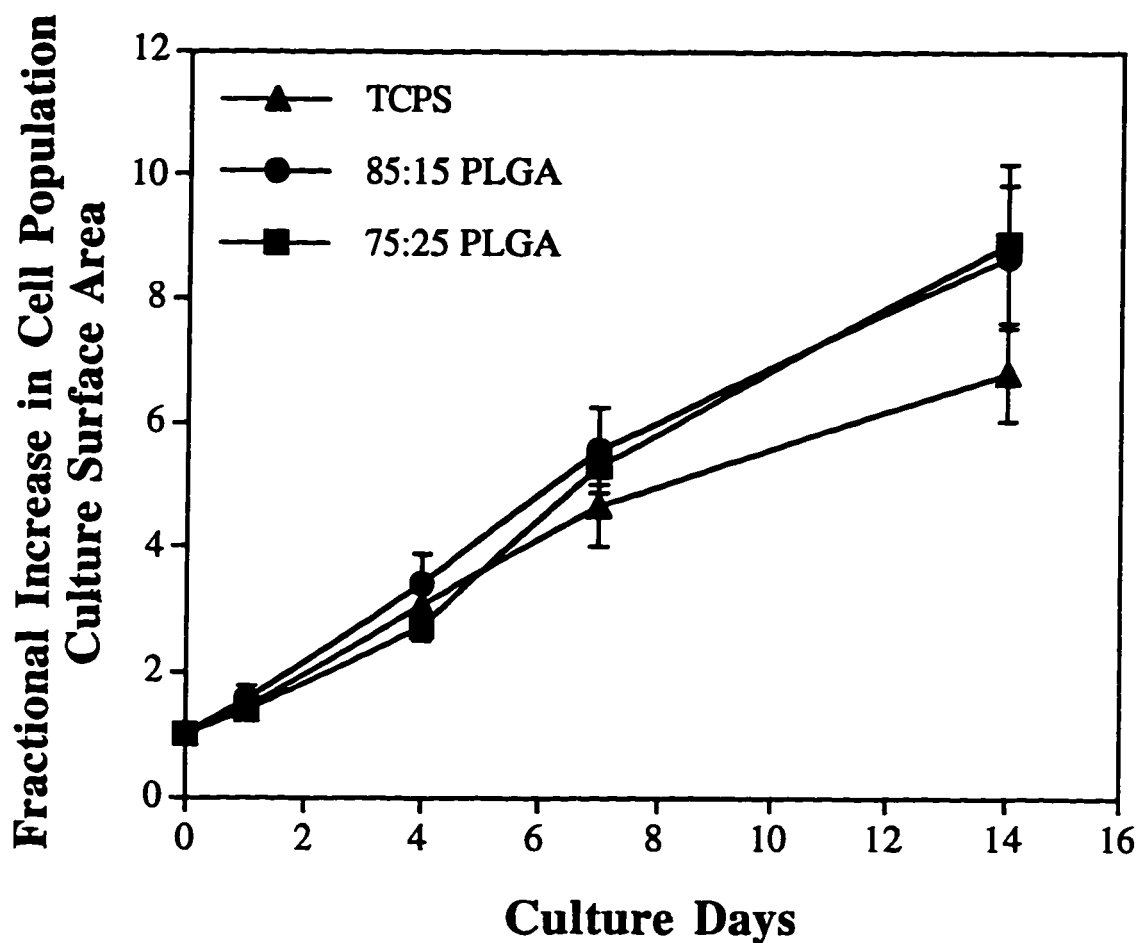


Figure 5-7. Fractional increase in osteoblast population culture surface area on 85:15 PLGA, 75:25 PLGA, and tissue culture polystyrene controls (TCPS) as a function of culture time. All osteoblast cultures were achieved by seeding 84,000 cells/cm² in the center area (17.8 mm²) of the Teflon fences. Data are means \pm s.d., n=3. The rate of increase in culture surface area was not different for osteoblasts grown on 75:25 and 85:15 PLGA, but was slightly slower ($p < 0.05$) for osteoblasts grown on TCPS when compared to the results for 75:25 PLGA.

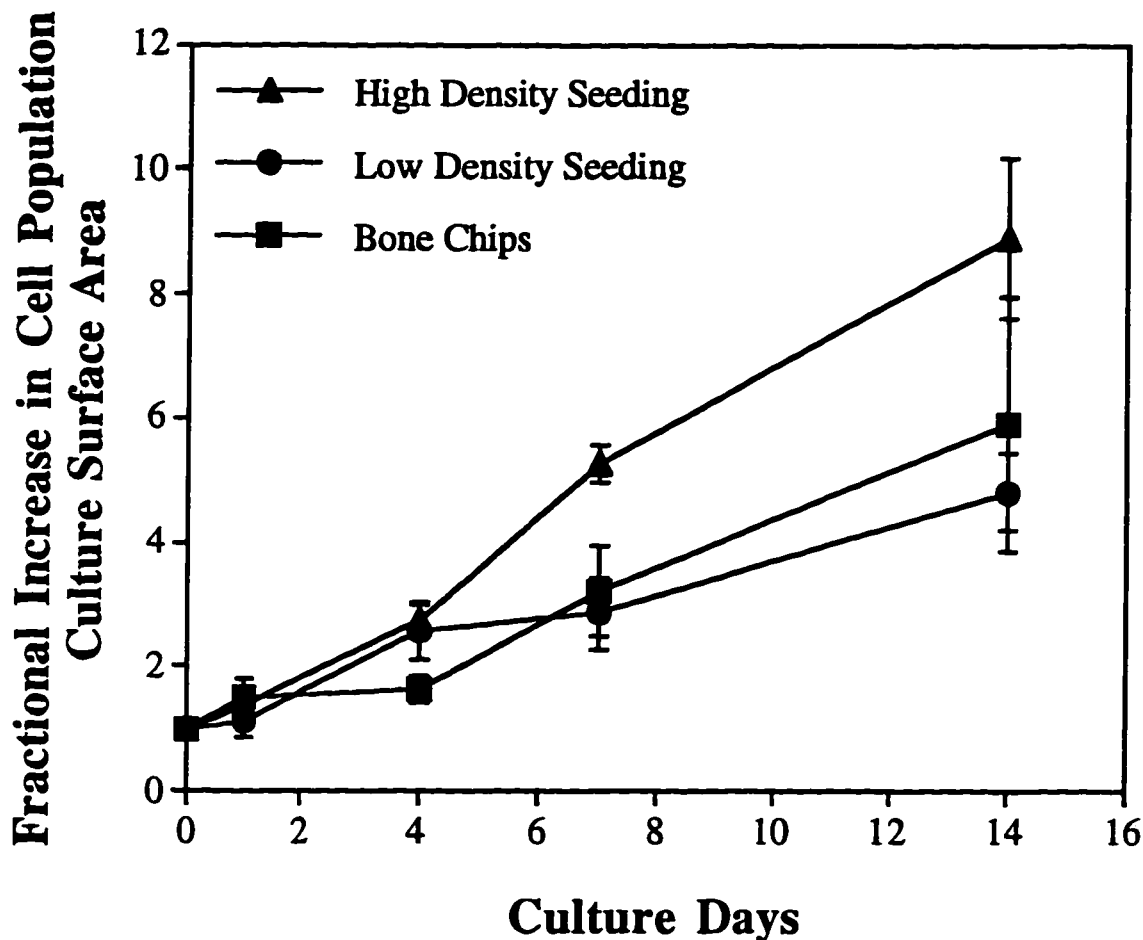


Figure 5-8. Fractional increase in osteoblast population culture surface area on 75:25 PLGA films as a function of culture time. Cell cultures achieved by seeding either 84,000 cells/cm² (high density seeding) or 42,000 cells/cm² (low density seeding) onto the polymer substrates with circular Teflon fences in place or by plating bone chips directly on the substrates. Data are means \pm s.d., n=3. The rate of increase in culture surface area for the high seeding density cultures was significantly greater ($p < 0.05$) than that for the low seeding density and bone chip cultures.

area coverage by the cultures had increased by 4.8 ± 0.6 and 5.9 ± 2.1 times for lower seeding density cultures and cultures originating from bone chips, respectively.

In addition to migration, osteoblasts continued to proliferate in all the cultures over the entire study period (Fig. 5-9). Proliferation rates of $5,100 \pm 600$ cells/day for the bone chip cultures, $8,300 \pm 700$ cells/day for the low density seeded cultures, and $9,900 \pm 600$ cells/day for the high density seeded cultures were obtained when linear regressions were fitted through the points in Figure 5-9. The number of cells that proliferated on 75:25 PLGA were similar for the high and low density seeded cultures throughout the study period. However, the number of cells that migrated and proliferated from the bone chips on the 75:25 PLGA was only similar to the low density cultures at days 4 and 7 and less ($p < 0.05$) than the number of cells that migrated from the high and low density seeded cultures on that same substrate after 14 days in culture. When the number of cells in the cultures are normalized to the culture area, the cell density in the colonies leveled off after an initial increase between 0 and 4 days (Fig. 5-10).

The molecular weight of the 75:25 PLGA substrates was monitored over the period of the study and did not decrease appreciably. The weight average molecular weight of all the 75:25 PLGA polymer films decreased by approximately 4 % by day 14. The polymer degradation rate did not depend on whether isolated osteoblasts or bone chips were cultured on the films, or on the seeding density of the isolated cell cultures (data shown in appendix, Fig. 5-11).

5.4 Discussion

Osteoblast migration and proliferation on poly(α -hydroxy esters) could play an important role in the successful seeding of porous poly(α -hydroxy ester) foam implants [Thomson et al., 1995] with cellular components and stabilization of these devices into *in*

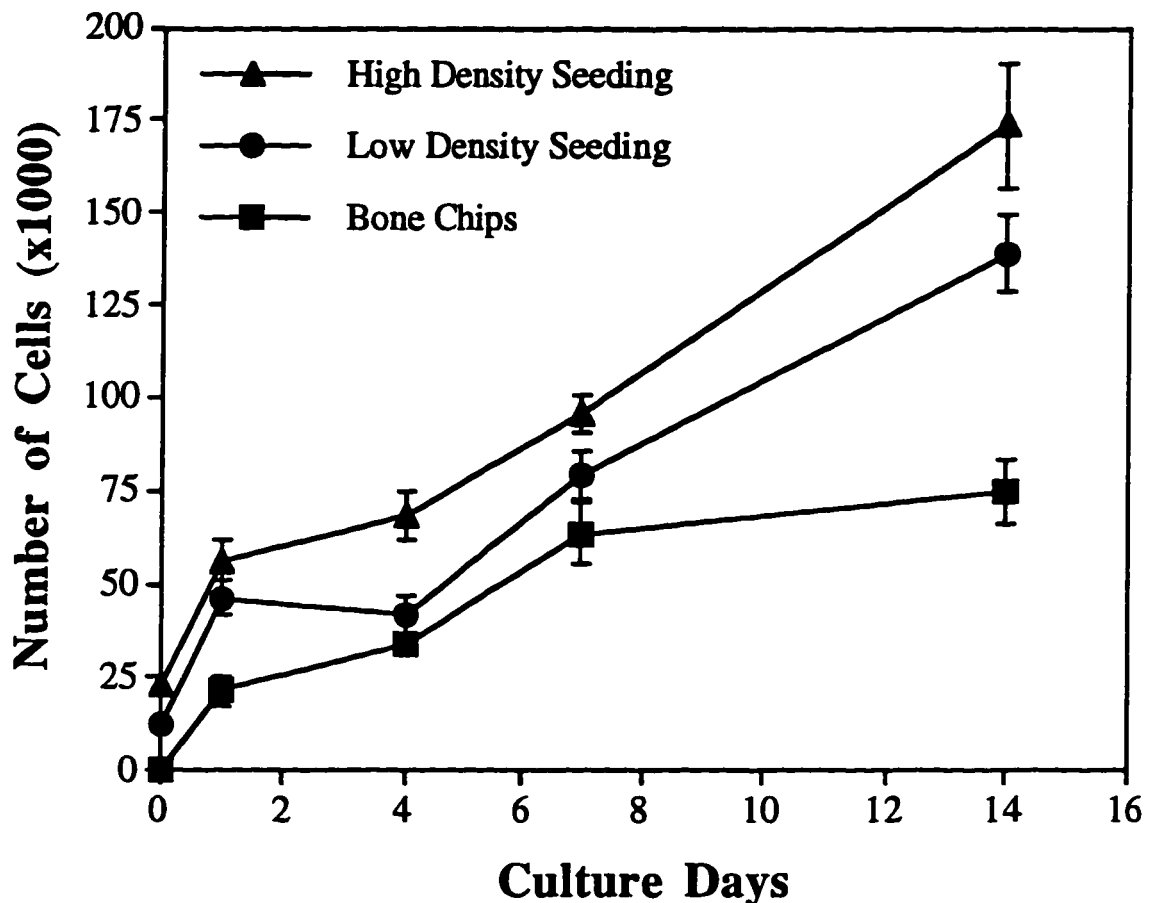


Figure 5-9. Osteoblast proliferation on 75:25 PLGA films as a function of culture time. Results are shown for preparations achieved by seeding either 84,000 cells/cm² (high density seeding) or 42,000 cells/cm² (low density seeding) onto the polymer substrates with circular Teflon fences in place or by plating bone chips directly on the substrates. Data are means \pm s.d., n=3. The proliferation rate for osteoblasts arising from the bone chip cultures was significantly less ($p < 0.05$) than that for the low and high density seeded cultures.

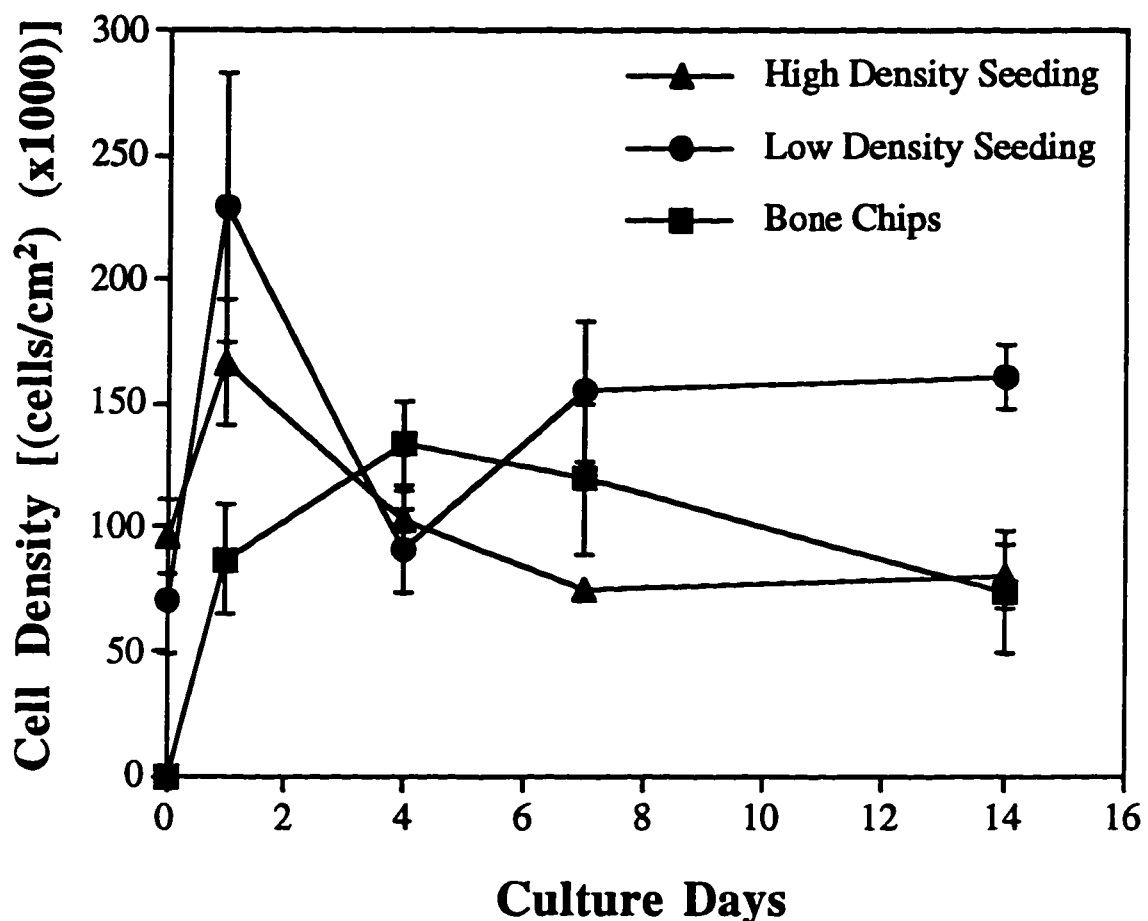


Figure 5-10. Cell densities obtained by dividing the number of cells in the cultures by the culture surface area for osteoblast cultures on 75:25 PLGA films as a function of time. Cell cultures were achieved by seeding 84,000 cells/cm² (high density seeding) or 42,000 cells/cm² (low density seeding) onto the polymer substrates with circular Teflon fences in place or by plating bone chips directly on the substrates. Data are means \pm s.d., n=3.

vivo sites. Our results have shown that osteoblasts, from both isolated osteoblast cultures and from bone tissue, readily migrate over the polymer films. This migration occurred initially as a monolayer of individual cells as seen in the migration fronts of the osteoblast cultures studied (Figs. 5-2 through 5-6). Multi-cell layers were observed in the interior of the cultures resulting from the proliferation and piling up of these non-contact inhibited cells (Figs. 5-2, 5-3, 5-5, and 5-6).

The rate of osteoblast migration did not depend on the PLGA copolymer composition used in this study. This result was not unexpected since it has been demonstrated that cellular migration (or movement speed) is greatly dependent on the adhesive interactions between cells and substratum, and the study described in chapter 4 has shown that osteoblast attachment was not greatly affected by the type of poly(α -hydroxy ester) substrate.

The osteoblast seeding density (or initial cell density) had an effect on the rate that surface area coverage by the cell populations increased. This could have resulted from a difference in the number of cells actively participating in the migration front. At the time the Teflon fences were removed (day 0) the cell densities of the isolated cultures on 75:25 PLGA for high and low seeding densities were $95,900 \pm 15,000$ cells/cm² and $70,700 \pm 21,700$ cells/cm² respectively. Given that a monolayer of osteoblasts contains approximately 53,000 cells/cm² (chapter 4) the initial preparation for the high density cultures were close to a bilayer of cells at day 0; this was not the case for the low density cultures. The differences in initial areas of the isolated cell cultures (Table 5-1) indicate that the osteoblast colonies created by seeding a high density of cells began to migrate under the edge of the fence prior to the fence removal (initial areas are greater than area created by the fence, 17.8 cm²), whereas the colonies created by the low seeding density were confined within the boundaries of the fence. It is possible that, when the fences were removed, osteoblasts from the bilayer of the high density cultures moved to the migration front on the

substrate surface to create a more densely packed migration front for the high density seeded cultures. Cells in low density cultures usually exhibit a random walk behavior [Dunn and Brown, 1987; Lauffenburger, 1991; Stokes and Lauffenburger, 1991; Lee et al., 1994] and less movement in a unilateral direction. However, when the cellular environment is more densely packed with cells in one region than another, there will be more cell-cell collisions in the densely packed region and less overall movement there. The overall result will be a greater cellular movement away from the region more densely packed with cells, or in the outwardly radial direction in the case of the more-densely-packed migration fronts. Conversely, in the less-densely-packed monolayer of cells present in the migration front of the lower initial seeding density cultures, individual cells could exhibit random walk behavior, resulting in lower overall cell population movement in the radial direction.

The same situation could be true for the osteoblasts that migrated to the substrates from bone chips. Osteoblasts must first escape from the tissue matrix prior to migrating on the substrates. The rate of cell escape from the bone tissue may be more similar to the rate at which cells migrate outwardly at the forefront of the lower seeding density cultures than the higher seeding density cultures. This could explain the similar rates of increase in surface area covered by the cell populations for the low seeding density cultures and bone chips. The lower rate of increase in cell population surface coverage for the bone chip cultures compared to the high seeding density cultures could also be due to a high probability that some edges of the bone chips were not touching the substrate as evidenced by the resulting irregular shaped osteoblast cultures produced by the bone chips (Fig. 5-3). It is also very probable that fewer cells are present on the outer edge of a bone chip than are contained in the isolated high density seeded cultures because the bone chip also contains extracellular matrix components.

Even though osteoblasts are not contact-inhibited cells, their growth slows down when they are confined to a given area and are forced to proliferate upwards (chapter 4). In the present study, the culture area was not confined and, therefore, the proliferation rate did not decrease over the study period. This observation may lend itself useful in the interpretation of how osteoblasts might grow into three-dimensional scaffolds having unlimited surface area available, at least initially.

The use of collagenase in the isolation method to obtain the osteoblasts and to create single cell suspensions prior to cell seeding might have temporarily damaged their plasma membrane and subsequently affected their function or mobility [Wong, 1990]. Moreover, the passaging of osteoblasts prior to seeding could explain the differences observed in the proliferation rates for the bone chip cultures and the cultures formed by isolated cell colonies.

A lower cell proliferation rate could result in a lower rate of culture area growth as was previously demonstrated with contact-inhibited cells [Zygourakis et al., 1991]. Therefore, the slower rate of proliferation for the bone chips could account for the slower rate of cell population surface area increase for these cell preparations. Conversely, either migration or motility can also affect cell proliferation rates [Barrandon and Green, 1987]. For example, greater rates in migration can result in increased cellular proliferation. The slower proliferation rate for the osteoblasts obtained from the bone chips could be due to slower cell migration rates.

When the number of cells in the cultures were normalized with respect to the culture area, cell density (cells/cm^2) increased between days 0 and 1 for the isolated osteoblast cultures and between days 0 and 4 for osteoblasts obtained from bone chips. This initial burst in cell density was caused by the accelerated cell growth (Fig. 5-9). Removal of the Teflon fence suddenly exposed the cells to available surface area for migration which may account for this burst of cell proliferation.

The weight average molecular weight of the 75:25 PLGA films used in this study decreased by only 4% from the solvent casted substrates to those obtained after the 14 day culture period. With such a slow degradation rate and the fact that the media was changed every two days, we do not expect that significant amounts of degradation products were present in the culture media to affect the cell migration and proliferation. Studies to investigate the effects of long-term degradation products on osteoblast function are currently in progress in our laboratory.

The two-dimensional studies reported here serve as models for the migration of osteoblasts into 3-dimensional polymer scaffolds *in vitro* and for the migration of osteoblasts into implant polymer scaffolds from the surrounding bone *in vivo*. Osteoblast migration is needed to achieve an even distribution of bone forming cells throughout implant polymer scaffolds, a requirement crucial in new bone formation and integration of implants into surrounding bone tissue.

CHAPTER 6

RAT MARROW OSTEOBLAST CULTURE IN THREE-DIMENSIONAL POLY(α -HYDROXY ESTER) FOAMS

6.1 Introduction

Two-dimensional cultures, as described in the previous two chapters, were necessary to establish the potential for using poly(α -hydroxy esters) as supportive material for osteoblast growth and function, but they are not the ideal form for transplanting into defect sites. Skeletal defects range in size and shape and require a 3-D graft material to fill or replace the missing tissue. Poly(α -hydroxy esters) can be fabricated into 3-D foams which can serve as a supportive scaffold for the culture and transplantation of osteoblasts[Thomson et al., 1995] and have the potential to fill skeletal defects of various sizes and shapes. These poly(α -hydroxy ester) foams have already been shown to allow for the penetration of vascular tissue[Wake et al., 1994] which will be essential to support the metabolic needs of the transplanted cells. Osteoblasts should populate the constructs by proliferation of the transplanted cells and the migration of cells into the construct from the surrounding tissue while the polymer scaffold gradually degrades. Eventually the construct will be filled with calcified extracellular matrix secreted by the osteoblasts and devoid of the synthetic biodegradable polymer.

An investigation of the effects of polymer foam morphology and culture conditions on cell proliferation and function was needed to elucidate the important parameters in the design of an *in vitro* osteoblast/foam culture system before osteoblast transplantation can be attempted *in vivo*. This is the focus of the present study. Rat stromal osteoblasts have been seeded onto highly porous PLGA foams with different pore sizes and cell seeding densities and cultured over a 56 day period. This study addresses 1) whether polymer

foam pore size in the range of 150-710 μm affects osteoblast proliferation and function *in vitro*, 2) whether osteoblast seeding density on polymer foams affects cell attachment, proliferation and function *in vitro* and 3) whether a 3-D osseous tissue can be formed by culturing osteoblasts in polymer foams *in vitro*.

6.2 Materials and Methods

Polymer foam fabrication

Polymer foams of three different pore sizes were fabricated by a solvent-casting particulate-leaching technique with NaCl as the leachable component [Mikos et al., 1994]. NaCl was sieved into particles ranging in diameter from 150-300, 300-500, or 500-710 μm and combined with 75:25 PLGA (Birmingham Polymers, Birmingham, AL) dissolved in chloroform to make 90% porous foams of various pore sizes. The foams were approximately 1.9 mm thick and cut into 7 mm diameter discs. They were stored under vacuum until use. Prior to cell seeding, the foams were pre-wetted with ethanol for 30 min to sterilize and enhance their water uptake [Mikos et al., 1994]. The ethanol was removed by soaking with agitation for 1 hour in 3 changes of phosphate buffered saline (PBS), and then for 3 hours in two changes of media.

Stromal osteoblast isolation, seeding, and culture

Stromal osteoblastic cells were obtained from the marrow of young adult male (6 weeks old, 150-170 g) Sprague Dawley rats [Maniatopoulos et al., 1988]. Following euthanasia by ethyl ether inhalation, femora were aseptically excised, cleaned of soft tissue, and washed in Dulbecco's Modified Eagle medium (DMEM) (Life Technologies, Grand

Island, NY) containing 250 µg/mL gentamicin sulfate (GS) (Sigma Chemical, St. Louis, MO). This concentration of antibiotics is 10 times the normal amount used in cell culture and was used as a precautionary measure to avoid contamination during the femora harvest. The metaphyseal ends were then cut off and the marrow was flushed from the midshaft with 5 mL of primary media (DMEM containing 10% fetal bovine serum (FBS) (Hyclone, Logan, Utah), and 25 µg/mL GS) using a syringe equipped with a 22 gauge needle and collected in a sterile petri dish. Cell clumps were broken up by repeatedly pipetting the cell suspension. The cells were then centrifuged at 400 g for 10 min. The resulting cell pellets were resuspended in 12 mL primary media and plated in a T-75 flask (cells from 2 femurs per flask). After 3 days, hematopoietic cells and other unattached cells were removed from the flasks by repeated washes with PBS. When confluent monolayers were reached (yielding approximately 2×10^6 cells/femur) the cells were enzymatically lifted from the flask using a 625 µg/mL solution of trypsin (enzyme cocktail recipe described in chapter 6). The cells were concentrated by centrifugation at 400g for 10 min and resuspended in a known amount of media. Cells were counted by Coulter Counter and diluted to concentrations of either 56,587,000 cells/mL (high density) or 17,525,000 cells/mL (low density) in complete media [consisting of DMEM supplemented with 10% FBS, 8 µg/mL GS, 10 mM Na β-glycerol phosphate (Sigma), and 50 µg/mL L-ascorbic acid (Sigma)] containing 10 nM dexamethasone (Sigma) [Cheng et al., 1994; Rickard et al., 1994]. Aliquots of 15 µL of either the high or the low density cell suspensions were seeded onto the top of prewetted foams placed in the wells of 24 well plates, resulting in a seeding density of 22.1×10^5 cell/cm² and 6.83×10^5 cells/cm² (or 849,000 and 263,000 cells/foam), respectively, when normalized to the top surface area of the foams. The foams were left undisturbed in an incubator for 3 hours to allow the cells to attach to the foams, after which time an additional 1 mL of complete media containing 10 nM Dexamethasone was added to each well. Medium was changed every 2-3 days. Osteoblasts were also

seeded into 35 mm tissue culture polystyrene (TCPS) dishes as a conventional 2-D control culture to monitor the functionality of the cells. The osteoblasts were seeded at a density of 2.1×10^4 cells/cm² in the TCPS dishes and used as a comparison for the alkaline phosphatase activity and qualitatively assessed for mineralization.

DNA assay

Cell numbers were determined by a fluorometric quantification of DNA in the foams by an assay adapted from West et al. [1985]. After 1, 7, 14, 28, and 56 days in culture, the foams and 2-D control cultures were harvested by rinsing with PBS and freezing at -80°C until assayed. Cell standards were prepared and frozen at -80°C as described. First, a stock solution of rat marrow osteoblasts was prepared by trypsinizing confluent monolayers of cells and resuspending them in DMEM to a final concentration of 10^6 cells/mL. Aliquots of 25-625 µL of the stock cell suspension were centrifuged at 400g for 10 min, washed once in PBS, and the resulting cell pellets (cell standards) were stored frozen at -80°C. DNA standards were prepared at the time of the assay from a stock of DNA solution. The aqueous stock solution of highly polymerized calf thymus DNA (type I, Sigma) was prepared by adjusting it spectrophotically to a concentration of 50 µg/mL (50 µg of DNA in 1.0 mL distilled H₂O produces 1.0 absorbance unit across a 1.0-cm light path at 260 nm). Aliquots of the DNA stock solution ranging from 0 - 160 µL were used as DNA standards. After thawing, the foams were homogenized in 1.4 mL of cold 10 mM ethylenediaminetetraacetic acid (EDTA) solution (pH 12.3), and the cell layers of the 2-D control cultures were scraped from the well bottom using disposable cell scrapers (Fisher Scientific, Springfield, NJ) into 1.4 mL of the EDTA solution. An equal amount of cold EDTA solution was added to thawed cell standards and DNA standards. All samples and standards were placed in a 37°C bath for 20 min and subsequently cooled on ice. The pH

of the samples and standards was adjusted to 7.0 by adding 200 μ L of 1M KH₂PO₄ prior to the addition of 1.5 mL of the fluorescent dye solution (200 ng/mL Hoechst 33258 dye (Polysciences, Warrington, PA), 100 mM NaCl, and 10 mM Tris adjusted to pH 7.0). Supernatant sample fluorescence emissions at 455 nm were read with the excitation set at 350 nm on a fluorescence spectrophotometer (series 2, SLM Amino Bowman, Urbana, IL). Cell number and DNA content in the foams were determined by comparing sample fluorescent results to the DNA and cell standard curves.

Alkaline phosphatase assay

Production of alkaline phosphatase (ALPase) was measured spectroscopically. Osteoblast seeded foams and 2-D osteoblast cultures of 7, 14, and 28 days were washed with PBS and then frozen. Upon thawing, the foams were homogenized with 1 mL Tris buffer (pH 8.0) (Sigma), and the osteoblasts of the 2-D control cultures were scraped from the well bottom using disposable cell scrapers into 1 mL Tris buffer. Both sets of samples were sonicated (Ultrasonik 300, J.M. Ney, Bloomfield, CT) for 4 min at 110 watts (50/60 Hz) on ice. Aliquots of 20 μ L were incubated with 1 mL of a p-nitrophenyl phosphate solution (16 mmol/L) (Diagnostic Kit 245, Sigma) at 30°C for up to 5 min. The production of p-nitrophenol in the presence of ALPase was measured by monitoring light absorbance by the solution at 405 nm at 1 min increments. The slope of the absorbance versus time plot was used to calculate the ALPase activity.

Confocal microscopy preparation

Osteoblast/foam constructs were prepared for confocal microscopy by staining the viable cells with the fluorescent dye 2', 7'-bis-(2-carboxyethyl)-5-(and-6)-

carboxyfluorescein, acetoxymethyl ester (BCECF-AM). The 3-D cultures were incubated with 5 mg/mL BCECF-AM in complete media for 1 hour. Following a rinse in PBS and replacement of fresh media, the cell cultures were examined using a confocal microscope (Zeiss LSM Axiovert, Carl Zeiss, Germany). Depth projection micrographs were constructed from 16 horizontal image sections through the cultures.

Histological preparation

Osteoblast/foam constructs were prepared for histology after 1, 14, 28, and 56 days in culture. The samples were fixed and stored in 10% neutral buffered formalin until ready for embedding. Standard dehydration in sequentially increasing ethanol solutions to 100% ethanol was performed followed by immersion in Hemo-De (Fisher Scientific, Pittsburg, PA), paraffin saturated Hemo-De, and finally molten paraffin. Tissue blocks were sectioned at 5 μ m and stained either by hematoxylin and eosin for visualization of cells and demonstration of tissue formation or by von Kossa's silver nitrate staining method for demonstration of matrix mineralization.

Histomorphometry

The volume per initial plating surface area and penetration depth of mineralized tissue was calculated by histomorphometry. Von Kossa stained tissue cross-sections were projected to an RGB color video camera (JVC, Model TK 107-OU) with a Jena 250-CF stereo light microscope (Micro-Tech Instruments, Dallas, TX). Output from the camera was routed to a digital image acquisition system (Quick Capture, Data Translation, Marlboro, MA) and analyzed with the public domain NIH Image software version 1.54. Images of the central cross-sectional region, 640 pixels or 3.9 mm wide, were captured for

each sample to be used for analysis. The mineralized tissue was distinguishable from the non-mineralized tissue and polymer material by its gray level intensity and was thus selected. The resulting measured areas in pixels were converted to areas in mm² following calibration of the system using a micrometer slide to determine pixel/mm ratio. The mineralized tissue area per length was calculated by dividing the mineralized tissue area by the width of the selected cross-sectional region. The standard stereological relationship that the area/length of a given phase in a two-dimensional field approximates the volume/surface area of that phase in three-dimensions was used to provide an estimate of the volume/surface area [Russ, 1986].

The penetration depth of mineralized tissue in the foams was calculated by manually measuring the maximum depth from the top surface of the polymer foam that mineralized tissue was detected on the same captured images used above. The average of 7 measurements taken at evenly spaced points along the width of the selected region was used to calculate the average mineralized penetration depth for each sample.

Gel Permeation Chromatography

The number and weight average molecular weights of the polymer foams were determined over the course of the experiment by gel permeation chromatography (Waters, Milford, MA) equipped with a differential refractometer (Waters, Series 410). The precipitates of homogenized foams from in the DNA assay were collected and dried overnight in a laminar flow hood. They were further dried and stored under high vacuum (50 mm Hg) to remove any remaining water. The homogenized and dried foams were dissolved in HPLC grade chloroform, and filtered with glass wool to remove any insoluble components. The solubilized samples were then eluted in a series configuration through a Phenogel 5 guard column (series 106337G, 50 x 7.8 mm, Phenomenex, Torrance, CA)

and a Phenogel 10 Linear column (series 106338, 300 x 7.8 mm, Phenomenex) at a flow rate of 1 mL/min. Polystyrene standards were used to construct a primary calibration curve.

Statistical Analysis

All measurements were collected in triplicate and expressed as means \pm standard deviations. Single factor analysis of variance (ANOVA) was employed to assess statistical significance of results for all the osteoblast/foam constructs whose single factor was pore size or seeding density. Scheffé's method was used for multiple comparison tests at a significance level of 95% and 99%. In addition, a two-tailed unpaired t-test was used to evaluate the significance of the cell seeding density effect on percent of cell attachment after 1 day of culture.

6.3 Results

Polymer foams

Polymer foams of controlled porosity, pore size, and thickness were fabricated with 75:25 PLGA by the solvent-casting particulate-leaching technique using salt particles as the leachable porogen. The resulting foam pore sizes were dictated by the size of the salt particles used in the fabrication process. Foams processed with salt particles sieved into the size ranges 150-300 μm (Fig. 6-1a), 300-500 μm (Fig. 6-1b) and 500-710 μm (Fig. 6-1c) exhibited pore sizes comparable to the size of the salt particles used in the fabrication process. An interconnected pore morphology was apparent in all foams which was possible because of the high porosity of the scaffolds.

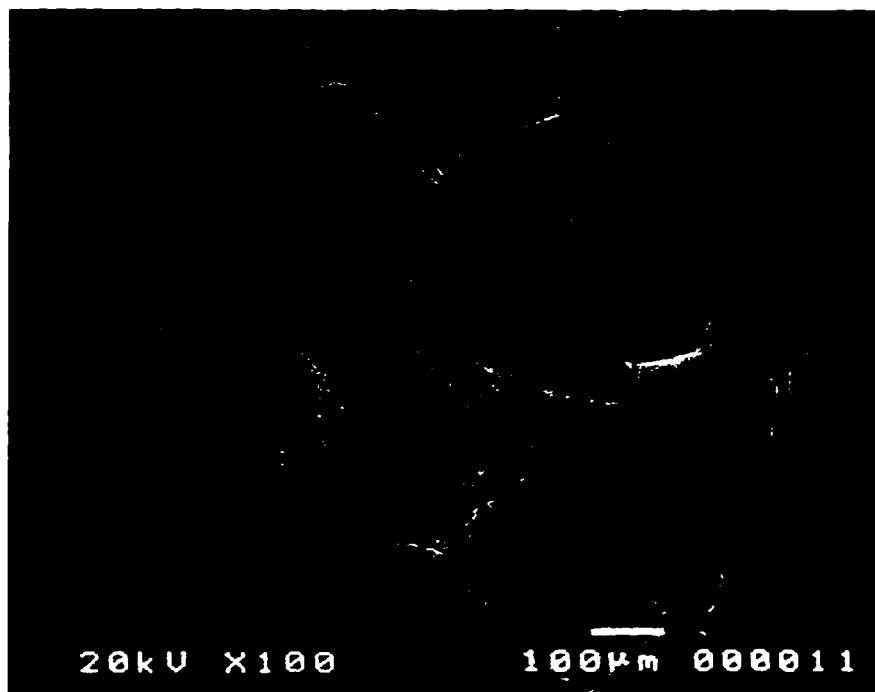


Figure 6-1a. Scanning electron micrographs of the top surface of 90% porous 75:25 PLGA foam fabricated by a solvent-casting particulate-leaching technique using sodium chloride particles of 150-300 μm in diameter as the leachable component. An interconnecting porous structure was achieved and the foams exhibited pore sizes comparable to the salt particle sizes used in the fabrication process.

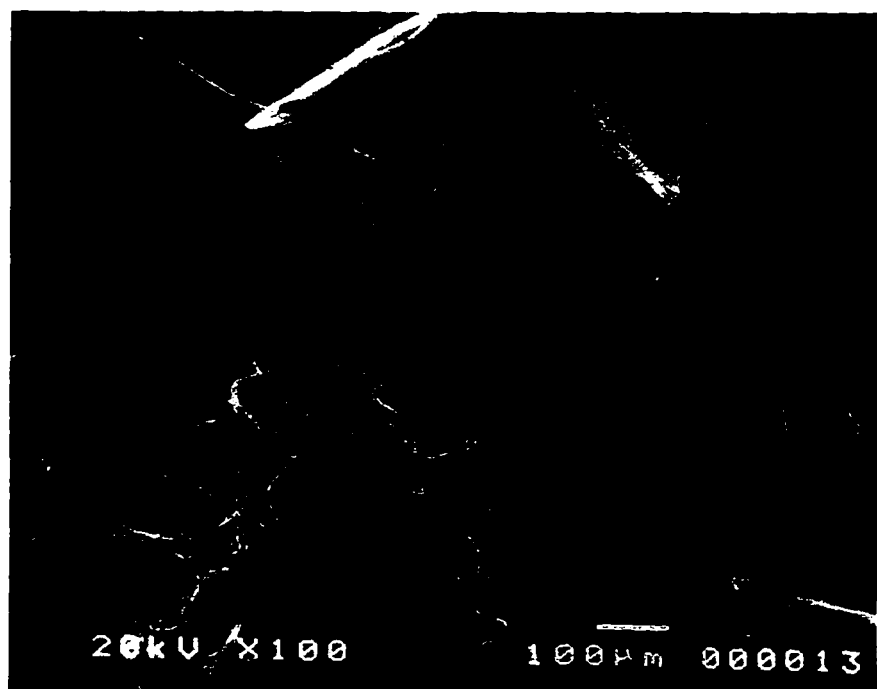


Figure 6-1b. Scanning electron micrographs of the top surface of 90% porous 75:25 PLGA foam fabricated by a solvent-casting particulate-leaching technique using sodium chloride particles of 300-500 μm in diameter as the leachable component.

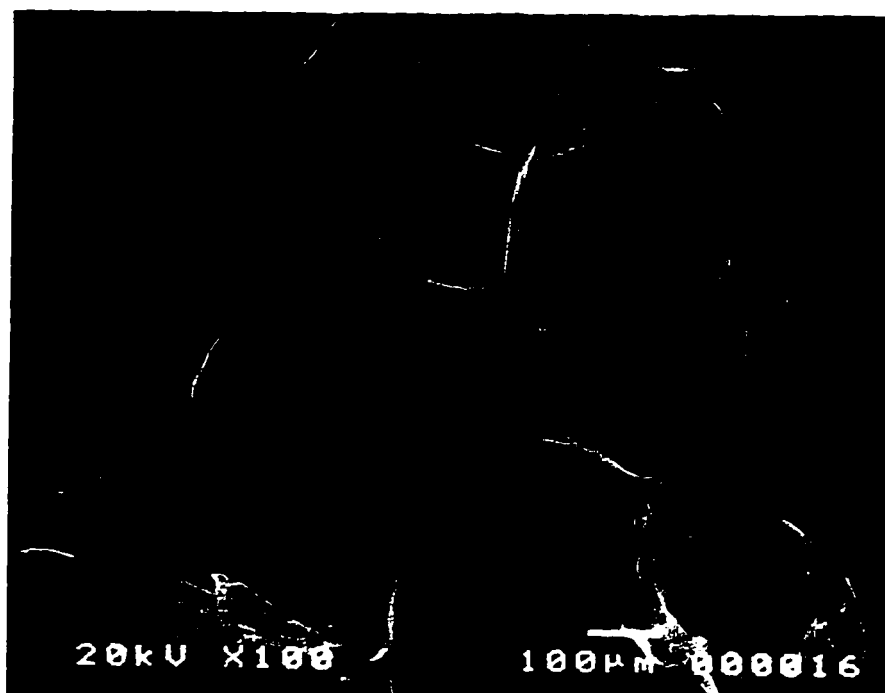


Figure 6-1c. Scanning electron micrographs of the top surface of 90% porous 75:25 PLGA foam fabricated by a solvent-casting particulate-leaching technique using sodium chloride particles of 500-710 μm in diameter as the leachable component.

Cell proliferation

Osteoblasts seeded onto 75:25 PLGA foams attached to the pore surfaces and continued to proliferate over the 56 day *in vitro* culture period on all the samples producing 3-D osteoblast/foam constructs. Scanning electron micrographs reveal the pore morphology of a foam created using salt particles 300-500 μm in diameter before (Fig. 6-1b) and after (Fig. 6-1d) osteoblast seeding. Osteoblasts can be seen covering the pore surfaces after 1 day in culture (Fig. 6-1d).

Only a fraction of the seeded cells remained attached to the polymer foams. The initial high seeding density of 22.1×10^5 cells/cm² resulted in only 11.8×10^5 cells/cm² remaining attached to the 300-500 μm foams after one day in culture, giving a percent attachment of $53 \pm 1\%$ after this 24 hour period. For the lower seeding density, 4.63×10^5 cell/cm² of the 6.83×10^5 cells/cm² seeded onto the 300-500 μm foams remained attached after 1 day in culture, giving a higher ($p < 0.01$) percent attachment of $68 \pm 5\%$.

Confocal depth projection micrographs demonstrated the initial rapid growth achieved when osteoblasts were seeded at a low density on polymer foams having pore sizes 300-500 μm in diameter (Fig. 6-2a through 6-2c). Proliferation results, as determined by quantification of DNA in the polymer foams, also indicated that osteoblasts grew more rapidly in the foams seeded with a lower cell density ($p < 0.01$, at day 1) eventually reaching comparable cell numbers to the foams seeded with a high cell density by day 7 (Fig. 6-3a). Comparable cell numbers were also found in the foams after 14 days in culture, however, by 28 and 56 days in culture the number of osteoblasts found in the foams seeded with a lower cell density was lower ($p < 0.05$) than that for the high density seeded foams after the same culture time. Osteoblast proliferation leveled off in all the osteoblast/foam constructs studied following 28 days in culture with no significant change in cell numbers between day 28 and 56 (Figs. 6-3a and 6-3b). Osteoblasts proliferated

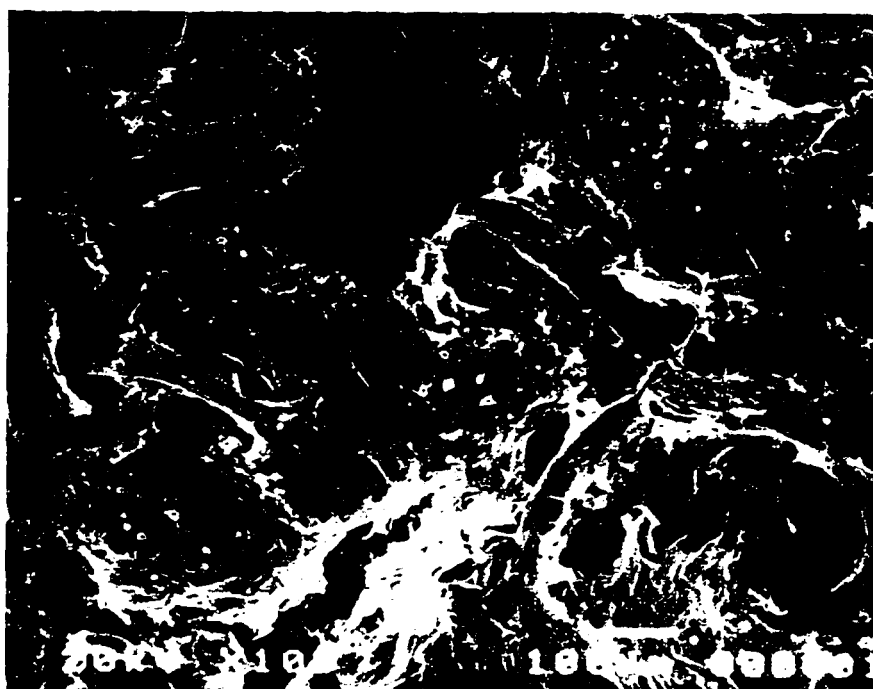


Figure 6-1d. A top view of a polymer foam prepared with salt particles ranging from 300-500 μm and seeded with high cell density (22.1×10^5 cells/ cm^2) reveals layers of osteoblasts covering the pores' surfaces after 1 day in culture.

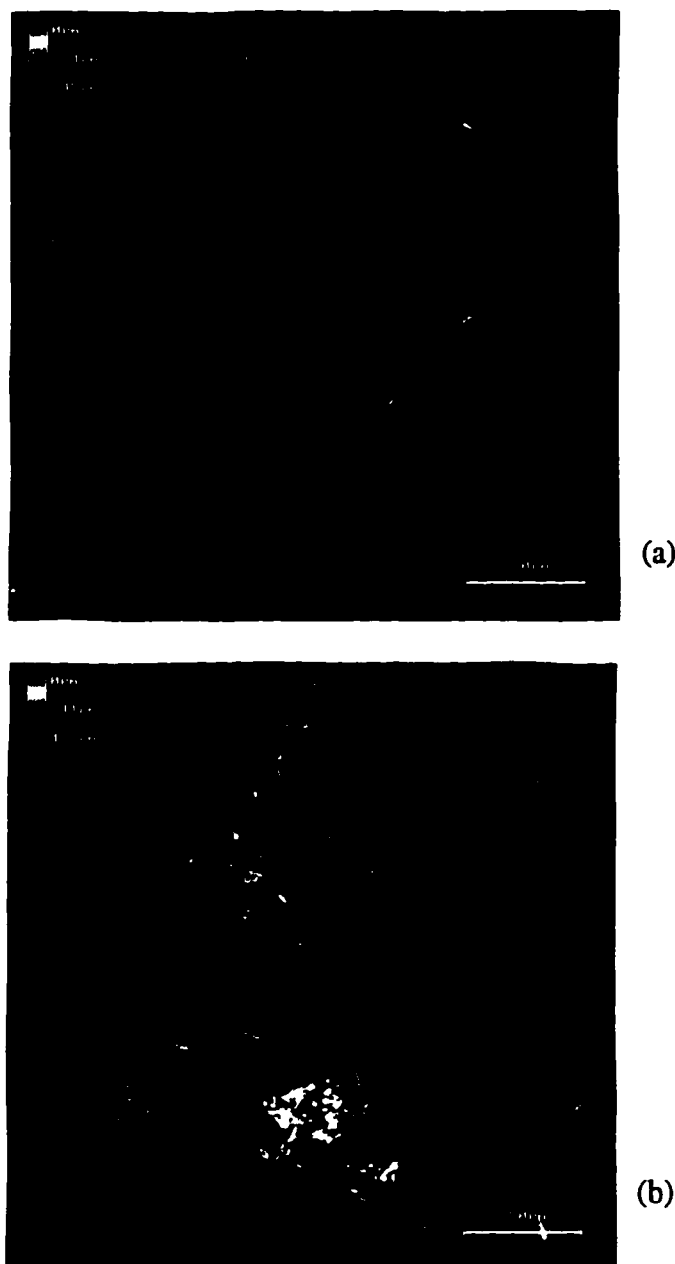


Figure 6-2 (a-b). Confocal micrographs of a 300-500 μm polymer foam seeded with a lower cell density ($6.83 \times 10^5 \text{ cells}/\text{cm}^2$) (a) and a high cell density ($22.1 \times 10^5 \text{ cells}/\text{cm}^2$) (b) after 1 day in culture revealing more cells covering the pores of the polymer in (b). Color corresponds to the depth from the polymer surface, with red being closest to the surface.

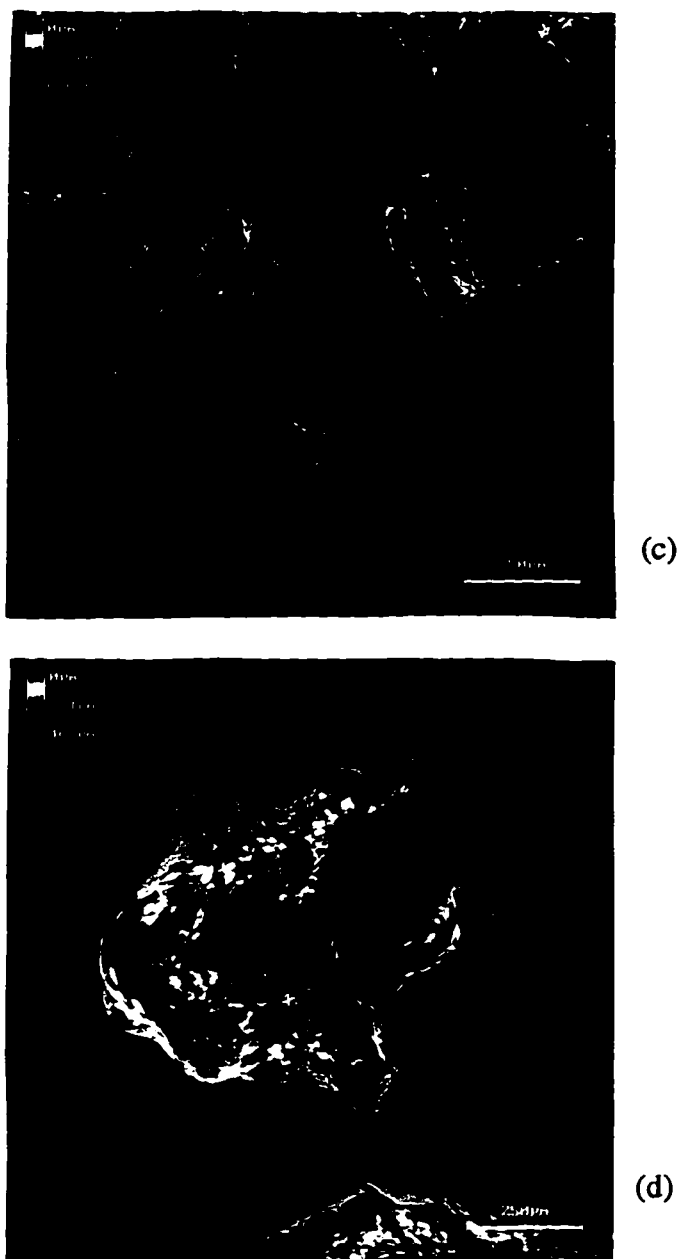


Figure 6-2 (c-d). Confocal micrographs depicting the rapid initial growth rate of osteoblasts seeded with a lower cell density (6.83×10^5 cells/cm 2) in 300-500 μ m foams. Pictures were taken after 4 (c), and 7 (d) days in culture and should also be compared to the picture 6-2a taken after 1 day in culture. Color corresponds to the depth from the polymer surface, with red being closest to the surface.

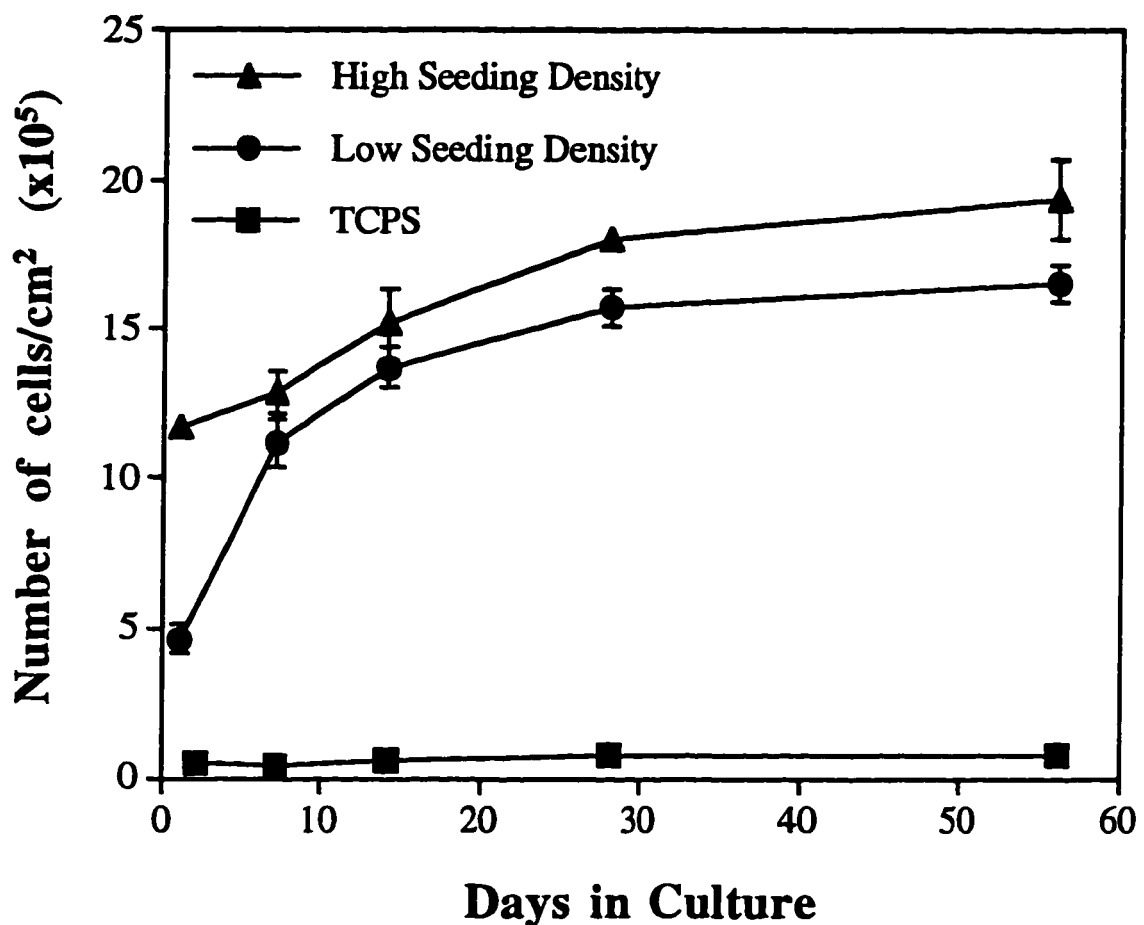


Figure 6-3a. Cellularity of osteoblast/foam constructs over time, expressed as number of cells per top cross-sectional surface area of the foams. Foams with 300-500 μm pores seeded with high seeding density (22.1×10^5 cells/ cm^2) and low seeding density (6.83×10^5 cells/ cm^2) had approximately the same number of cells by day 7, indicating a very fast initial growth rate in the lower seeding density foams. The proliferation kinetics of osteoblasts seeded on tissue culture polystyrene (TCPS) with a 2.1×10^4 cells/ cm^2 seeding density is also shown. Error bars designate means \pm s.d. for n=3.

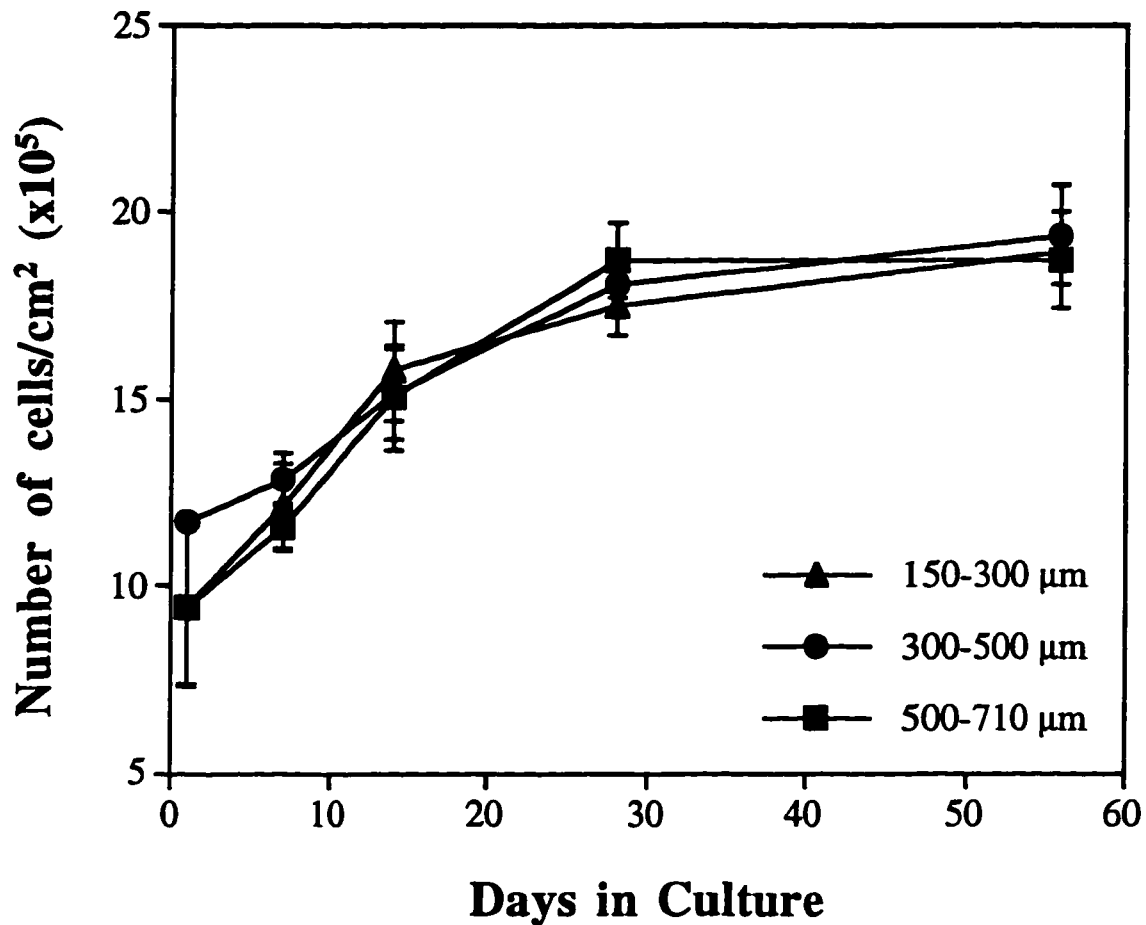


Figure 6-3b. Cellularity of osteoblast/foam constructs over time, expressed as number of cells per top cross-sectional surface area of the foams. Osteoblast proliferation continued in all foams throughout the 56 day culture period with no significant difference in cellularity between foams fabricated with different pore sizes and seeded initially with a high cell density (22.1×10^5 cells/cm²). Error bars designate means \pm s.d. for n=3.

equally well on polymer foams of all pore sizes studied (Fig. 6-3b). The rate of osteoblast proliferation on TCPS should not be compared to the osteoblast/foam construct rates of proliferation because they were seeded at a much lower cell density. ALPase activity for these cultures will be compared to activity results of the osteoblast/foam constructs in the next section.

Alkaline phosphatase activity

All osteoblast/foam cultures expressed high alkaline phosphatase activity which increased substantially over time in culture (Figs. 6-4a and 6-4b). Osteoblasts seeded at a low cell density on polymer foams of 300-500 μm appeared to express higher levels of ALPase activity compared to foams seeded with a higher cell density at all days in culture; nevertheless, these results were not significantly different (Fig. 6-4a). Measurement of ALPase activity of osteoblasts cultured on standard TCPS were included for comparison to the 3-D substrates. The cells in the constructs were expressing comparable levels of ALPase activity to the standard 2-D osteoblast cultures after 7 and 14 days in culture (Fig. 6-4a); with the exception of day 28 where slightly higher activity ($p < 0.05$) was observed for osteoblasts cultured on TCPS than in osteoblast/foam constructs initially seeded with a high cell density. Polymer foam pore size did not affect the expression of ALPase activity of the osteoblasts at any culture period (Fig. 6-4b).

Histology

In addition to growth, the osteoblasts began to lay down osteoid demonstrated by the pink regions of H & E stained sections of a construct after 56 days in culture (Figs. 6-5a and 6-6a). Osteoblasts appear to be embedded in the newly formed tissue matrix which

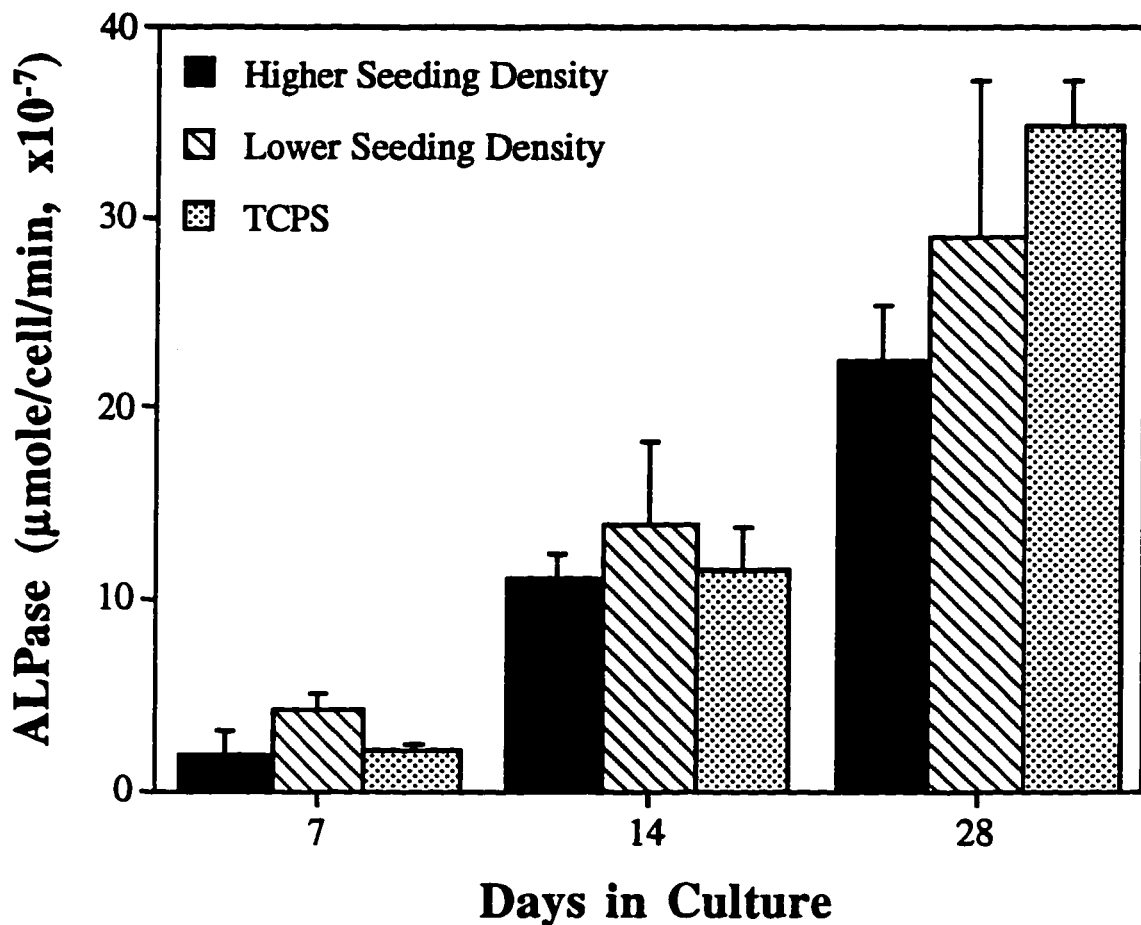


Figure 6-4a. Alkaline phosphatase (ALPase) activity in the osteoblast/foam constructs over time for foams with pore size 300-500 μm and seeded with either a high (22.1×10^5 cells/cm 2) or low (6.83×10^5 cells/cm 2) cell seeding density. High levels of ALPase activity were detected and increased significantly over time in all osteoblast/foam constructs but were independent of cell seeding density. ALPase activity in the polymer foams were comparable to those achieved in standard 2-D cultures on tissue culture polystyrene (TCPS) on a per cell basis. Error bars designate means \pm s.d. for n=3.

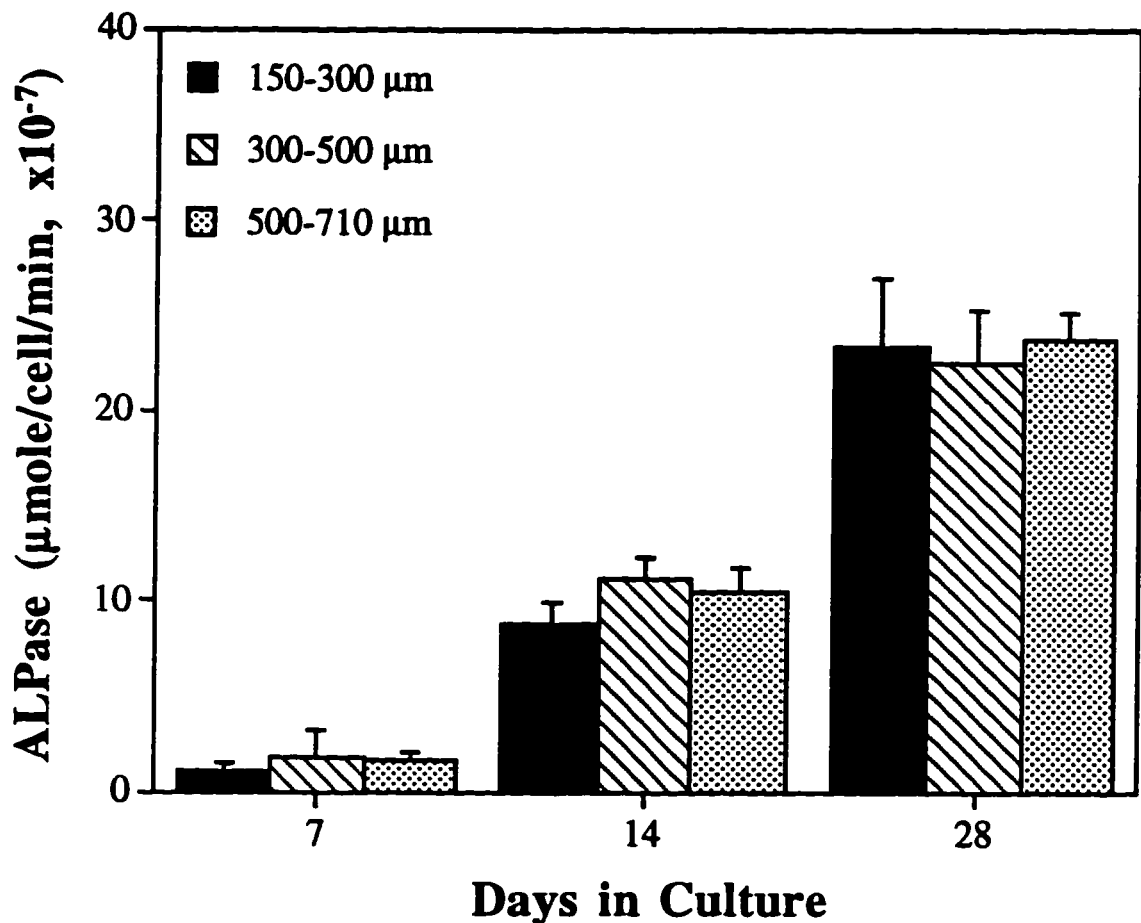


Figure 6-4b. Alkaline phosphatase (ALPase) activity in the osteoblast/foam constructs over time for foams of various pore sizes seeded with a high cell seeding density (22.1×10^5 cells/cm 2). High levels of ALPase activity were detected and increased significantly over time in all osteoblast/foam constructs, and were independent of foam pore size. Error bars designate means \pm s.d. for n=3.



Figure 6-5a. Light micrograph of a horizontal cross section of a 300-500 μm pore size polymer foam initially seeded with 22.1×10^5 cells/cm 2 and cultured for 56 days. The section was stained with hematoxylin and eosin to visualize tissue formation (25x).



Figure 6-5b. Light micrographs of a parallel cross section to that in figure 6-5a but stained using Von Kossa's staining method (with safranin O as counterstain) which stains calcium phosphate deposits black (25x).

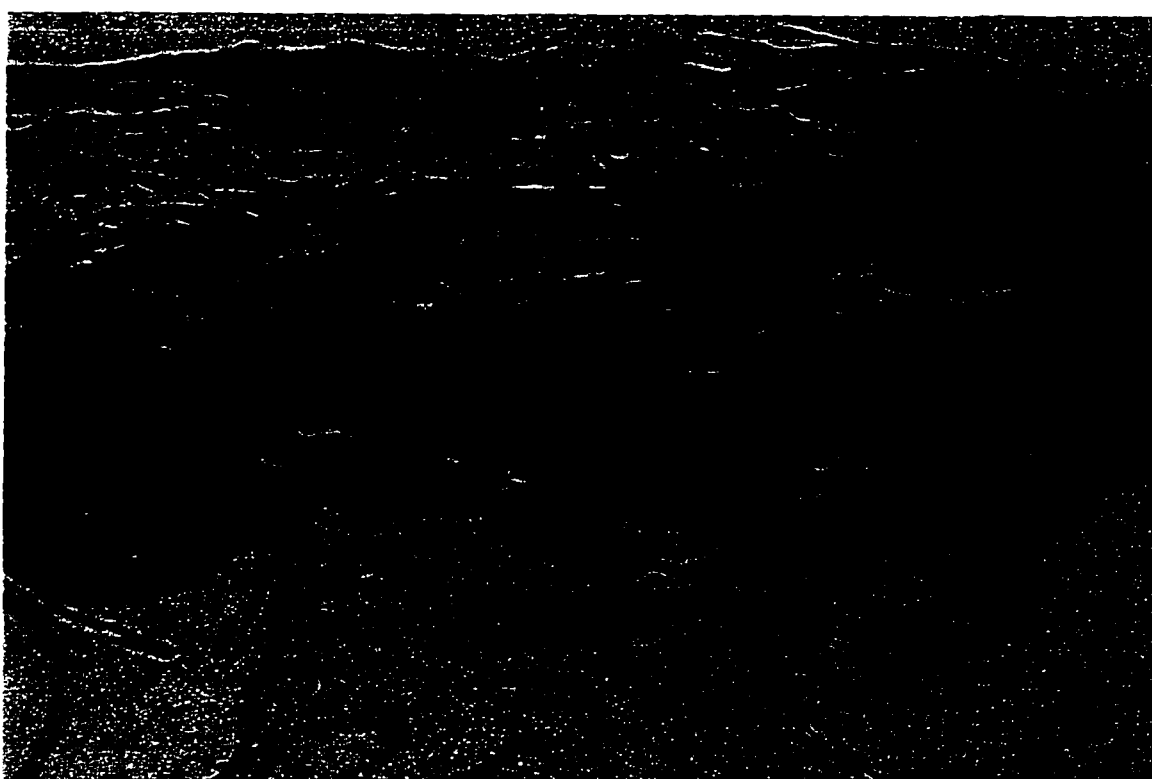


Figure 6-6a. Light micrograph of a vertical cross section of a 300-500 μm pore size foam initially seeded with 22.1×10^5 cells/cm 2 and cultured for 56 days. The section was stained with hematoxylin and eosin (100x)



Figure 6-6b. Light micrographs of a parallel cross section to that in figure 6-6a but stained using von Kossa's staining method (100x). Digitized images of sections similar to this section were used for histomorphometric quantification of mineralized tissue.

is characteristic of the natural osteoblast differentiation and their progression into osteocytic cells. Von Kossa's staining of parallel histological sections reveals that portions of the tissue matrix have been mineralized with the mineral deposits predominantly covering the surface of the construct (Figs. 6-5b and 6-6b).

Mineralization

Vertical cross-sections of the osteoblast/foam constructs stained by von Kossa's method, such as the one shown in figure 6-6b, were used to quantify the mineralized tissue by histomorphometric techniques. The penetration depth of osseous tissue into the construct (distance from polymer surface to bottom of mineralized tissue front) was found to increase over the study period for all samples (Fig. 6-7a). A maximum penetration depth of mineralized tissue of $240 \pm 82 \mu\text{m}$ was reached for osteoblast/foam constructs of pore size 300-500 μm initially seeded with a low cell density. The penetration depth of mineralized tissue was significantly affected ($p < 0.05$) by initial osteoblast seeding density only at day 14 in culture and was not affected by foam pore size at any time point (Fig. 6-7a).

The ratio of the mineralized tissue volume to top surface area of the foams increased dramatically for all the osteoblast/foam constructs over the 56 day culture period (Fig. 6-7b). Neither polymer foam pore size nor initial cell seeding density had any significant effect on the mineralized volume to surface area, with the exception of foams with pore size 500-710 μm resulting in a greater ($p < 0.05$) mineralized volume to surface area than foams with pore size 150-300 μm after 14 days in culture.

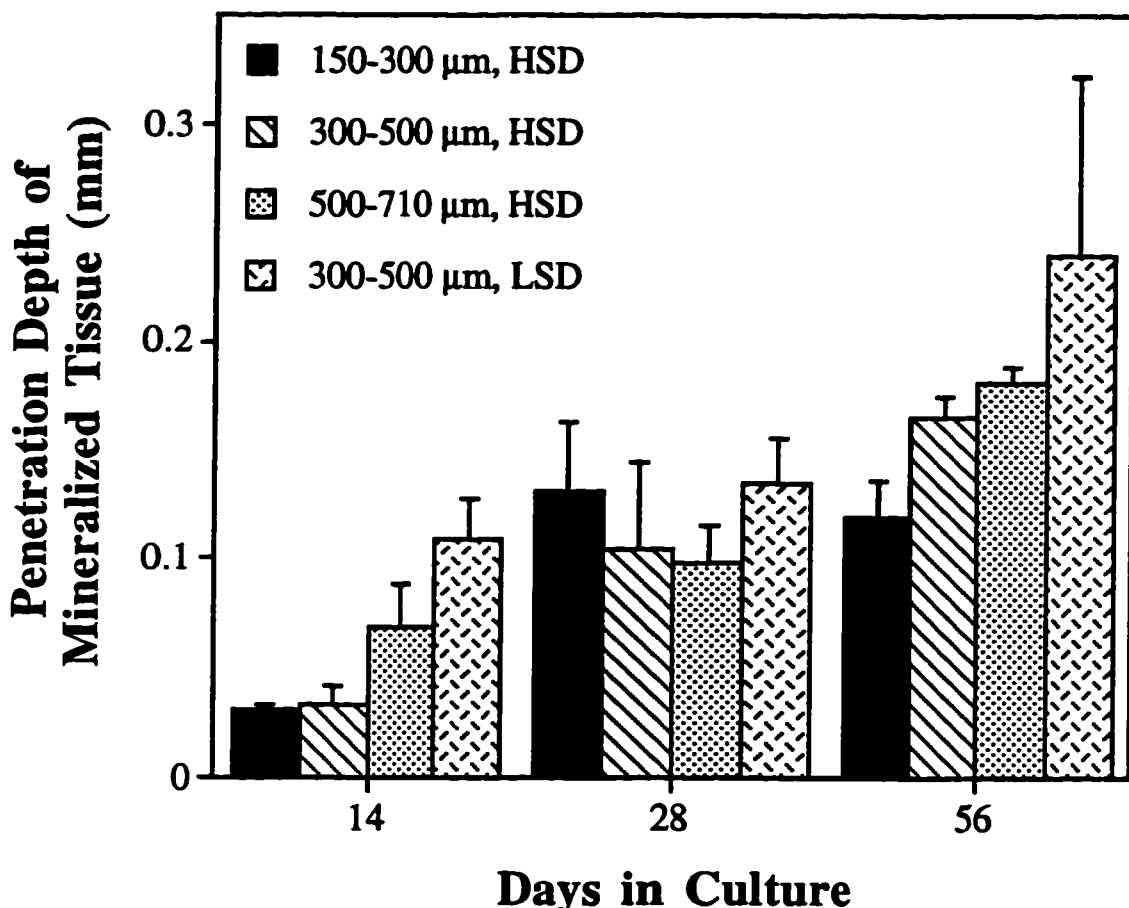


Figure 6-7a. Average maximum depth below the polymer surface that mineralized tissue was deposited in the osteoblast/foam constructs over culture time. These values were determined by histomorphometry using vertical tissue cross sections of the constructs stained with Von Kossa's silver nitrate method (similar to that shown in figure 6-6b). Mineralization was initially detected in the foams by day 14 in culture and increased significantly throughout the 56 day culture time. No significant differences were seen between foams of different pore sizes and cell seeding densities, where HSD and LSD stand for high seeding density (22.1×10^5 cells/cm²) and low seeding density (6.83×10^5 cells/cm²), respectively. Error bars designate means \pm s.d. for n=3.

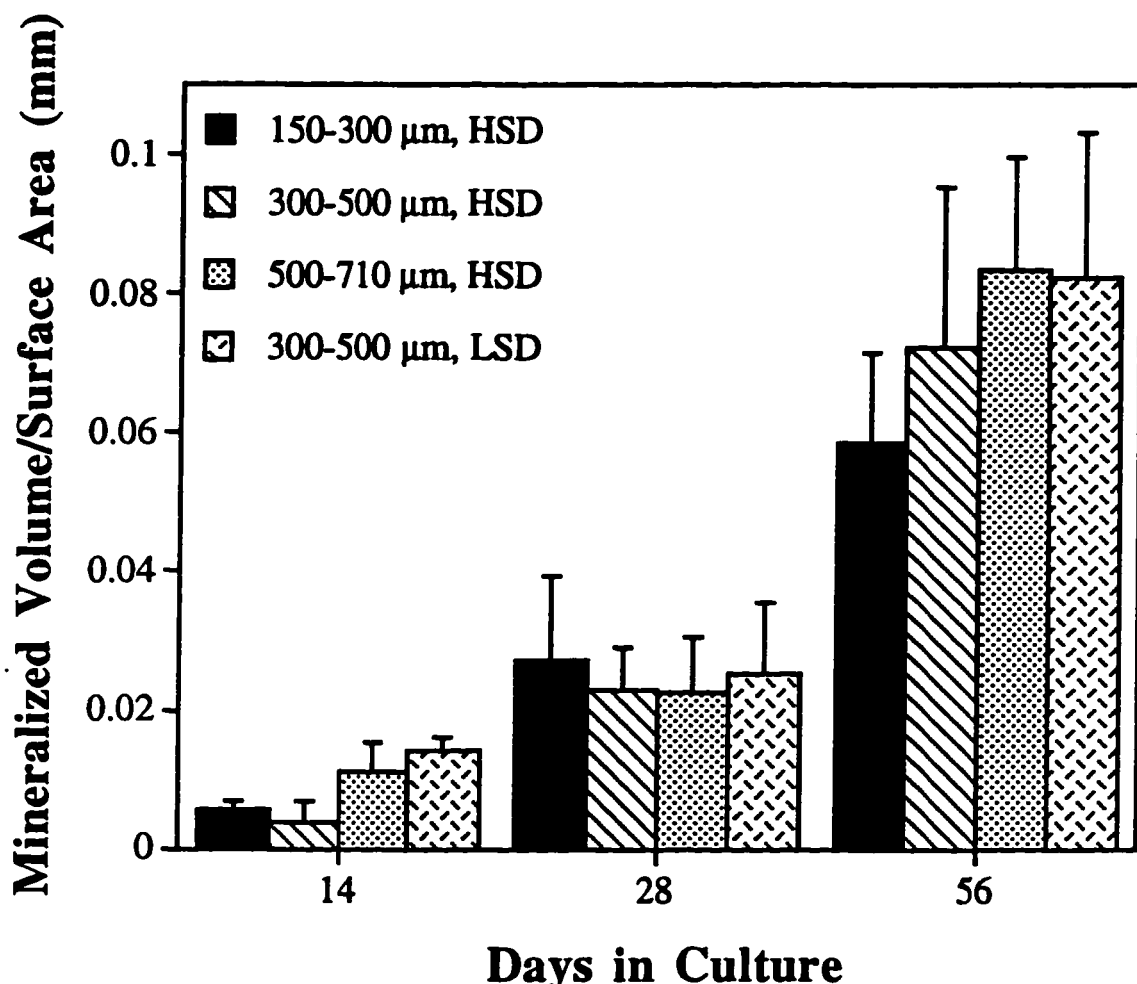


Figure 6-7b. Total mineralized volume/surface area in the osteoblast/foam constructs over culture time. These values were determined by histomorphometry using vertical tissue cross sections of the constructs stained with Von Kossa's silver nitrate method (similar to that shown in figure 6-6b). The mineralized volume/surface area in 3-D was taken to be proportional to the mineralized tissue area per length in the 2-D sections. No significant differences were seen between foams of different pore sizes and cell seeding densities, where HSD and LSD stand for high seeding density (22.1×10^5 cells/cm²) and low seeding density (6.83×10^5 cells/cm²), respectively. Error bars designate means \pm s.d. for n=3.

Polymer degradation

All the foams degraded throughout the culture period of the study as measured by their decrease in weight average molecular weight (Fig. 6-8). Neither foam pore size (Fig. 6-8) nor seeding density (data shown in appendix, Fig. 6-9) significantly affected the degradation of the constructs. The average decrease in weight average molecular weight of the polymer in all the osteoblast/foam constructs from day 1 to day 56 was $69 \pm 5\%$.

6.4 Discussion

This study intended to answer the following questions: 1) whether differences in polymer foam pore size in the range of 150-710 μm affect osteoblast proliferation and function *in vitro*, 2) whether osteoblast seeding density on polymer foams affects cell attachment, proliferation and function *in vitro* and 3) whether a 3-D osseous tissue can be formed by culturing osteoblasts in polymer foams *in vitro*.

To answer the first question, we cultured stromal osteoblasts in polymer foams having pores in the size range of 150-300, 300-500, or 500-710 μm . We found that differences in polymer foam pore size within a range of 150-710 μm did not significantly affect osteoblast proliferation or function *in vitro* based on DNA content, ALPase activity, and mineral deposition in the osteoblast/foam constructs. Pore size was investigated because an optimum pore size of 200-400 μm had been observed *in vivo* for bone growth in studies using ceramic materials [Dennis et al., 1992]. Since bone is a vascular tissue, this pore size range may be optimal because it provides sufficient space for growth of vascular tissue. One reason why we may not have seen any effects based on pore size is because there is no angiogenesis (new vessel formation) in our *in vitro* culture system. It has also been suggested that the pore size range of 200-400 μm is preferred by osteoblasts

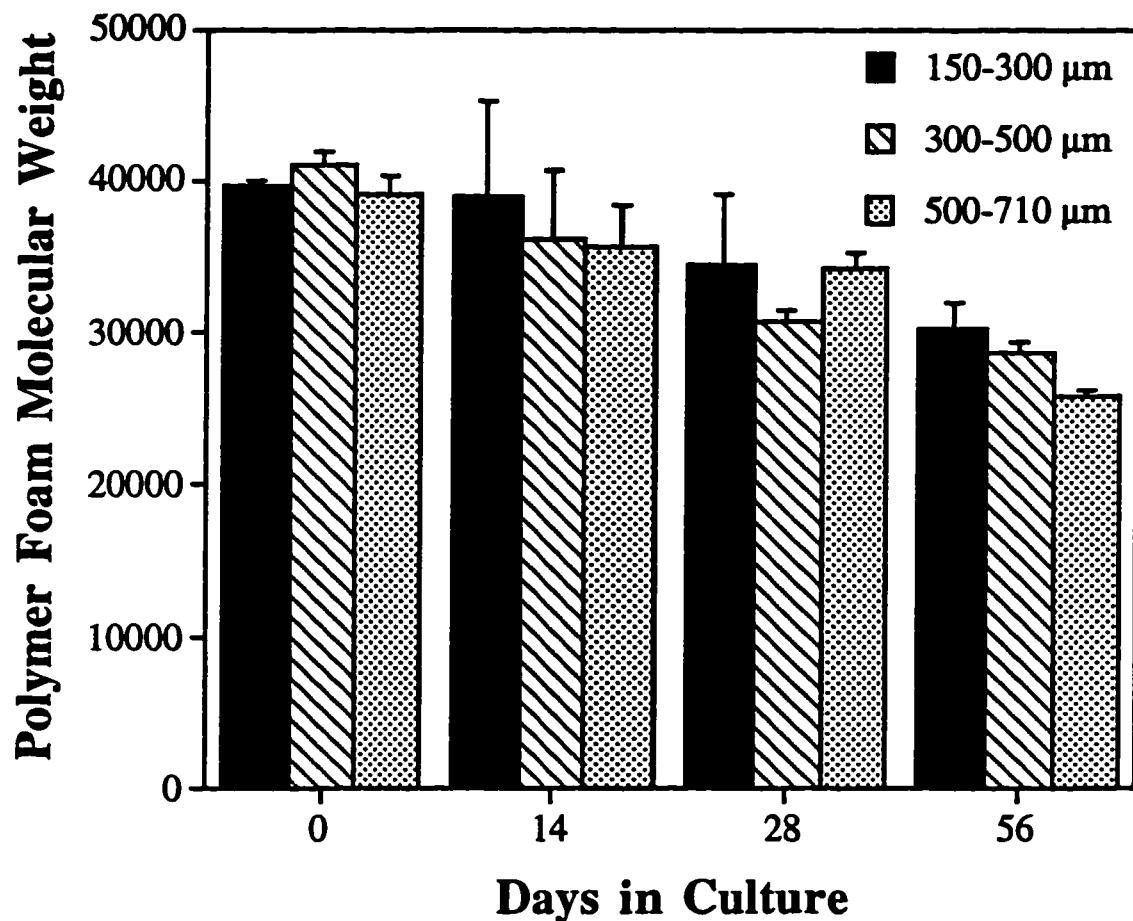


Figure 6-8. Weight average molecular weights of the 75:25 PLGA polymer foams, initially seeded with a high cell density (22.1×10^5 cells/cm²), over time. No significant difference in the weight average molecular weight was seen between the polymer foams of different pore size. Similar results were found for the foams seeded with a lower cell density (data not shown). Error bars designate means \pm s.d. for n=3.

because it provides the optimum compression and tension on the osteoblast's mechanoreceptors [Boyan et al., 1996], which may also explain the independency on pore size observed in our static culture system having no mechanical stimuli. Studies in progress in our laboratory aim to investigate the effect of the pore size on bone formation *in vivo* following the orthotopic and ectopic implantation of PLGA foams seeded with autogenous stromal osteoblasts.

To determine what effect seeding density had on osteoblast attachment, proliferation and function, we seeded osteoblasts onto the top surface of polymer foams of pore size 300–500 μm at two different cell densities ($22.1 \times 10^5 \text{ cell/cm}^2$ and $6.83 \times 10^5 \text{ cells/cm}^2$). The seeding densities were the same magnitude as those reported for cultures on 3-D collagen [Casser-Bette et al., 1990; Schoeters et al., 1992] and PGA matrices [Vacanti et al., 1993]. Only a fraction of the osteoblasts that we initially seeded actually attached to the polymer foam. As little as $53 \pm 1\%$ of the high density and $68 \pm 5\%$ of the low density seeded osteoblasts attached after 1 day. It is possible that the surface area available for cell seeding on the top of foams may be a limiting factor. Even though the initial percent of attachment was lower for the constructs created with a high seeding density, the absolute number of attached cells at day 1 was much greater than constructs seeded at a lower density of osteoblasts ($p < 0.01$). Nevertheless, by day 56 the difference between the two groups was not as significant ($p < 0.05$), due to the rapid proliferation of osteoblasts in the lower seeding density constructs between days 1 and 7 in culture. In contrast, osteoblast function as measured by ALPase activity and mineralized matrix deposition was not affected by osteoblast seeding density after 56 days in culture.

Finally, hematoxylin and eosin stained matrix and mineralized matrix deposition observed in histological sections of the osteoblast/foam constructs has provided evidence that a 3-D osseous-like tissue was formed *in vitro*. The culture environment at the outer surface of the foams seems to be favorable for osteoblasts to lay down osteoid.

This is the first study to demonstrate 3-D osseous tissue formation *in vitro* using poly(α -hydroxy ester) biodegradable foams as a scaffolding substrate for seeded osteoblasts. Previously, osteoblasts have been successfully cultured on 2-D poly(α -hydroxy ester) substrates, but skeletal defect replacement therapies require a three-dimensional osteoconductive material. Initial studies involving osteoblast-like cell culture in 3-D poly(lactic acid) foams for the eventual use in skeletal reconstruction have been investigated; however, tissue formation was not observed nor were any quantitative data reported [Lo et al., 1994]. The approach of osteoblast transplantation in polymer foams can be easily adapted to the clinical setting since extraction of bone marrow is a simple outpatient procedure and the ability to culture osteoblasts from human bone marrow has already been established [Ashton et al., 1985; Haynesworth et al., 1992; Cheng et al., 1994]. Also, poly(α -hydroxy esters) have already been FDA approved for certain clinical uses such as degradable sutures. The poly(α -hydroxy ester) used in the foam construction can be tailored to degrade over periods ranging from weeks to years, depending on clinical needs [Thomson et al., 1995]. Replacement of the resorbed polymer scaffold by the host bone would subsequently result in natural bone regeneration in the defect site.

Although 3-D osteoblast cell culture has been demonstrated on a variety of matrices, such as poly(glycolic acid) meshes, [Vacanti et al., 1993] collagen matrices, [Sudo et al., 1986; Casser-Bette et al., 1990] ceramics, [Cheung Haak, 1989] and polyphosphazenes, [Laurencin et al., 1996] we believe the PLGA constructs offer distinct advantages over other methods. Poly(glycolic acid) meshes inherently have low mechanical strength and their relatively thin 100 μm sheets make repairing larger defects more challenging. Collagen matrices are also relatively weak and their enzymatically dependent degradation may result in unpredictable degradation rates. In addition, the success of transplanted collagen/osteoblast matrices may be compromised due to immunological responses to collagen obtained from xenogeneic or allogeneic sources or contaminants from transfected

cell line collagen purifications. The slow degradation of ceramic matrices may pose a problem for the replacement of these devices with new host bone, and may alter the mechanical properties of the newly formed bone. Finally, the biocompatibility of polyphosphazenes still needs to be tested as they are fairly new materials. In contrast, poly(lactic-co-glycolic acid) foams can be fabricated in any size, degrade by hydrolysis in a controllable fashion, and are biocompatible.

In addition to *in vivo* regenerative potential, these 3-D osteoblast cultures may provide a better *in vitro* model of osteoblast function than do conventional 2-D systems because osteoblasts are naturally found in a 3-dimensional network *in vivo*. More accurate responses of osteoblasts to pharmacological or mechanical stimuli may thus be determined. We are presently investigating osteoblast responses to mechanical loads in a three-dimensional environment using this culture system [Jen et al., 1996]. Three-dimensional osteoblast cultures also have the potential to yield greater cellularity than do 2-D cultures. As discussed in chapter 4, calvarial osteoblast proliferation plateaued at approximately 1×10^5 cells/cm² on flat 75:25 PLGA films compared to cellularities ranging from $17-19 \times 10^5$ cells/cm² achieved in the 3-D foams after 14 days in culture. This may be attributed to the larger surface area provided by the interconnected pores and the three-dimensional nature of the constructs. Similar trends between 2-D and 3-D cultures were found when osteoblast-like cells were cultured on polyphosphazene matrices [Laurencin et al., 1996].

Direct comparisons between the present study and previous ones can be made but are difficult because of differences in initial seeding density. Three-dimensional polyphosphazene matrices (of average pore size of 165 μm) supported the growth of 8×10^5 cells/cm² after 14 days in culture, but we produced 3-D cultures in 75:25 PLGA foams of 150-300 μm pores having 15×10^5 cells/cm². The greater number of cells found in our 3-D constructs is most likely due to the greater 22×10^5 cells/cm² seeding density which was used in our study, compared to the 1×10^5 cells/cm² density used to seed the

polyphosphazene matrices. Osteoblasts cultured on porous calcium phosphate ceramic [Cheung Haak, 1989] originally seeded with approximately 2.6×10^5 cells/cm² had 12×10^5 cell/cm² after 70 days in culture, whereas we achieved comparable osteoblast densities after only 7 days in culture. Again, the difference can be attributed to the seeding density variance between both studies.

The primary limitation of this culture system is the depth of cell growth. Histological sections revealed considerable cell proliferation and mineralized tissue formation within approximately 120-250 μm of the polymer foam surface with only a minimal number of cells located in the center. This might be due to diffusion limitations of the media into the center of the foams because of distance and physical obstruction by cells and mineralized matrix present on the upper polymer surfaces. This problem may be alleviated by alterations in culture conditions or seeding methods, such as culturing the osteoblast/foam constructs under mixed conditions [Freed et al., 1994]. The cells may also be seeded into the center of the foam rather than onto the surface, eliminating the possibility of surface obstruction to diffusion. For *in vivo* applications, however, diffusion limitations may eventually be overcome by the ingrowth of vascular tissue if viability is maintained until neovascularization is complete [Wake et al., 1994]. The mineralized volume to surface area increased more dramatically than the penetration depth of mineralized tissue. This suggests that as long as the metabolic needs of the osteoblast are met, as they are on the surface, they will continue to lay down new osteoid tissue.

CHAPTER 7

RAT CALVARIAL OSTEOBLAST CULTURE IN THREE-DIMENSIONAL POLY(α -HYDROXY ESTER) FOAMS

7.1 Introduction

This chapter describes a similar study to the study conducted in chapter 6 with the exception that rat calvarial osteoblasts instead of rat stromal osteoblasts were used in this study and a higher concentration of dexamethasone was used in the culture medium. It is very likely that osteoblasts derived from stromal origins give rise to a more heterogeneous population of cells than osteoblasts derived from rat calvaria, which could affect the proliferation and function of the cells and result in a different type tissue being produced in the polymer foams. In addition, studies describing the induction or stimulation of the osteoblast phenotype with dexamethasone give conflicting recommended concentrations ranging from 10 nM to 100 nM. We were interested to see if osteoblasts isolated from a different source and cultured with a higher concentration of dexamethasone would effect the proliferation of osteoblasts in the polymer foams and the mineralized tissue deposition. Another difference between this study and the chapter 6 study is that the lower cell seeding density used in this study is twice as high as that used in chapter 6.

7.2 Materials and Methods

Polymer foam fabrication

Polymer foams of two different pore sizes (150-300 and 500-710 μm) and two thicknesses (1.9 mm and 3.0 mm) were fabricated by a solvent-casting particulate-leaching

technique with NaCl as the leachable component as described in chapter 6 to make 90% porous foams. The foams with thickness of approximately 1.9 mm thick were casted with 5 mL of a 0.1 g/mL polymer solution combined with 4.5 g NaCl, and 3.2 mm foams were casted with 5 mL of a 0.18 g/mL polymer solution with 8.1 g NaCl into a 60 mm glass petri dish. The 7 mm diameter foams that were cut from the 60 mm casted and leached foams were prewetted prior to cell seeded as described in chapter 6.

Calvarial osteoblast isolation, seeding, and culture

Osteoblasts were isolated from neonatal (less than 1 day old) Sprague Dawley rat calvaria by an enzymatic digestive process described in chapter 4. The isolated and passaged cells were pooled, pelleted, and resuspended in a known amount of media. Cells were counted by Coulter Counter and diluted to concentrations of either 56,587,000 cells/mL (high density) or 28,431,447 cells/mL (low density) in complete media containing 100 nM dexamethasone (Sigma) [Bellows et al., 1987; Shalhoub et al., 1992; Pockwinse et al., 1995]. Aliquots of 15 μ L of either the high or the low density cell suspensions were seeded onto the top of prewetted foams placed in the wells of 24 well plates, resulting in a seeding density of 22.1×10^5 cell/cm² and 11.1×10^5 cells/cm² (or 849,000 and 426,000 cells/foam), respectively, when normalized to the top surface area of the foams. The foams were left undisturbed in an incubator for 3 hours to allow the cells to attach to the foams, after which time an additional 1 mL of complete media containing 100 nM dexamethasone was added to each well. Medium containing 100 nM dexamethasone was changed every 2-3 days.

DNA assay

The number of cells in the foams after 1, 7, 14, and 56 days in culture were determined by a fluorometric quantification of DNA found in the foams by the assay described in chapter 6.

Alkaline phosphatase assay

ALPase production for osteoblasts cultured in foams for 7 and 14 days was measured spectrophotically as described in chapter 6.

Confocal microscopy preparation

Osteoblast/foam constructs were prepared for confocal microscopy as described in chapter 6.

Histological preparation and Histomorphometry

Osteoblast/foam constructs were prepared for histology after 1, 14, 21, 28, and 56 days in culture as described in chapter 6. The penetration depth of mineralized tissue and the mineralized tissue volume per surface area in the foams were calculated from digitized images of the histological sections also described in chapter 6.

Statistical Analysis

Statistical analysis was performed as described in chapter 6.

7.3 Results

Polymer foams

The polymer foams used in this study were similar to those fabricated in chapter 6 which were shown to have a controlled porosity, pore size, and thickness. Polymer foams with the same porosity and pore size but with greater thickness were achieved by increasing the amount of polymer and salt used in the solvent-casting particulate leaching technique.

Cell proliferation

The 75:25 PLGA foams supported the attachment and proliferation of seeded osteoblasts over the 56 day *in vitro* culture period for all the samples. A confocal depth projection micrograph reveals the osteoblast distribution over the pore surfaces of a foam having 150-300 μm pores after 3 days in culture and initially seeded with 22.1×10^5 cell/cm² (Fig. 7-1). A high percent of the seeded cells remained attached to the polymer foams. The initial high seeding density of 22.1×10^5 cells/cm² resulted in only $15.1 \pm 1.0 \times 10^5$ cells/cm² remaining attached to the 150-300 μm , 1.9 mm thick foams after one day in culture, giving a percent attachment of $68.6 \pm 4.7\%$ after this 24 hour period. For the lower seeding density, $8.4 \pm 0.1 \times 10^5$ cell/cm² of the 11.1×10^5 cells/cm² seeded onto 1.9 mm thick foams of pore size 150-300 μm remained attached after 1 day in culture, giving a greater percent attachment of $75.6 \pm 1.1\%$. Proliferation results, as determined by quantification of DNA in the polymer foams, indicated that the number of osteoblasts continued to increase throughout the study, but eventually began to level off near 56 days in culture. The results also indicated that osteoblasts grew more rapidly in the foams seeded with a lower cell density ($p < 0.05$, at day 1) eventually reaching comparable cell

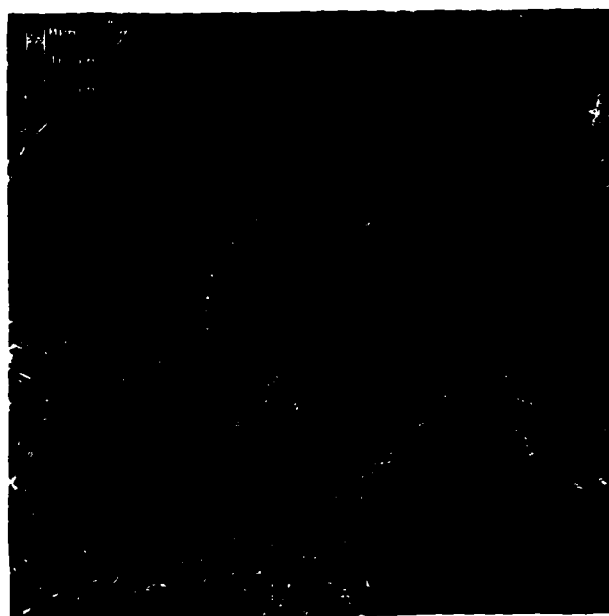


Figure 7-1. Confocal depth projection micrograph of a 1.9 mm thick foam having 150-300 μm pores and initially seeded with a high cell density ($22.1 \times 10^5 \text{ cells/cm}^2$). Picture was taken after 3 days in culture. Color corresponds to the depth from the polymer surface, with red being closest to the surface.

numbers to the foams seeded with a high cell density by day 7 (Fig. 7-2a). Comparable cell numbers were also found between the foams seeded with different cell densities at the later time points in the study (after 14 and 56 days in culture). Osteoblasts also proliferated equally well on polymer foams of the two pore sizes and foam thicknesses, with no significant differences observed in cell numbers at any time point studied (Fig. 7-2b).

Alkaline phosphatase activity

All osteoblast/foam cultures expressed high alkaline phosphatase activity which increased substantially over time in culture (Figs. 7-3a and 7-3b). Comparisons were only made between foams which varied in only one parameter. Osteoblasts seeded at a low cell density on polymer foams of 150-300 μm expressed higher levels of ALPase activity compared to foams seeded with a higher cell density ($p < 0.05$) after 7 days in culture but by 14 days in culture no significant differences were found between the foams seeded with different osteoblast densities (Fig. 7-3a). The ALPase activity for foams with pore size 500-710 μm and thickness 1.9 mm was significantly greater than the activity for foams with pore size 150-300 μm and the same thickness after 7 days in culture; this difference, however, was not significant after 14 days in culture (Fig. 7-3b). In addition, no differences were found for foams having pore size 150-300 μm and different thicknesses, 1.9 mm and 3.2 mm, at either time.

Histology

After 14 days in culture, extracellular matrix depositions began appearing in the foams. This matrix appeared pink in the H & E stained sections (Figs. 7-4a and 7-4b). Osteocytic-like cells also were seen embedded in the newly formed tissue matrix (Fig. 7-

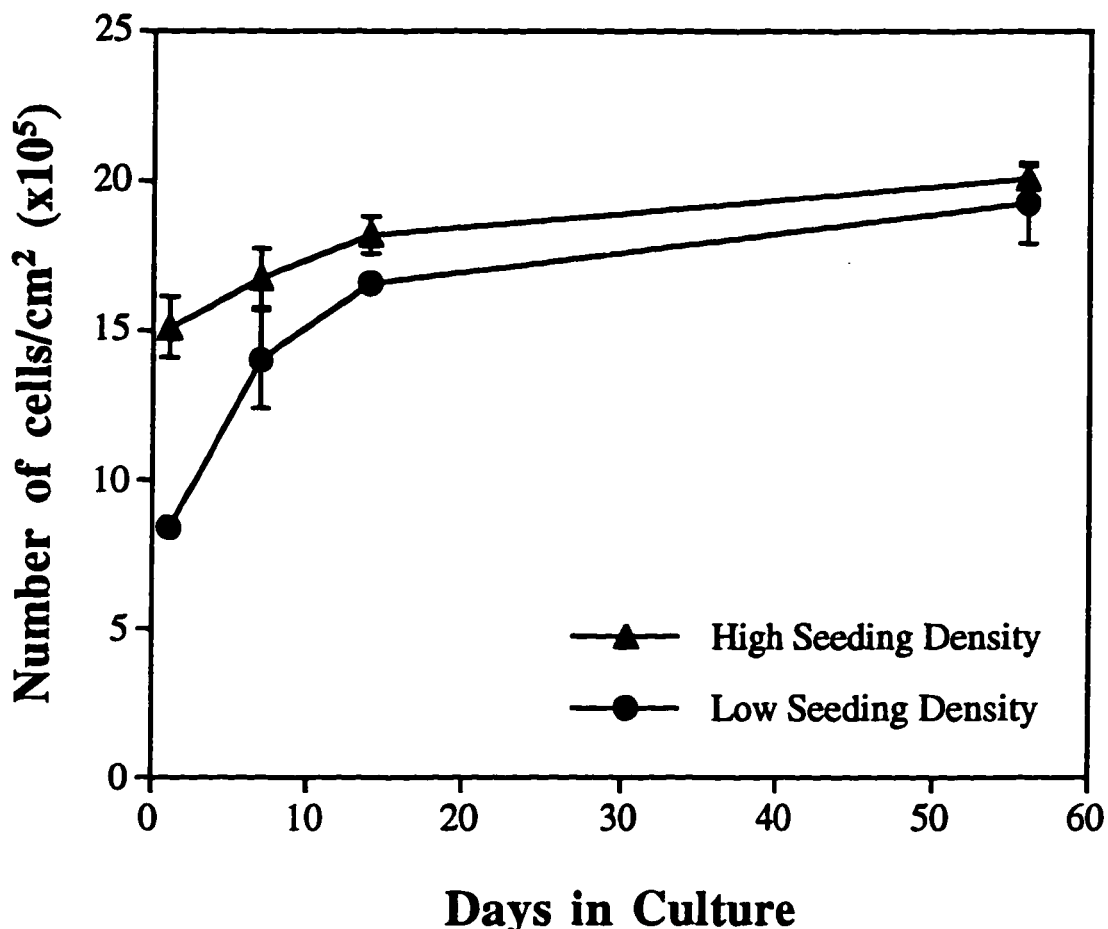


Figure 7-2a. Cellularity of osteoblast/foam constructs over time, expressed as number of cells per top cross-sectional surface area of the foams. Foams having pores in the range of 150-300 μm in diameter and seeded with either a high seeding density (22.1×10^5 cells/cm²) or a low seeding density (11.1×10^5 cells/cm²) showed significant differences only at Day 1, indicating a very fast initial growth rate in the lower seeding density foams. Error bars designate means \pm s.d. for n=3.

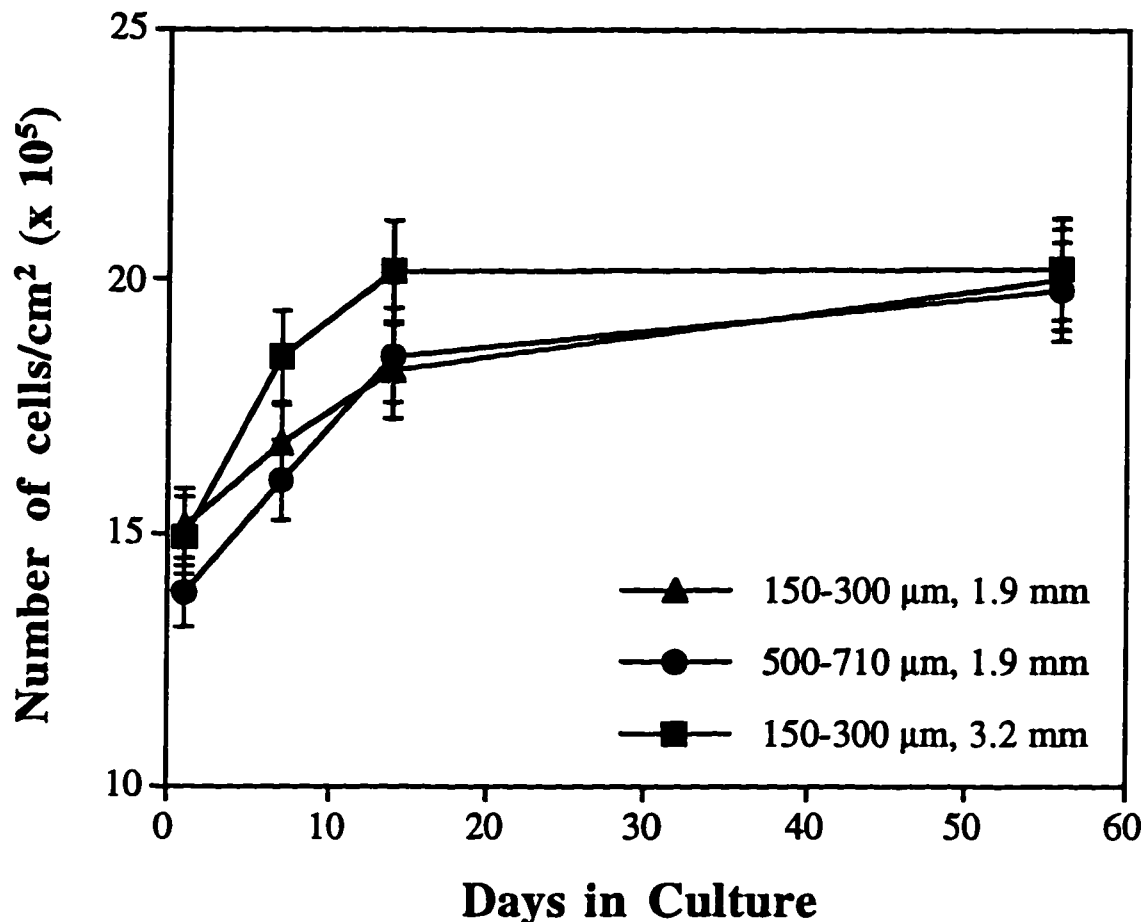


Figure 7-2b. Cellularity of osteoblast/foam constructs over time, expressed as number of cells per top cross-sectional surface area of the foams. Osteoblast proliferation continued in all foams throughout the 56 day culture period with no significant difference in cellularity for foams seeded initially with a high cell density (22.1×10^5 cells/cm²) and fabricated with different pore sizes and thicknesses. Error bars designate means \pm s.d. for n=3.

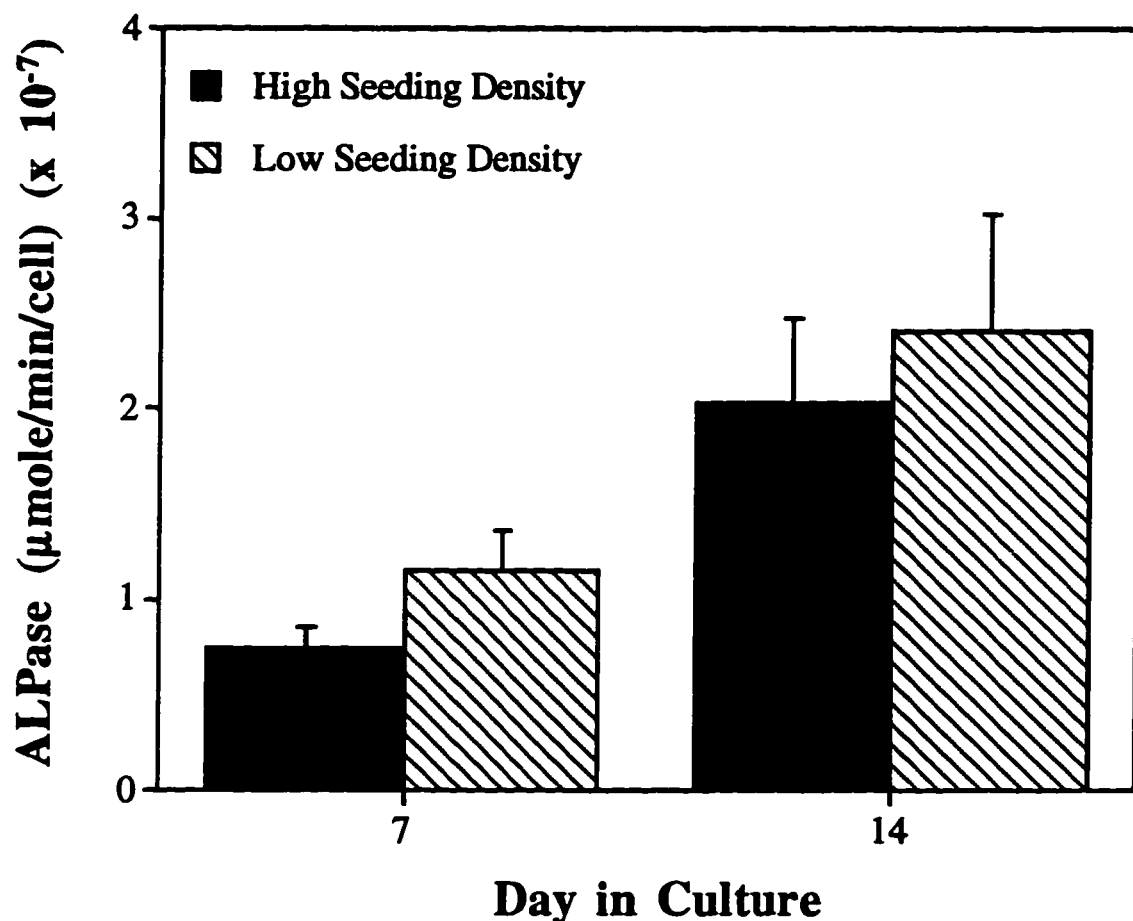


Figure 7-3a. Alkaline phosphatase (ALPase) activity in the osteoblast/foam constructs over time for foams of pore size 150-300 μm and initially seeded with either a high or low cell density. High ALPase activity was detected and increased significantly over time ($p < 0.05$). The enzyme activity was found to be greater ($p < 0.05$) for the foams seeded with a lower osteoblast seeding density after 7 days in culture, but the difference after 14 days in culture was not found to be significant. Error bars designate means \pm s.d. for $n=3$.

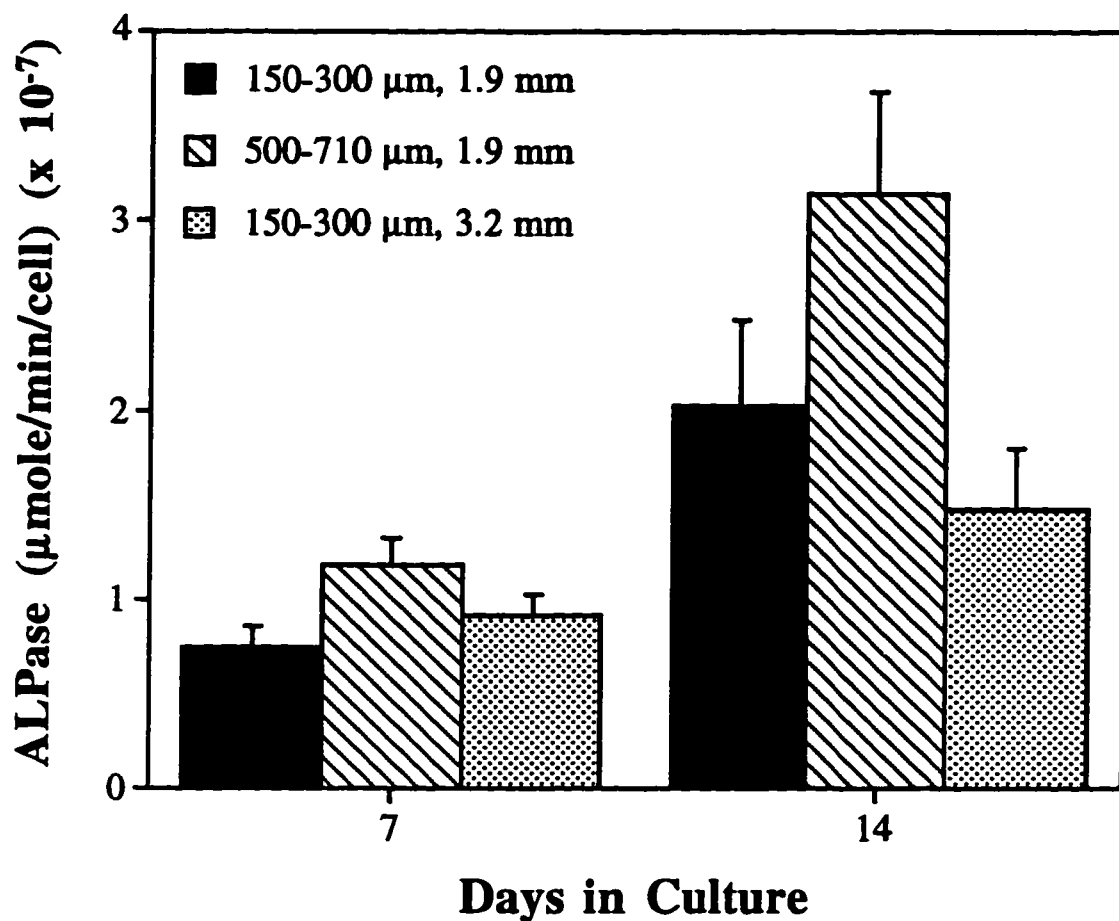


Figure 7-3b. Alkaline phosphatase (ALPase) activity over time for osteoblast/foam constructs having pore sizes of either 150-300 μm or 500-710 μm and thicknesses of either 1.9 mm or 3.2 mm and seeded initially with a high cell density ($22.1 \times 10^5 \text{ cell/cm}^2$). High ALPase activity was detected and increased significantly over time. The enzyme activity was found to be greater ($p < 0.05$) for the foam with pore size 500-710 μm after 7 days in culture (when compared to 150-300 μm foams with the same 1.9 mm thickness); however, the difference after 14 days in culture was not found to be significant. Error bars designate means \pm s.d. for $n=3$.

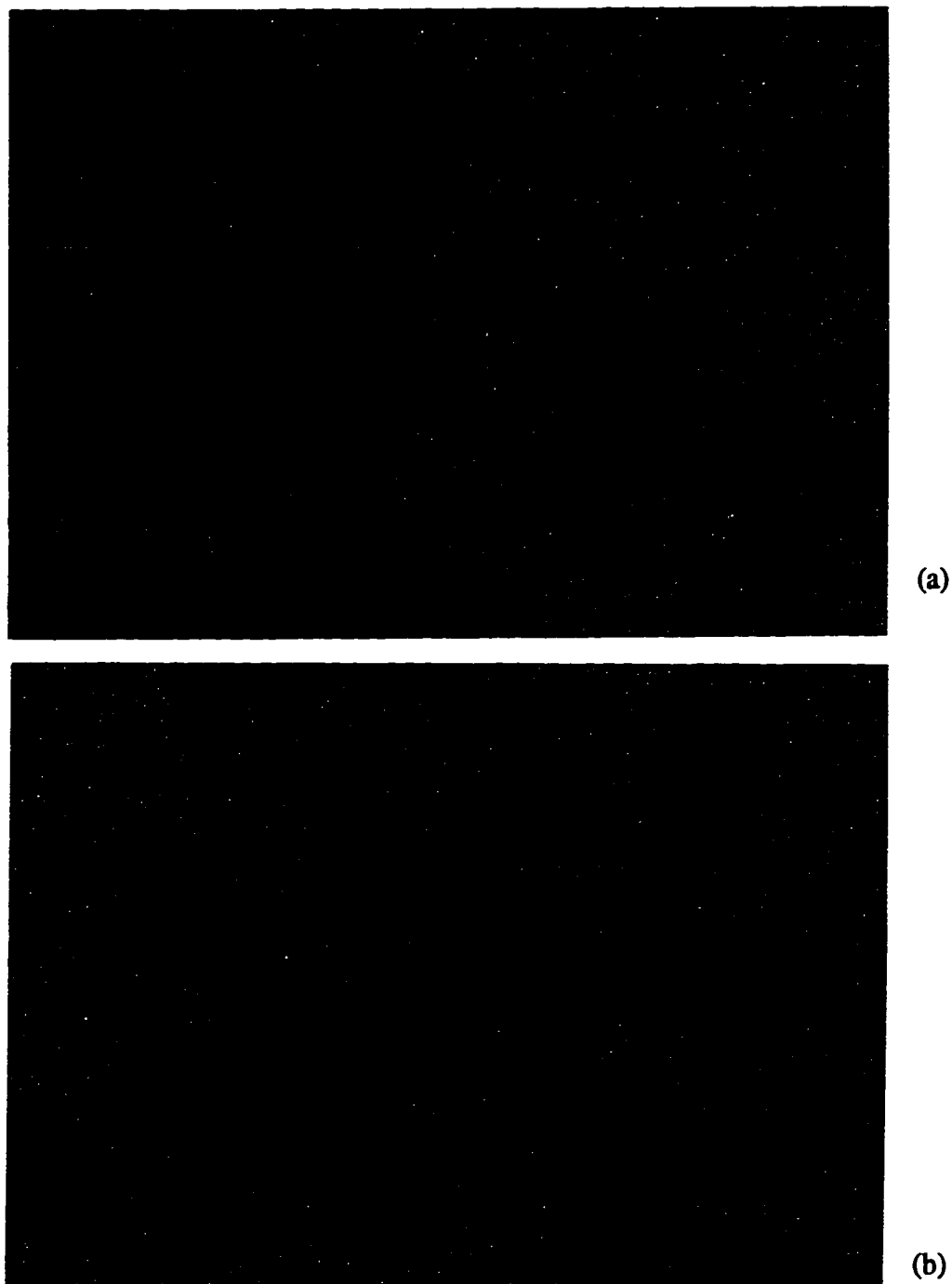


Figure 7-4. Light micrographs of vertical cross-sections of a 500-710 μm pore size polymer foam of thickness 1.9 mm (a) and a 150-300 μm pore size polymer foam of thickness 3.2 mm (b); both of which were initially seeded with 22.1×10^5 cells/cm 2 and cultured for 14 days. The sections were stained with hematoxylin and eosin to visualize osteoblasts and tissue formation. Magnification: 25x (a) and 100x (b).

4b). The extracellular matrix deposited by the osteoblasts had been mineralized as demonstrated by the von Kossa's staining of the histological foam sections. One such foam section is shown in Figure 7-5 which also reveals that the mineral deposits is predominantly covering the top surface of the construct similar to that observed in chapter 6.

Mineralization

Vertical cross-sections of the osteoblast/foam constructs stained by von Kossa's method, such as the one shown in Figure 7-5, were used to quantify the mineralized tissue by histomorphometric techniques. A maximum penetration depth of osseous tissue in the construct (distance from polymer surface to bottom of mineralized tissue front) of 218 ± 41 μm was reached for osteoblast/foam constructs of pore size 150-300 μm initially seeded with a high cell density (22.1×10^5 cells/cm²) after 56 days in culture (Fig. 7-6a). The penetration depth of mineralized tissue was found to be independent of polymer foam pore size, foam thickness, and initial osteoblast seeding density. The ratio of the mineralized tissue volume to top surface area of the foams after 56 days in culture was also independent of foam pore size, thickness, and initial seeding density (Fig. 7-6b).

7.4 Discussion

This study was carried out similarly to the previous study (described in chapter 6) with the exception that rat calvaria osteoblasts were seeded in the polymer foams instead of rat stromal osteoblasts and 100 nM of dexamethasone was supplemented to the culture media as opposed to 10 nM. Considering the notion that rat calvarial osteoblasts are a more homogenous population of osteoblasts and that higher concentrations of dexamethasone



Figure 7-5. Light micrographs of vertical cross sections of a 500-710 μm pore size foam initially seeded with 22.1×10^5 cells/cm 2 and cultured for 56 days. The sections were stained using Von Kossa's staining method (with safranin O as counterstain) which stains calcium phosphate deposits black. Digitized images of sections similar to these were used for histomorphometric quantification of mineralized tissue. Magnification: 25x.

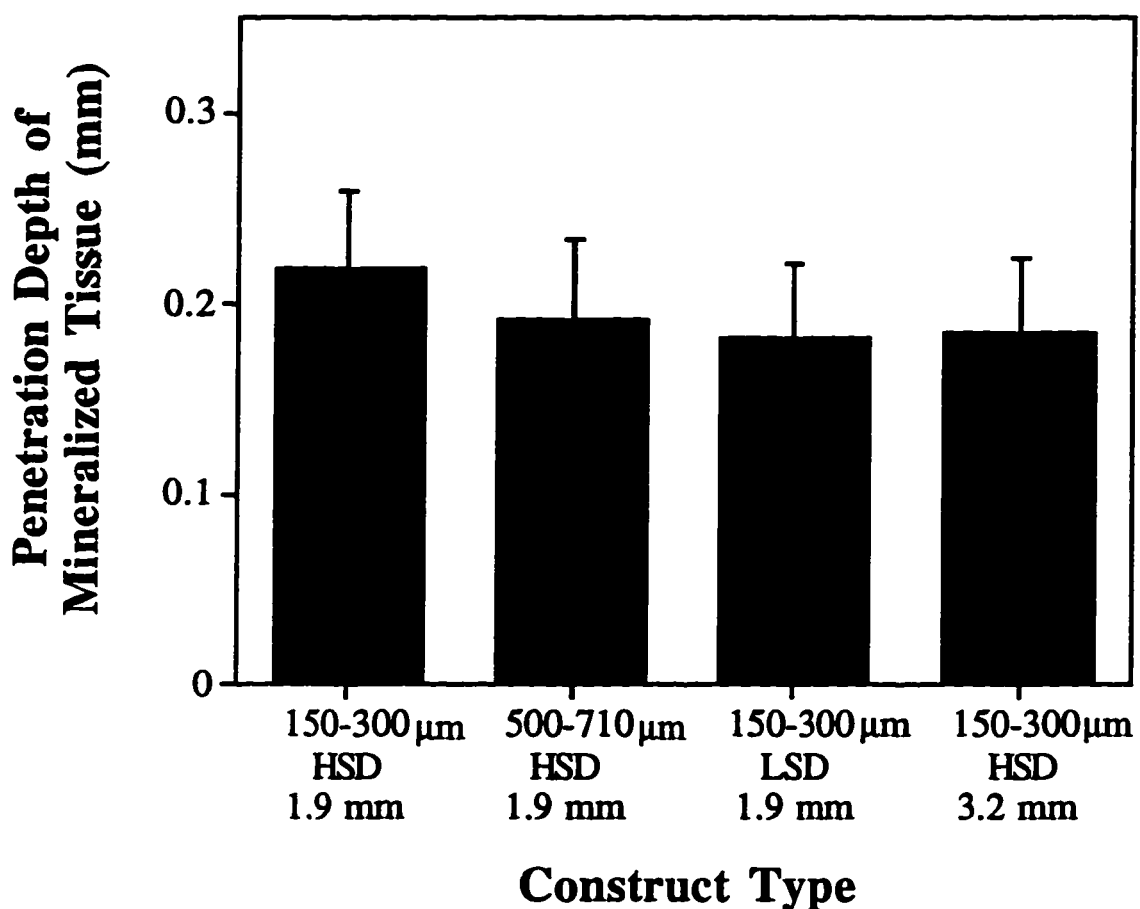


Figure 7-6a. Average maximum depth below the polymer surface that mineralized tissue was deposited in the osteoblast/foam constructs after 56 days in culture. These values were determined by histomorphometry using vertical tissue cross sections of the constructs stained with Von Kossa's silver nitrate method (similar to that shown in fig. 7-5). No significant differences were seen between constructs with different foam pore sizes, cell seeding densities, and thicknesses. The numbers in the abscise expressed in microns stand for the pore sizes of the foams, the HSD and LSD stand for high seeding density (22.1×10^5 cells/cm²) and low seeding density (11.1×10^5 cells/cm²), respectively, and the number expressed in millimeters stand for the thicknesses of the foams. Error bars designate means \pm s.d. for n=3.

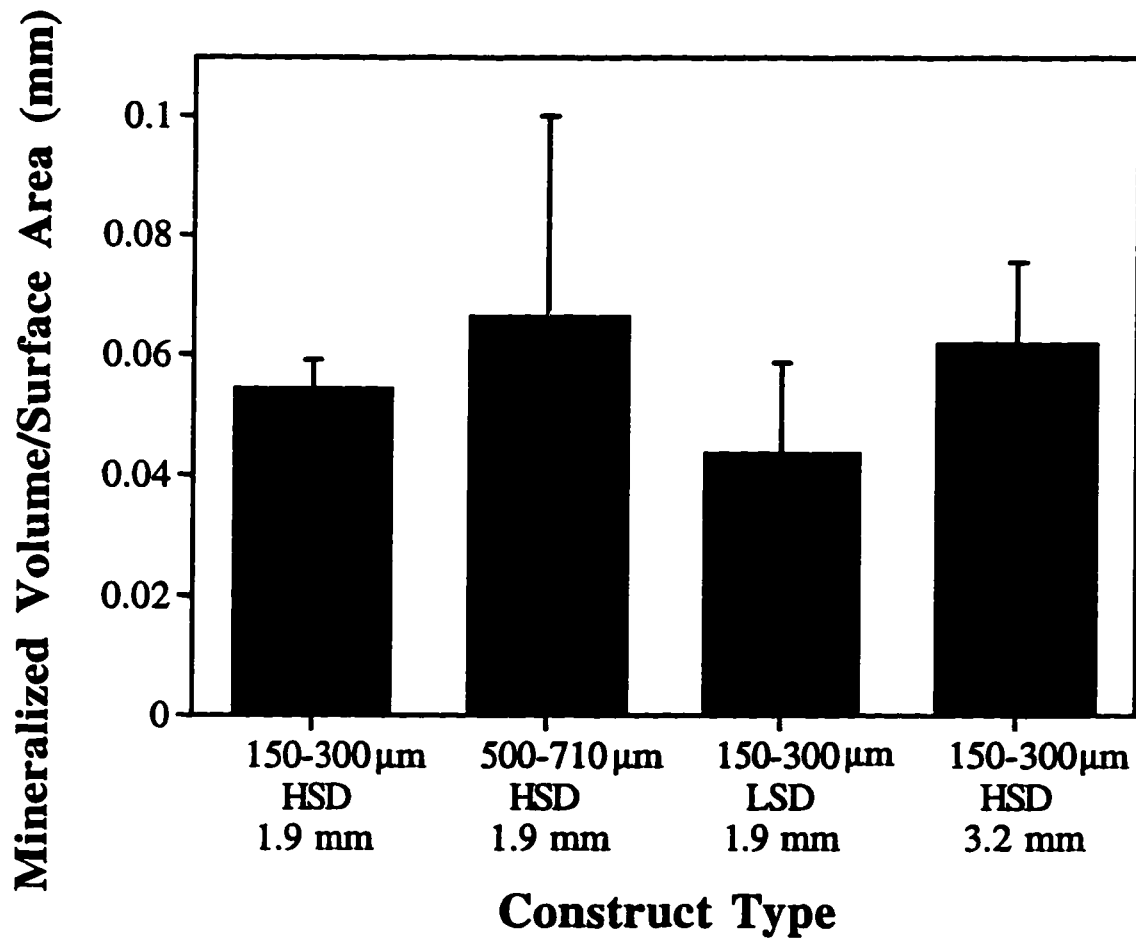


Figure 7-6b. Total mineralized volume/surface area in the osteoblast/foam constructs after 56 days in culture. These values were determined by histomorphometry using vertical tissue cross sections of the constructs stained with Von Kossa's silver nitrate method (similar to that shown in Fig. 7-5). No significant differences were seen between constructs of different foam pore sizes, thicknesses, and cell seeding densities. The numbers in the abscise expressed in microns stand for the pore sizes of the foams, the HSD and LSD stand for high seeding density (22.1×10^5 cells/cm 2) and low seeding density (11.1×10^5 cells/cm 2), respectively, and the number expressed in millimeters stand for the thicknesses of the foams. Error bars designate means \pm s.d. for n=3.

could potentially stimulate greater differentiated function, we were interested if rat calvarial osteoblasts cultured with a higher concentration of dexamethasone could proliferate, function, and produce more mineralized matrix than stromal osteoblasts cultured with 10 times less dexamethasone.

We found that the trends observed in this study are in agreement with those observed in the previous study. These trends include rapid osteoblast proliferation in foams seeded with a lower seeding density, eventually reaching comparable cell numbers to foams seeded with a higher osteoblast density at later times; increased alkaline phosphatase activity for all osteoblast/foam constructs over time and independency of ALPase activity on foam morphology or osteoblast seeding density at later times; and no significant differences in mineralized tissue penetration depth and mineralized tissue volume/surface area between foams with different pore size and seeding densities. Absolute experimental values for the cell counts and penetration depth were also comparable between the two studies; however, ALPase activity and mineralized tissue volume/surface area were less for the osteoblast/foam constructs in this study. This could be due to the higher dexamethasone concentration which was used in the culture media, indicating that a dexamethasone concentration closer to 10 nM than 100 nM can better stimulate the osteoblastic phenotype. This results is in agreement with a study by Bellows et al. [Bellows et al., 1987] where they found that a dexamethasone concentration of 10 nM resulted in greater numbers of mineralized nodules for rat calvarial osteoblasts than cultures with 100 nM dexamethasone.

CHAPTER 8

ECTOPIC BONE FORMATION BY IMPLANTATION OF OSTEOBLAST-SEEDED POLY(α -HYDROXY ESTER) FOAMS INTO THE RAT MESENTERY

8.1 Introduction

We have shown in chapter 4 that PLGA copolymers are suitable substrates for rat calvarial osteoblast attachment and proliferation. We have also demonstrated that rat calvarial osteoblasts readily migrate on these polymers (chapter 5). Finally, we have established three-dimensional cultures of rat marrow stromal osteoblasts in PLGA foams *in vitro*, suggesting the feasibility of producing bone-like tissue *in vivo* (chapter 6).

In this study, we have investigated ectopic bone formation in the rat mesentery by transplantation of polymer/cell constructs and asked the following questions: 1) Will osteoblasts grown *in vitro* on polymer scaffolds survive transplantation into a well vascularized site? 2) Will bone tissue be formed *in vivo*? 3) Does pore size of the polymer scaffolds in the range of 150 to 710 μm affect the extent of new bone growth?

8.2 Materials and Methods

Polymer foam fabrication

PLGA foams of two different pore sizes were fabricated by a solvent-casting particulate-leaching technique described in chapter 6. The two types of polymer foams were made 90% porous with 75:25 PLGA (Birmingham Polymers) having pores ranging in diameter from either 150-300 or 500-710 μm . The foams were approximately 1.9 mm

thick and cut into 7 mm diameter discs. They were stored, prewetted and washed as described in chapter 6.

Stromal osteoblast isolation, seeding, and culture

Stromal osteoblastic cells were obtained from the marrow of young adult male (6 weeks old, 150-170 g) Fisher 344 rats (Harlan Sprague Dawley, Indianapolis, IN) as described in chapter 6. Cells were counted by Coulter Counter and diluted to 17,525,000 cells/mL in complete media (chapter 4) containing 10 nM dexamethasone (Sigma). Aliquots of 15 µL of the cell suspensions were seeded onto the top of pre-wet foams placed in the wells of 24 well plates, resulting in a seeding density of 6.83×10^5 cells/cm² (or 263,000 cells/foam) when normalized to the top surface area of the foams (this is equivalent to the lower cell seeding density used in the study described in chapter 6). The foams were left undisturbed in an incubator for 3 hours to allow the cells to attach to the foams, after which time an additional 1 mL of complete media containing 10 nM dexamethasone was added to each well. The cell-seeded foams were cultured for 7 days prior to implantation, with the medium containing 10 nM dexamethasone changed every 2 days.

In Vivo Implantation

Fisher 344 rats (250 g) were anesthetized by methoxyflurane (Pitman-Moore, Mundelein, IL) inhalation and secured in a supine position. After aseptic preparation, the abdomen was incised in the midline and a portion of the small bowel was withdrawn from within the abdominal cavity. Two foams were implanted in each of 24 rats at distal locations between folds of the mesentery [Mikos et al., 1993]. The foams were

immobilized by suturing the mesenteric folds together, forming a pocket. One 150-300 μm and one 500-710 μm osteoblast seeded polymer foam were implanted into each test rat. Foams without cells (pre-wet and soaked in media) of each pore size were also implanted as controls into a separate group of animals. The two implanted foams were distinguishable by using different colored non-absorbable suture material (monofilament, 5-0, Ethicon, Somerville, NJ) used for their immobilization. The mesentery and intestines were returned to the abdominal cavity and the abdominal wall was closed with an absorbable suture. Animals were maintained for 1, 7, 28, or 49 days then euthanized by ethyl ether inhalation. Six rats were euthanized at each time; three with foams seeded with cells and three with control foams without cells. The foams were harvested and stored in 10% neutral buffered formalin until embedded.

Histological preparation

The fixed foam constructs were cut in half with a razor blade, and one of each half was decalcified in a 14% EDTA solution ($\text{pH}=7.4$) for 36 hours. Standard dehydration in sequentially increasing ethanol solutions to 100% ethanol was performed on both construct halves, followed by immersion in Hemo-De (Fisher Scientific, Pittsburgh, PA), paraffin saturated Hemo-De, and finally molten paraffin. Tissue blocks were sectioned at 5 μm . The decalcified samples were stained with hematoxylin and eosin (H&E) for visualization of cells and demonstration of bone tissue formation and the non-decalcified samples were stained with von Kossa's silver nitrate staining method for demonstration of matrix mineralization.

Histomorphometry

The elements identified for histomorphometry were mineralized bone-like tissue, non-mineralized bone-like tissue, fibrovascular tissue, residual polymer, and void space (representing empty pores remaining in the polymer). The penetration depth of mineralized bone tissue, the bone volume per surface area (both mineralized bone tissue and total bone tissue), and the percent mineralized bone tissue in the volume of the foams penetrated by mineralized bone tissue were calculated by histomorphometric techniques. Instrument setup is described in chapter 6.

The penetration depth of mineralized tissue in the foams was determined by manually drawing a line with a software tool on the digitized image of the von Kossa stained cross-section from the outer edge surface, normal to the edge, to each mineralized deposit (black-colored) found in the sections. These length measurements in pixels were converted to mm by calibration of the system using a micrometer slide to determine pixel/mm ratio. The number of penetration depth measurements for each section depended on the number of mineralized deposits found in each section which ranged from 3 to 20. Measurements of each and every mineralized deposit were taken and averaged to obtain a mean penetration depth for each section.

The mineralized tissue (black stained regions in the von Kossa stained sections) and the total bone-like tissue (from the H&E sections) were distinguishable from the other tissue, such as fibrovascular tissue, and polymer material by their gray level intensity and were thus selected and measured for area. The resulting measured areas in pixels were converted to areas in mm^2 following calibration of the system. The length of each cross-section was also determined using a software tool as described above. The bone area per length was calculated by dividing the bone tissue areas (total or mineralized) by the length of the respective cross-sectional region. The standard stereological relationship that the

area/length of a given phase in a two-dimensional field approximates the volume/surface area in three-dimensions was used to provide an estimate of the bone volume/surface area.

The percent of mineralized tissue in the foam volume containing mineralized deposits was calculated by dividing the total mineralized area (determined above) by the total area that had been penetrated by mineralized tissue (estimated by multiplying the penetration depth by the length of the sections). Percent areas are equivalent to percent volumes in this case because the third dimension is the same for both quantities.

Gel Permeation Chromatography

The weight average molecular weight of the polymer foams was determined for all samples by gel permeation chromatography. After sectioning, histological samples were removed from paraffin and rehydrated by immersing the foams in molten paraffin, paraffin saturated Hemo-De, and sequentially decreasing solutions of ethanol. Samples were first dried overnight in a fume hood and then placed under vacuum (50 mm Hg) to remove remaining water. The scaffolds were dissolved in HPLC grade chloroform and filtered with a glass syringe equipped with a 0.45 μm filter to remove any insoluble components. The dissolved samples were then measured for molecular weight as described in chapter 6.

Statistical Analysis

All measurements were collected in triplicate sections and expressed as means \pm standard deviations. Single factor analysis of variance (ANOVA) was employed to assess statistical significance of results for all the polymer/cell constructs whose single factor was pore size, bone tissue type, or day. In addition, a two-tailed unpaired t-test was used to

evaluate the significance of the pore size on penetration depth of mineralized tissue after 1, 28, or 49 days post-implantation time.

8.3 Results

An organized, mineralized bone-like tissue, which was not present at day 1 post-implantation, began to form in the polymer/cell constructs by day 7 *in vivo* (Figs. 8-1 and 8-2) indicating that transplanted cells survived and maintained their differentiated function. This bone-like tissue was found in all cell seeded foam samples at all time points up the final study point, 49 days post-implantation (Fig. 8-3). Osteocyte-like cells appeared embedded in the bone tissue matrix deposited by the transplanted osteoblasts (Figs. 8-1 and 8-3). Capillaries were seen running adjacent to the islands of bone-like tissue (Fig. 8-3b). Fibrovascular tissue filled the remaining areas in the constructs not occupied by bone-like tissue, polymer material or void space. The control foams (without seeded cells) contained only fibrovascular tissue with no traces of bone-like tissue (section not shown).

The penetration depth of mineralized tissue in the foams remained constant over time and was not effected by pore size. At day 7 post-implantation the average penetration depth was $288 \pm 33 \mu\text{m}$ and $294 \pm 49 \mu\text{m}$ for cell seeded foams with pore sizes of 150-300 and 500-710 μm , respectively. The average penetration depth of mineralized tissue found in the constructs explanted after 49 days *in vivo* ranged from $190 \pm 50 \mu\text{m}$, for foams with 500-710 μm pores, to $370 \pm 160 \mu\text{m}$, for foams with 150-300 μm pores (Fig. 8-4).

The mineralized tissue volume per surface area (calcified tissue stained using von Kossa's method) and the total bone-like tissue volume per surface area (decalcified tissue stained with H&E) remained constant over time and were independent of pore size in the range of 150-710 μm (Figs. 8-5 and 8-6). For example, at day 28 post-implantation the mineralized tissue volume per surface area was $16.9 \pm 10.4 \mu\text{m}$ for a 150-300 μm pore size

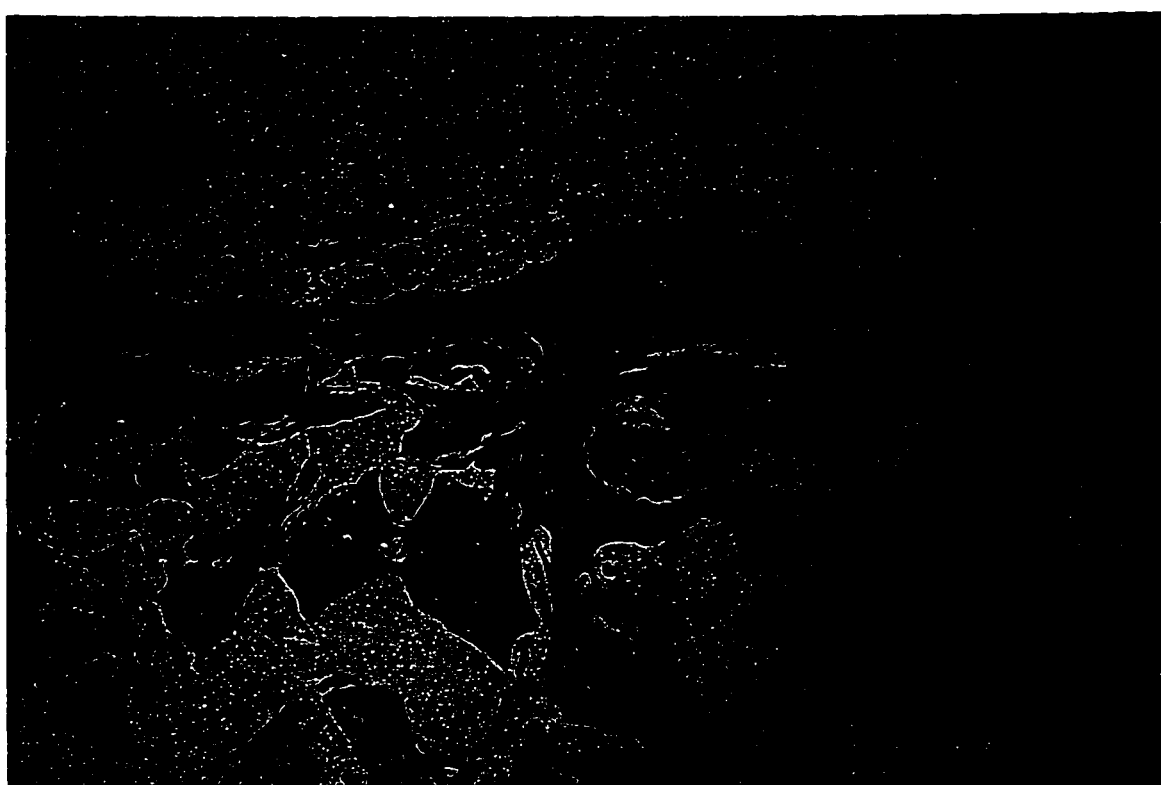


Figure 8-1. Histological cross-section of a cell-seeded polymer foam having a pore size range of 150-300 μm which was explanted from the rat mesentery after 7 days *in vivo*. The foam was initially seeded with 6.83×10^5 cells/cm 2 and cultured for 7 days *in vitro* prior to implantation. Bone-like tissue is distinguishable from fibrovascular tissue by its greater abundance of extracellular matrix (light pink) and has fewer cells. Polymer material, and possibly void space, occupied the remaining volume of the construct which appear clear in the stained section. The sample was de-calcified and stained with H&E. Magnification: 25 X.

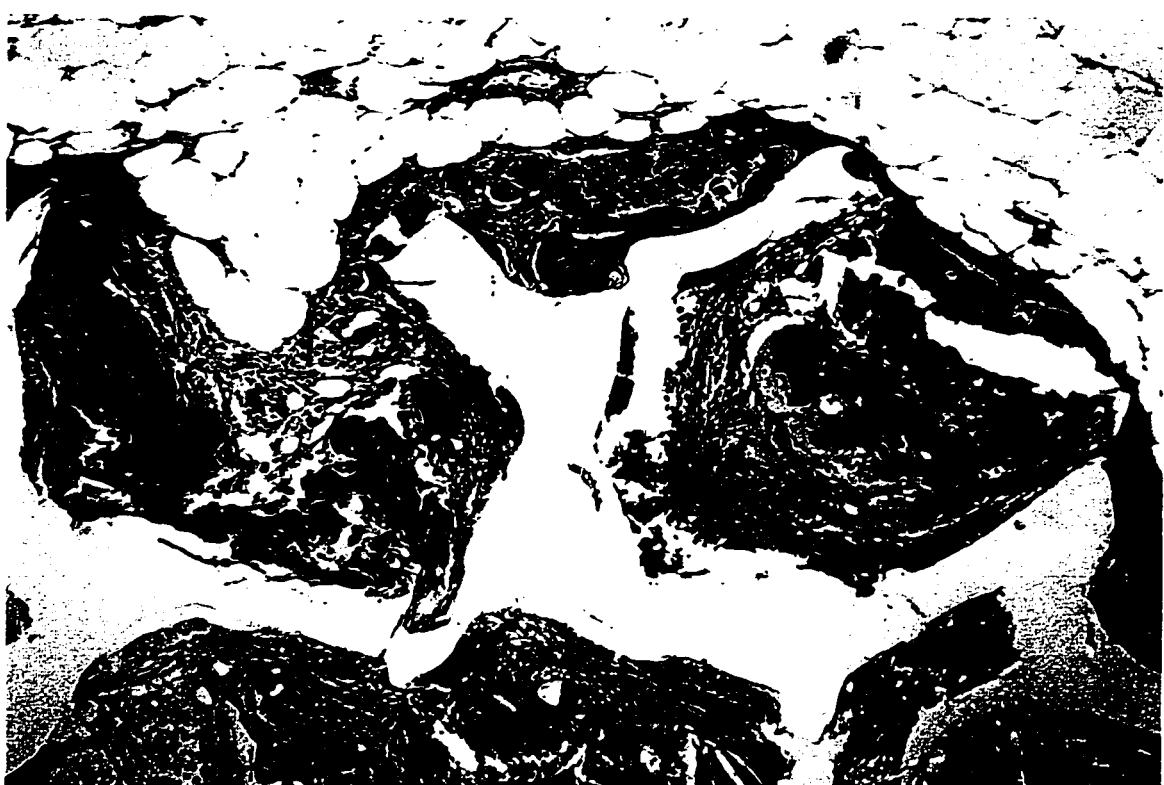


Figure 8-2. Histological cross-section of a cell-seeded polymer foam having a pore size range from 500-710 μm explanted from the rat mesentery after 7 days *in vivo*. The foam was initially seeded with 6.83×10^5 cells/cm 2 and cultured for 7 days *in vitro* prior to implantation. The sample was stained using von Kossa's method which stains calcium phosphate deposits black. Mineralized bone-like tissue has formed near the outer edge of the foam and is surrounded by fibrovascular tissue. Non-mineralized bone with embedded osteocyte-like cells is also visible surrounding some of the mineralized tissue. Polymer material, and possibly void space, occupied the remaining volume of the construct which appear clear in the stained section. Magnification: 25 X.

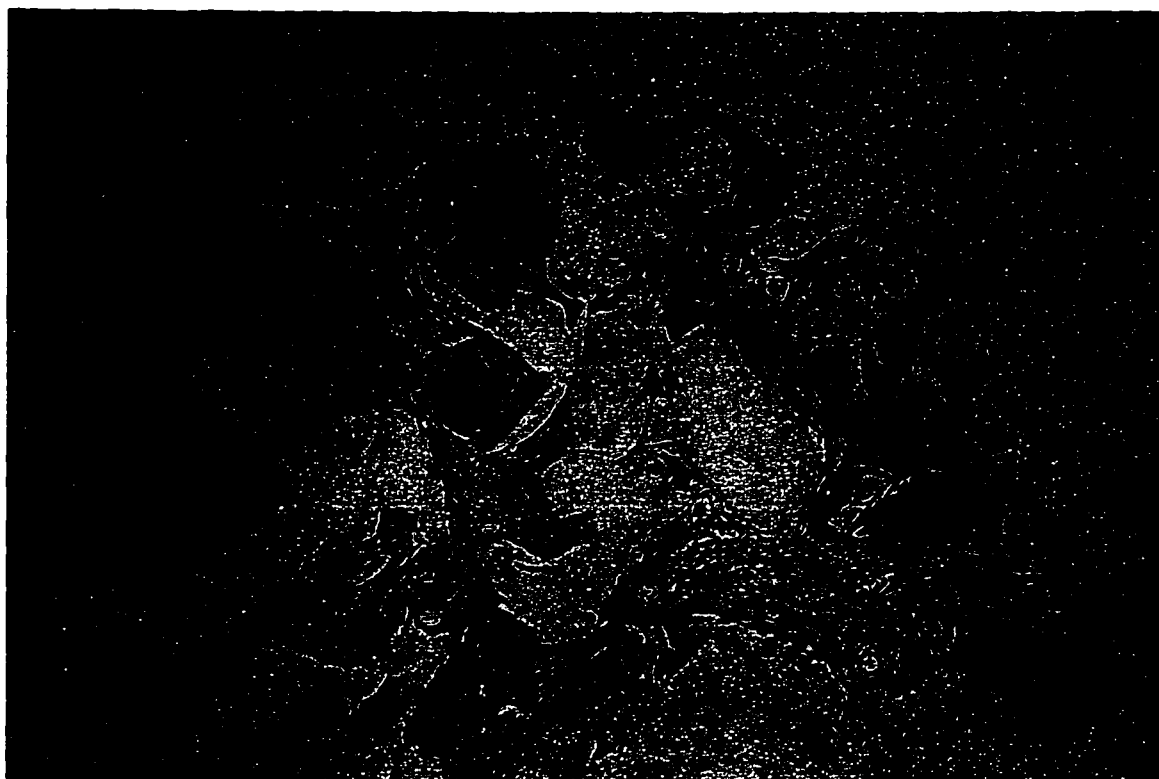


Figure 8-3a. Histological cross-section of a cell-seeded polymer foam having a pore size range from 150-300 μm explanted from the rat mesentery after 49 days *in vivo*. The foam was initially seeded with 6.83×10^5 cells/cm 2 and cultured for 7 days *in vitro* prior to implantation. The picture taken shows the edge of the sample near one end of the cross-section. Bone-like tissue has formed near the outer edge of the foam (light pink region with fewer cells) and is surrounded by fibrovascular tissue. The sample was decalcified and stained with H&E. Magnification: 25 X.

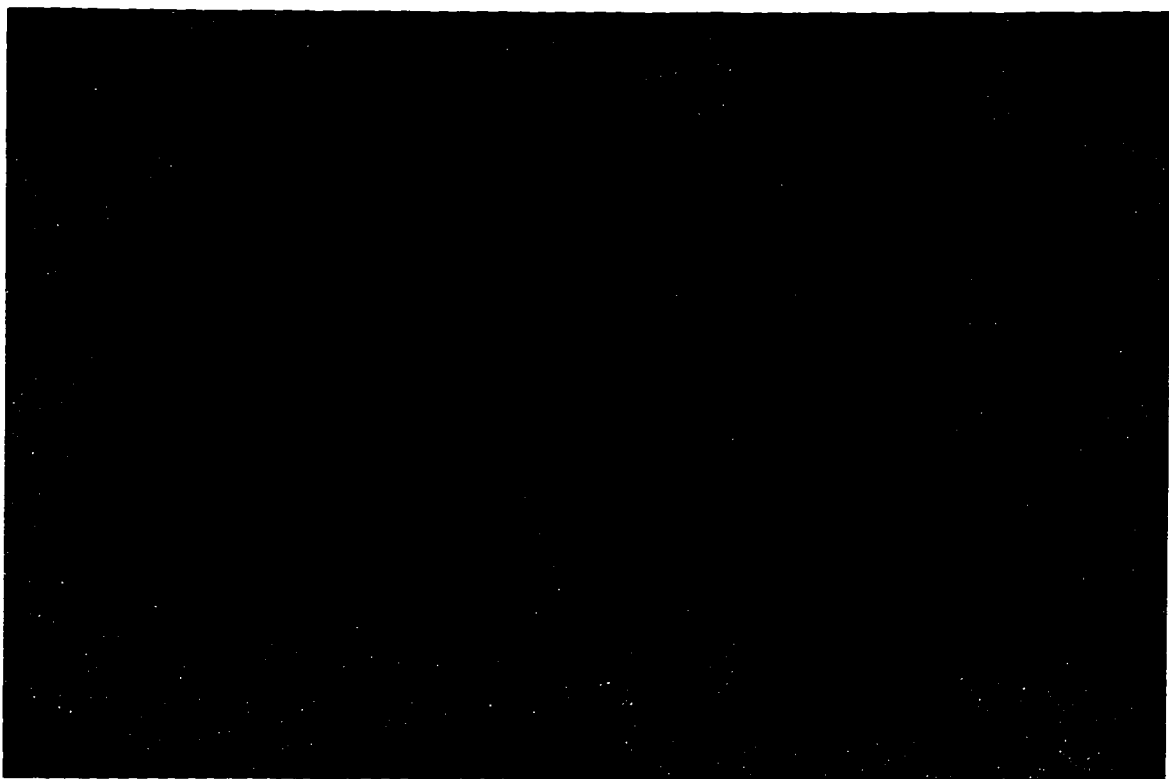


Figure 8-3b. Magnified view of the histological section in figure 8-3b. Osteocytic cells appear embedded in the tissue matrix deposited by the transplanted osteoblasts. Capillaries are seen running through the fibrovascular tissue adjacent to the bone-like tissue. Magnification: 100 X

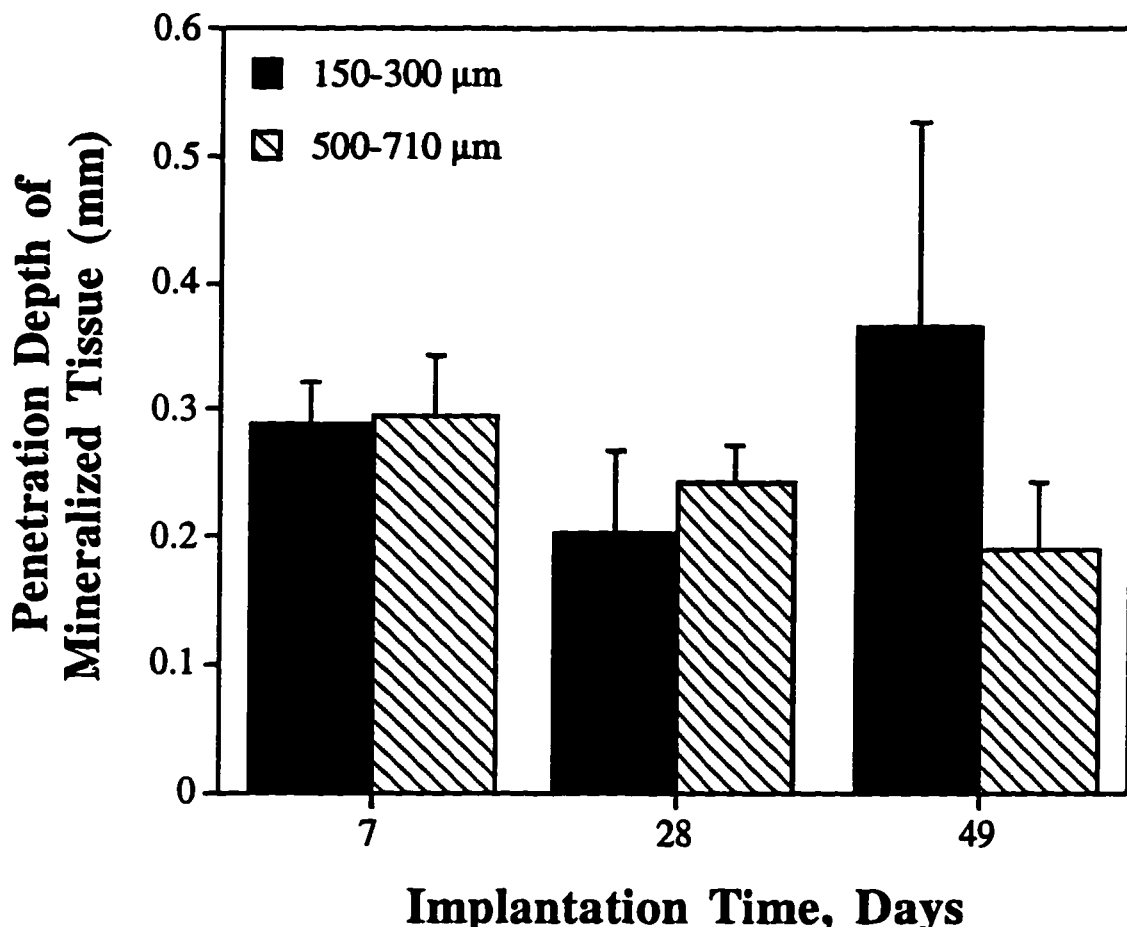


Figure 8-4. Average maximum depth from the outer edge of the polymer foams that mineralized deposits were found in the polymer foam constructs (penetration depth) at different implantation time points and for foams with two different pore sizes. Histomorphometric analysis of von Kossa stained cross-sections of the constructs were used to determine the average depths. No significant differences were found between the foams of different pore sizes or at different implantation times. Error bars designate means \pm s.d. for n=3.

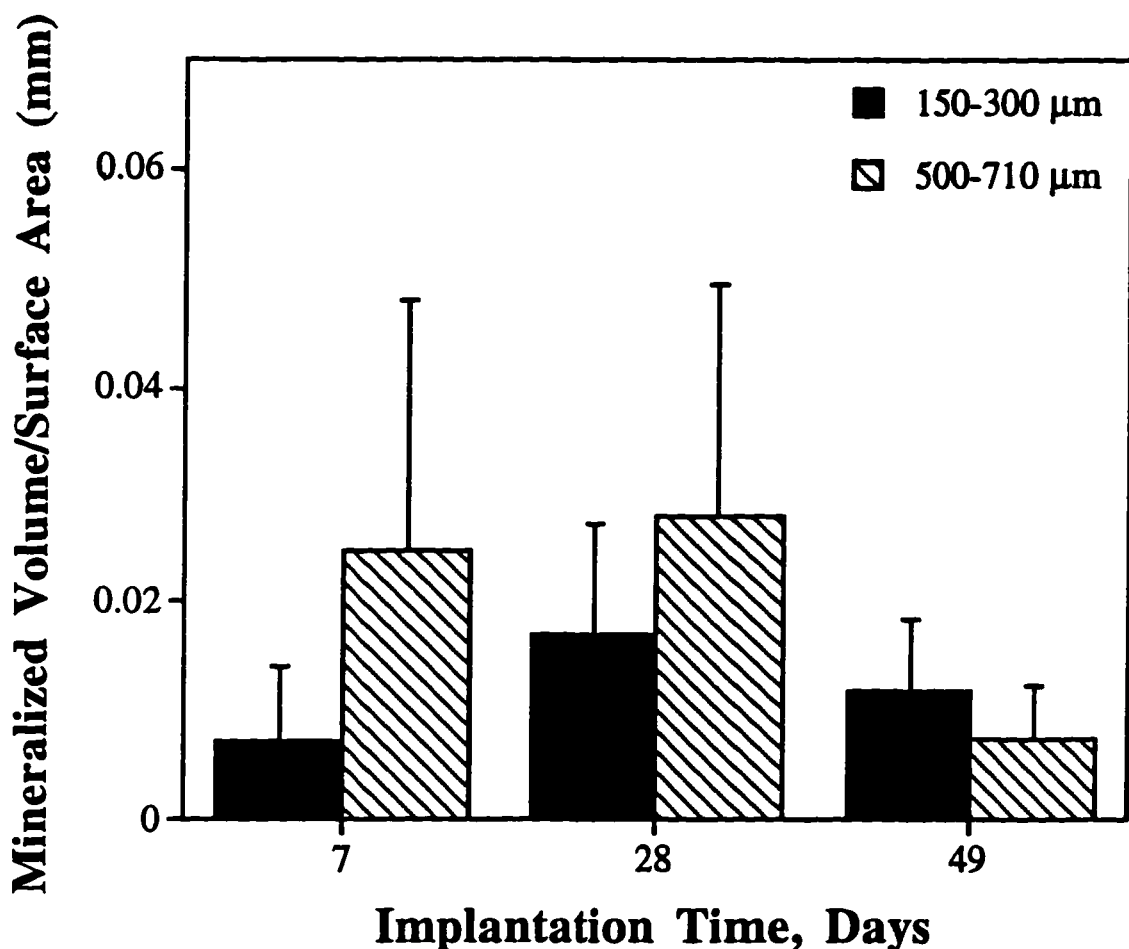


Figure 8-5. Total mineralized bone tissue volume normalized to the surface area of the constructs as a function of implantation time and foam pore size. These values were determined by histomorphometric analysis of vertical cross-sections through the constructs stained using von Kossa's method (similar to that shown in Fig. 2). No significant differences were found between the foams of different pore sizes or at different implantation times. Error bars designate means \pm s.d. for n=3.

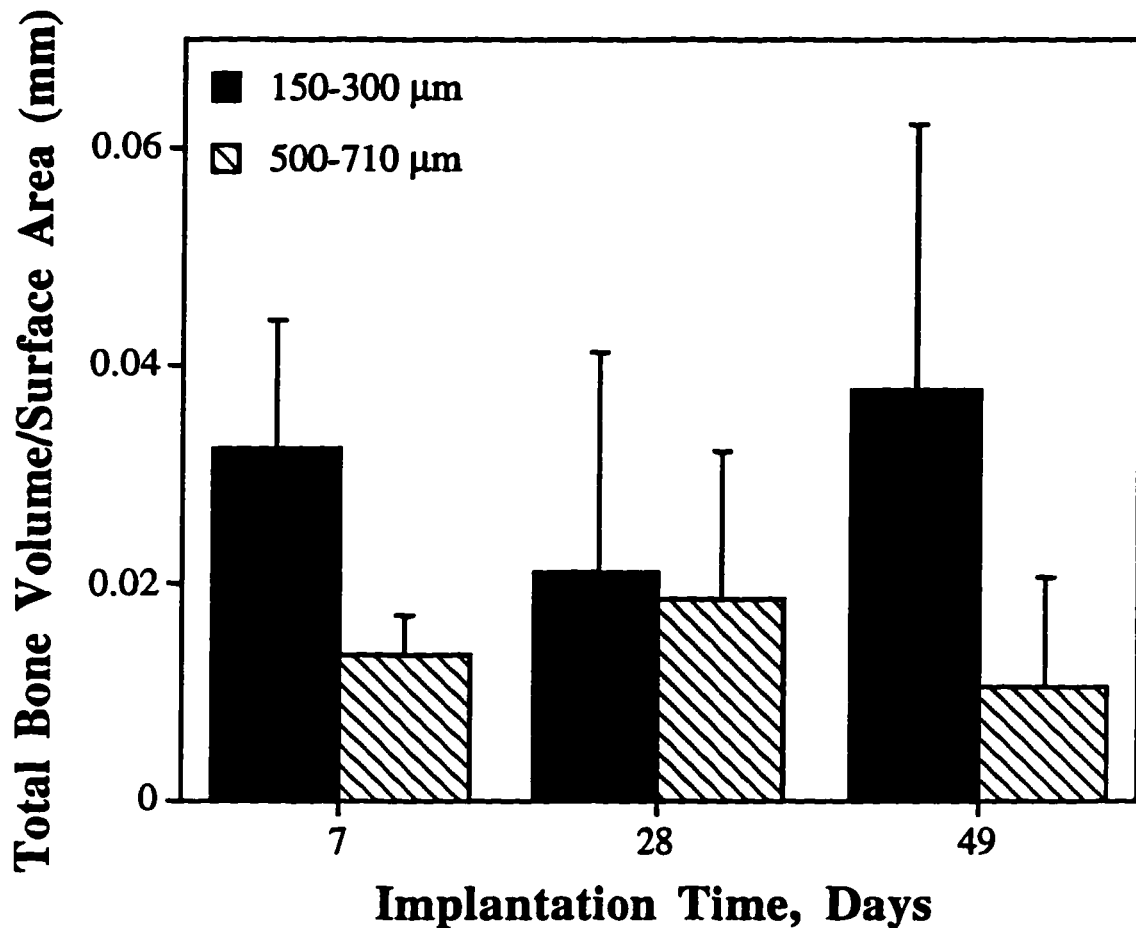


Figure 8-6. Total bone-like tissue volume normalized to the surface area of the constructs as a function of implantation time and foam pore size. These values were determined by histomorphometric analysis of vertical cross-sections through the constructs stained with H&E (similar to that shown in Fig. 1). No significant differences were found between the foams of different pore sizes or at different implantation times. Error bars designate means \pm s.d. for n=3.

foam and $28.0 \pm 21.4 \mu\text{m}$ for a 500-710 μm pore size foam. The total bone (both mineralized and non-mineralized) volume/surface area in the foam constructs was not significantly greater than the mineralized volume/surface area at any time point, indicating that most of the bone in the constructs was in the mineralized form. Moreover, the percent of mineralized tissue found within the volume of the construct where mineralization occurred did not depend significantly on foam pore size or the amount of time the foams were implanted (Fig. 8-7).

Weight average molecular weight was found to decrease significantly over time for both cell seeded samples (Fig. 8-8) and no cell control scaffolds (data not shown). For example, the weight average molecular weights of 150-300 μm and 500-710 μm pore size, cell seeded scaffolds decreased from $30,700 \pm 5400$ and $26,200 \pm 4400$ respectively at day 1 after implantation to $13,800 \pm 1300$ and $12,000 \pm 1200$ respectively at 49 days post-implantation.

8.4 Discussion

Transplantation of rat marrow stromal cells on polymer scaffolds into the mesentery of the rat was performed to determine 1) whether cells could survive when transplanted into a well-vascularized site, such as the mesentery; 2) the amount of bone tissue, if any, the transplanted cells would produce; and 3) whether pore size of the scaffolds in the range of 150 to 710 μm would affect the extent of new bone growth. Our results demonstrated that these transplanted cells were able to survive and continue functioning in this well-vascularized *in vivo* site. Similar cell transplantation success into the rat mesentery has been achieved with hepatocytes in poly(lactic acid) sponges [Mooney et al., 1995] and poly(glycolic acid) woven sheets [Johnson et al., 1994].

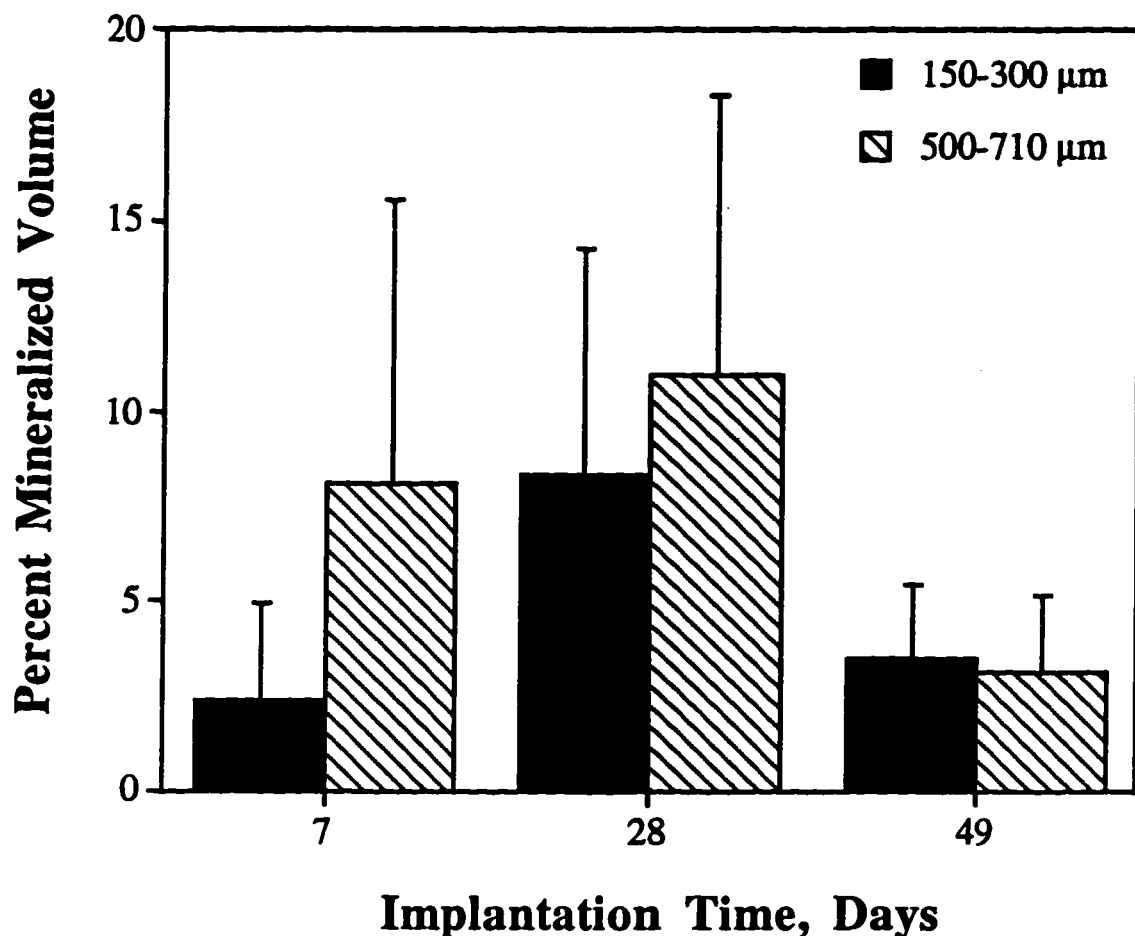


Figure 8-7. Percent of mineralized tissue found in the volume of the construct penetrated by bone-like tissue as a function of implantation time and foam pore size. The area of mineralized tissue in the sections stained by von Kossa's method (black stained regions) was normalized to the area within the construct, from the surface, in which bone-like tissue was found. No significant differences were found between the foams of different pore sizes or at different implantation times. Error bars designate means \pm s.d. for n=3.

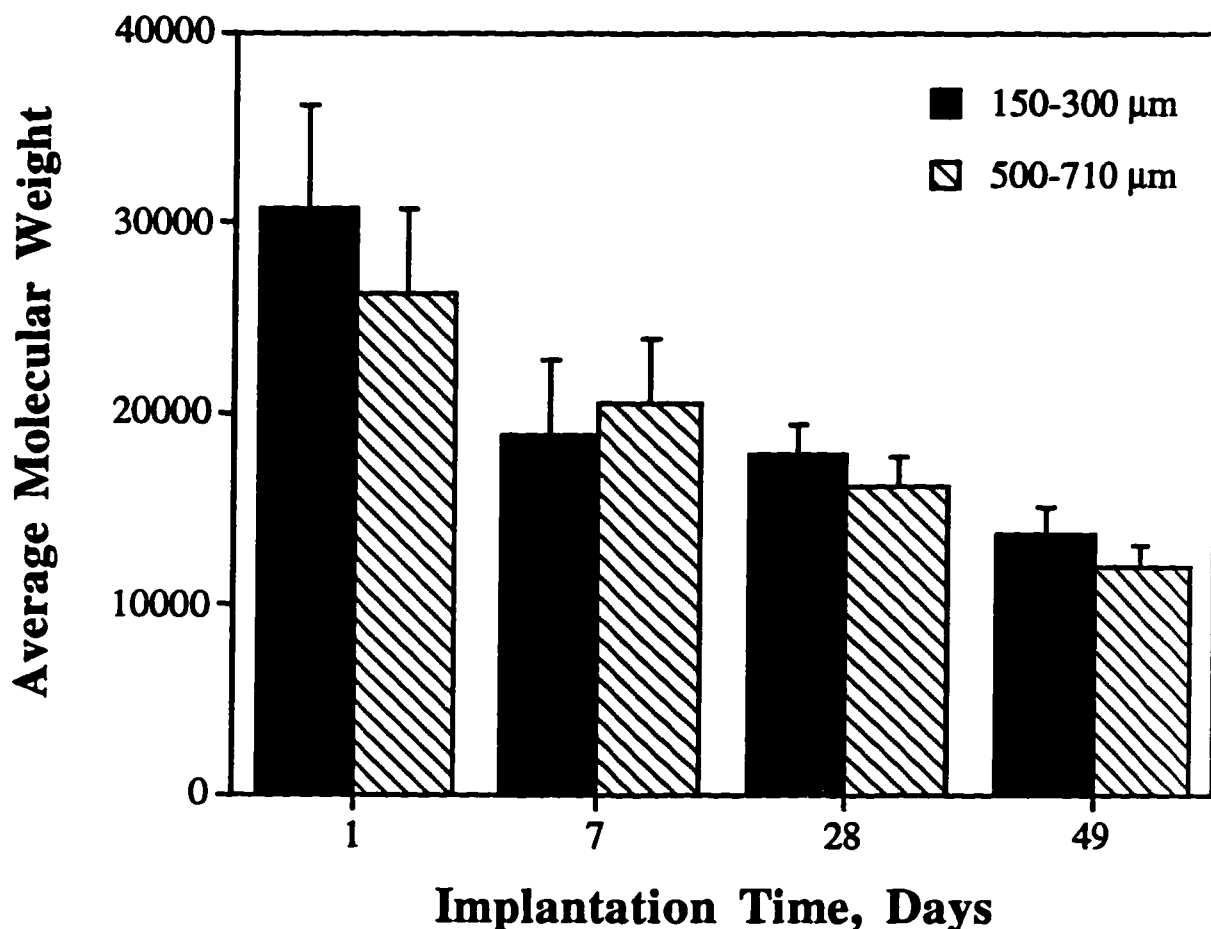


Figure 8-8. Change in the weight average molecular weight over time *in vivo* for cell seeded foams of different pore sizes. Molecular weights were determined by gel permeation chromatography and were found to significantly decrease over time. Before cell seeding (that is 7 days prior to implantation), the molecular weights of the 150-300 μm and 500-710 μm polymer foams were $39,600 \pm 270$ and $39,200 \pm 1200$, respectively. No significant differences were found between the foams of different pore sizes. Error bars designate means \pm s.d. for n=3.

We estimate that there were approximately 1.8×10^5 cells/foam at the time of implantation based on previous cell count results from chapter 6 using the same seeding density and foams with a pore size range of 300-500 μm . Most of the bone-like tissue was found within 300 μm of the outer edge of the construct. The fact that the cells were only on one side of the construct is due to the non-homogeneous cellular distribution in the foams prior to implantation, resulting from our method of cell seeding on only one side of the foams. It was not expected to see cells deeper than 300 μm from the surface at the time of implantation because osteocyte survival by diffusion is limited to distances of 200-300 μm [Heslop et al., 1960; DeLeu and Trueta, 1965].

In the study described in chapter 6, marrow stromal cells were seeded at the same cell density by the same technique and cultured up to 56 days *in vitro*. Results from the 56 days in culture can be compared to results from this study at 49 days post-implantation because the cells were cultured for an additional 7 days *in vitro* prior to implantation. The penetration depth of mineralized tissue found for constructs at the final time point was comparable for both studies, but they differed at earlier time points. While the penetration depth remained fairly constant over time in the present study, an increase in penetration depth between days 14 and 56 was observed *in vitro*. We believe that this was caused by the invasion of vascular tissue which supplied cells on the interior of the foams better access to nutrients than their counterparts being cultured *in vitro*. Based on studies of pore effects on the fibrovascular tissue ingrowth into polymer foams [Wake et al., 1994], we estimate that most of the available void space is filled with vascular tissue by 7 days post-implantation. Because the metabolic needs of the cells *in vivo* were better being met, they were able to secrete more matrix and mineralize more quickly at early time points than cells *in vitro*.

The mineralized volume per surface area and total bone-like volume per surface area found in the foam constructs had maximal values of 0.028 ± 0.021 mm (500-710 μm pore

size, day 28) and 0.038 ± 0.024 mm (150-300 μm pore size, day 49), respectively. However, in our previous *in vitro* study, the mineralized volume per surface area was as great as 0.083 ± 0.021 after 56 days in culture for foams with a pore size range of 300-500 μm seeded with the same cell density. The mineralized tissue volume per surface area increased significantly over time for the previous study, whereas, there was no significant change over time for this study. This result indicates that the osteoblasts continued to lay down new matrix at the outer polymer surface edge (adjacent to the media) *in vitro* as long as space was available and their metabolic needs were being met. It may be that the rapid ingrowth of fibrovascular tissue may be overtaking the available space in the foam constructs implanted *in vivo*, reaching up to 100% by as little as 7 days [Wake et al., 1994], and thereby impeding the osteoblasts to continue to lay down new bone matrix at later implantation time points. This would explain why the percent of mineralized tissue in the volume penetrated by bone-like tissue did not significantly change over time either.

Pore size has been found to be an important parameter for bone ingrowth into ceramics [Dennis et al., 1992] and fibrovascular invasion into polymer scaffolds [Wake et al., 1994]. We were therefore interested to determine if it had any affect on the growth of transplanted bone cells. Penetration depth, mineralized tissue per surface area, and percent of bone formation were all found to be independent of pore size in this study. Both bone ingrowth into ceramics and fibrovascular invasion into polymer scaffolds rely on the migration or movement of the tissue in question. The bone-like tissue that was formed in the polymer constructs in this study originated from the transplanted cells which were already present in the foams upon implantation. This suggests that pore size may only affect the ingrowth of cells and tissue and not tissue growth in general, at least in the range of 150-710 μm .

The degradation rate of the PLGA foams *in vivo* was higher than that observed *in vitro* for the same pore sizes and cell seeding densities (chapter 6). Although the polymer

degradation products (lactic and glycolic acid) are processed through normal metabolic pathways and are ultimately eliminated from the body, a sudden rise in their concentration can render the local tissue environment acidic resulting in bone demineralization [Thomson et al., 1995]. However, our data suggest that any released degradation products were removed by the vascular tissue grown into the foam constructs and did not affect the extent of mineralization during the course of the 49 day experiment.

CHAPTER 9

CONCLUSIONS

Early passaged rat osteoblasts were cultured on synthetic biodegradable polymers as an *in vitro* model of bone formation. Osteoblasts attached to, and proliferated on, all the poly(α -hydroxy ester) films examined during a 14 day culture period. Cultured osteoblasts also retained their phenotype throughout the experimental period as indicated by high expression of ALPase activity and collagen synthesis. The osteoblast ALPase activity was different from that of osteoblast-like cells. The results of osteoblast function on biodegradable polymers are also in good agreement with reports of osteoblast cultures on non-degradable orthopedic biomaterials.

Rat calvarial osteoblasts from isolated cultures and bone chips were also cultured on poly(α -hydroxy ester) films and allowed to migrate and proliferate for up to 14 days. Confocal and light micrographs illustrated that a monolayer of osteoblasts was present in the migration fronts and multi-cell layers formed shortly behind the fronts. Osteoblast migration was observed for all the cultures and did not depend on the copolymer ratio between the 85:15 PLGA and 75:25 PLGA substrates examined. However, the migration rate was greater for osteoblast cultures seeded with a higher cell density. This data suggests that it may be feasible to create biodegradable polymer/osteoblast constructs for the regeneration and repair of bone tissue by relying on the migration of osteoblasts into polymer foams from the bone surrounding the implant site.

Rat stromal osteoblasts cultured on 3-D porous poly(lactic-co-glycolic acid) foams can form a calcified bone-like tissue *in vitro*. Osteoblast proliferation and function were not affected by polymer foam pore size in the range of 150-710 μm but increased over time for all constructs. Cell seeding density affected initial osteoblast attachment and proliferation rates, but differences became less significant over time with no measurable difference in

function. Similar cultures of rat calvarial cells on these foams demonstrated similar trends and also established that foam thickness has no effect on osteoblast proliferation and function in these constructs. Viable cells may be supported for only short distances into the 3-D matrices under static culture conditions. Achieving cell survival beyond 240 μm from the outer surface in large 3-D porous scaffolds may require altering culture conditions to improve delivery of nutrients deep within the constructs.

The ability to grow bone-like tissue by osteoblast transplantation in a well vascularized ectopic site was established in our final study. The bone-like tissue formed islands which were surrounded by fibrovascular tissue. This fibrovascular tissue is believed to be responsible for the large penetration depth of mineralized tissue seen initially in the study compared to the penetration depths for a previous *in vitro* study by providing the metabolic needs for the osteoblasts in the interior region of the constructs. We have also concluded that the fibrovascular tissue ingrowth is responsible for the lower mineralized bone volume/surface area found at later times in this study compared to an *in vitro* study because it occupied the remaining available space and thereby impeded osteoblast growth. These results are encouraging and indicate the regenerative potential of osteoblast seeded polymer scaffolds for new bone growth when implanted in orthotopic sites where transplanted cells and secreted bone growth factors may further induce bone ingrowth from adjacent bone.

These studies have shown that poly(α -hydroxy esters) have great potential as a scaffolding material for bone regeneration by osteoblast transplantation. The polymers are able to support the attachment, proliferation and function of osteoblasts both in two-dimensional and three-dimensional culture systems. They also allow for the ingrowth of vascular tissue which is necessary to support the metabolic needs of the transplanted cells.

REFERENCES

- Arnow, M.A., Gerstenfeld, L.C., Owen, T.A., Tassinari, M.S., Stein, G.S. , Lian, J.B. (1990): Factors that Promote Progressive Development of the Osteoblast Phenotype in Cultured Fetal Rat Calvaria Cells. *J. Cell. Phys.* **143**:213-221.
- Ashton, B.A., Abdullah, F., Cave, J., Williamson, M., Sykes, B.C., Couch, M. , Poser, J.W. (1985): Characterization of Cells with High Alkaline Phosphatase Activity Derived from Human Bone and Marrow: Preliminary Assessment of their Osteogenicity. *Bone* **6**:313-319.
- Atala, A., Vacanti, J.P., Peters, C.A., Mandell, J., Retik, A.B. , Freeman, M.R. (1992): Formation of Urothelial Structures *In Vivo* from Disassociated Cells Attached to Biodegradable Polymer Scaffolds *In Vitro*. *J. Urol.* **148**:658-662.
- Aubin, J.E., Bellows, C.G., Turksen, K., Liu, F. , Heersche, J.N.M. (1992): Analysis of the Osteoblast Lineage and Regulation of Differentiation. In: *Chemistry and Biology of Mineralized Tissues*, Slavkin H Price P, eds., New York: Elsevier Science, 267-277.
- Bajpai, P.K. (1983): Biodegradable Scaffolds in Orthopedic, Oral, and Maxillofacial Surgery. In: *Biomaterials in Reconstructive Surgery*, Rubin LR, eds., St. Louis: C. V. Mosby Co., 312-328.
- Barrandon, Y. , Green, H. (1987): Cell Migration Is Essential for Sustained Growth of Keratinocyte Colonies: The Role of Transforming Growth Factor- α and Epidermal Growth Factor. *Cell* **50**:1131-1137.
- Beck, L.S., Deguzman, L., Lee, W.P., Xu, Y., McFatridge, L.A., Gillett, N.A. , Amento, E.P. (1991): TGF- β_1 Induces Bone Closure of Skull Defects. *J. Bone Miner. Res.* **6**:1257-1265.

- Bellows, C.G., Aubin, J.E. , Heersche, J.N.M. (1987): Physiological Concentration of Glucocorticoids Stimulate Formation of Bone Nodules from Isolated Rat Calvaria Cells *In Vitro*. *Endocrin.* **121**:1985-1992.
- Bellows, C.G., Aubin, J.E., Heersche, J.N.M. , Antosz, M.E. (1986): Mineralized Bone Nodules Formed *In Vitro* from Enzymatically Released Rat Calvaria Cell Populations. *Calcif. Tissue Int.* **38**:143-154.
- Beresford, J.N., Gallagher, J.A., Gowen, M., McGuire, M.K.B., Poser, J.W. , Russell, R.G.G. (1983): Human Bone Cells in Culture. A Novel System for the Investigation of Bone Cell Metabolism. *Clin. Sci.* **64**:38-39.
- Beresford, J.N., Gallagher, J.A., Poser, J.W. , Russell, R.G.G. (1984): Production of Osteocalcin by Human Bone Cells *In Vitro*. Effects of $1,25(\text{OH})_2\text{D}_3$, $24,25(\text{OH})_2\text{D}_3$, Parathyroid Hormone, and Glucocorticoids. *Metab. Bone Dis. Rel. Res.* **5**:229-234.
- Bobyn, J.D., Mortimer, E.S., Glassman, A.H., Engh, C.A., Miller, J.E. , Brooks, C.E. (1992): Producing and Avoiding Stress Shielding. *Clin. Orthop. Rel. Res.* **274**:79-96.
- Boonekamp, P.M., Hekkelman, J.W., Hamilton, J.W., Cohn, D.V. , Jilka, R.L. (1984): Effect of Culture on the Hormone Responsiveness of Bone Cells Isolated by an Improved Sequential Digestion Procedure. *Proc. K. Ned. Akad. Wet.* **B87**:371-381.
- Bortell, R., Barone, L.M., Tassinari, M.S., Lian, J.B. , Stein, G.S. (1990): Gene Expression during Endochondral Bone Development: Evidence for Coordinate Expression of Transforming Growth Factor β and Collagen Type I. *J. Cell. Biochem.* **44**:81-91.
- Bos, R.R.M., Boering, G., Rozema, F.R. , Leenslag, J.W. (1987): Resorbable Poly(L-lactide) Plates and Screws for the Fixation of Zygomatic Fractures. *J. Oral Maxillofac. Surg.* **45**:751-753.

- Bos, R.R.M., Roszema, F.R., Boering, G., Nijenhuis, A.J., Penning, A.J., Verwey, A.B., Nieuwenhuis, P. , Jansen, H.W.B. (1991): Degradation of and Tissue Reaction to Biodegradable Poly(L-lactide) for Use as Internal Fixation of Fractures: A Study in Rats. *Biomaterials* 12:32-36.
- Böstman, O.M. (1991): Absorbable Implants for the Fixation of Fractures. *J. Bone Joint Surg.* 73:148-153.
- Boyan, B.D., Hummert, T.W., Dean, D.D. , Schwartz, Z. (1996): The Role of Material Surfaces in Regulating Bone and Cartilage Cell Response. *Biomaterials* 17:137-146.
- Buckwalter, J.A., Glimcher, M.J., Cooper, R.R. , Recker, R. (1995): Bone Biology, Part1: Structure, Blood Supply, Cells, Matrix, and Mineralization. *J. Bone Joint Surg.* 77A:1256-1275.
- Casser-Bette, M., Murray, A.B., Closs, E.I., Erfle, V. , Schmidt, J. (1990): Bone Formation by Osteoblast-Like Cells in a Three-Dimensional Cell Culture. *Calcif. Tissue Int.* 46:46-56.
- Cheng, S.L., Yang, J.W., Rifas, L., Zhang, S.F. , Avioli, L.V. (1994): Differentiation of Human Bone Marrow Osteogenic Stromal Cells *In Vitro*: Induction of the Osteoblast Phenotype by Dexamethasone. *Endo.* 134:277-286.
- Cheung, H.S. , Haak, M.H. (1989): Growth of Osteoblasts on Porous Calcium Phosphate Ceramic: An *In Vitro* Model for Biocompatibility Study. *Biomaterials* 10:63-67.
- Chu, C.C. (1982): The Effect of pH on the *in vitro* Degradation of Poly(Glycolide Lactide) Copolymer Absorbable Sutures. *J. Biomed. Mater. Res.* 16:117-124.
- Chu, C.C. (1985): Degradation and Biocompatibility of Suture Materials. *CRC Critical Reviews in Biocompatibility* 1:261-321.
- Clark, R.A.F. , Henson, P.M., Ed. (1988). *The Molecular and Cellular Biology of Wound Repair*. New York, Plenum Press.

- Cowin, S.C., Moss-Salentijn, L. , Moss, M.L. (1991): Candidates for the Mechanosensory System in Bone. *J. Biomechan. Eng.* **113**:191-197.
- DeBoer, H.H. (1988): History of Bone Grafts. *Clin. Orthop. Rel. Res.* **226**:292-298.
- DeLeu, J. , Trueta, J. (1965): Vascularization of Bone Grafts in the Anterior Chamber of the Eye. *J. Bone Joint Surg.* **47B**:319.
- Dennis, J.E., Haynesworth, S.E., Young, R.G. , Caplan, A.I. (1992): Osteogenesis in Marrow-Derived Mesenchymal Cell Porous Ceramic Composites Transplanted Subcutaneously: Effect of Fibronectin and Laminin on Cell Retention and Rate of Osteogenic Expression. *Cell Transplantation* **1**:23-32.
- Dunn, G.A. , Brown, A.F. (1987): A Unified Approach to Analysing Cell Motility. *J. Cell. Sci. Suppl.* **8**:81-102.
- Ecarot-Charrier, B., Glorieux, F.H., van der Rest, M. , Pereira, G. (1983): Osteoblasts Isolated from Mouse Calvaria Initiate Matrix Mineralization. *J. Cell Biol.* **96**:639-643.
- Elgendi, H.M., Norman, M.E., Keaton, A.R. , Laurencin, C.T. (1993): Osteoblast-Like Cell (MC3T3-E1) Proliferation on Bioerodible Polymers: An Approach Towards the Development of a Bone-Bioerodible Polymer Composite Material. *Biomaterials* **14**:263-269.
- Engelberg, I. , Kohn, J. (1991): Physico-Mechanical Properties of Degradable Polymers Used in Medical Applications: A Comparative Study. *Biomaterials* **12**:292-304.
- Freed, L.E., Marquis, J.C., Nohria, A., Emmanuel, J., Mikos, A.G. , Langer, R. (1993): Neocartilage Formation *In Vitro* and *In Vivo* Using Cells Cultured on Synthetic Biodegradable Polymers. *J. Biomed. Mater. Res.* **27**:11-23.
- Freed, L.E., Marquis, J.C., Vunjak-Novakovic, G., Emmanuel, J. , Langer, R. (1994): Composition of Cell-Polymer Cartilage Implants. *Biotechn. Bioeng.* **43**:605-614.

- Friedlaender, G.E. (1987): Current Concepts Review. Bone Grafts. The Basic Science Rationale for Clinical Applications. *J. Bone Joint Surg.* **69A**:786-790.
- Gehron Robey, P. , Termine, J.D. (1985): Human Bone Cells *In Vitro*. *Calcif. Tissue Int.* **37**:453-460.
- Gibson, L.J. , Ashby, M.F. (1988): *Cellular Solids, Structure and Properties*. New York: Pergamon Press.
- Gilding, D.K. , Reed, A.M. (1979): Biodegradable Polymers for Use in Surgery-Polyglycolic/Poly(lactic acid) homo- and copolymers. *Polymer* **20**:1459-1464.
- Groessner-Schreiber, B. , Tuan, R.S. (1992): Enhanced Extracellular Matrix Production and Mineralization by Osteoblasts Cultured on Titanium Surfaces *In Vitro*. *J. Cell Sci.* **101**:209-217.
- Guillemin, G., Patat, J.L., Fournie, J. , Chetail, M. (1987): The Use of Coral as a Bone Graft Substitute. *J. Biomed. Mater. Res* **21**:557-567.
- Haynesworth, S.E., Goshima, J., Goldberg, V.M. , Caplan, A.I. (1992): Characterization of Cells with Osteogenic Potential from Human Marrow. *Bone* **13**:81-88.
- Heslop, B.F., Zeiss, I.M. , Nisbet, N.W. (1960): Studies on Transference of Bone: I. Comparison of Autologous and Homologous Implants with Reference to Osteocyte Survival, Osteogenesis, and Host Reaction. *Br. J. Exp. Pathol.* **41**:269.
- Holland, S.J., Tighe, B.J. , Gould, P.L. (1986): Polymers for Biodegradable Medical Devices. 1. The Potential of Polyesters as Controlled Macromolecular Release Systems. *J. Controlled Release* **4**:155-180.
- Hollinger, J.O. (1983): Preliminary Report on the Osteogenic Potential of a Biodegradable Copolymer of Polylactide and Polyglycolide. *J. Biomed. Mater. Res.* **17**:71-82.
- Hollinger, J.O. , Battistone, G.C. (1986): Biodegradable Bone Repair Materials: Synthetic Polymers and Ceramics. *Clin. Orthop. Rel. Res.* **207**:290-305.

- Holmes, R.E., Wardrop, R.W. , Wolford, L.M. (1988): Hydroxylapatite as a Bone Graft Substitute in Orthognathic Surgery. *J. Oral Maxillofac. Surg.* **46**:661-671.
- Howlett, C.R., Cavé, J., Williamson, M., Farmer, J., Ali, S.Y., Bab, I. , Owen, M.E. (1986): Mineralization in *In Vitro* Cultures of Rabbit Marrow Stromal Cells. *Clin. Orthop. Rel. Res.* **213**:251-263.
- Jarcho, M., Bolen, C.H., Thomas, M.B. , al., e. (1976): Hydroxylapatite Synthesis and Characterization in Dense Polycrystalline Form. *J. Mater. Sci.* **11**:2027-2035.
- Jen, A.C., Ishaug, S.L., Yaszemski, M.J., McIntire, L.V. , Mikos, A.G. (1996): Three Dimensional *In Vitro* Mechanical Model for Bone Formation. *Trans. World Biomater. Congress* **5**:I-979.
- Johnson, L.B., Aiken, J., Mooney, D., Schloo, B.L., Griffith-Cima, L., Langer, R. , Vacanti, J.P. (1994): The Mesentery as a Laminated Vascular Bed for Hepatocyte Transplantation. *Cell Transpl.* **3**:273-281.
- Kent, J.N., Quinn, J.H., Zide, M.F. , al., e. (1983): Alveolar Ridge Augmentation using Nonresorbable Hydroxylapatite With or Without Autogenous Cancellous Bone. *J. Oral Maxillofac. Surg.* **41**:629-642.
- Langer, R. , Vacanti, J.P. (1993): Tissue Engineering. *Science* **260**:920-926.
- Lauffenburger, D.A. (1991): Models for Receptor-Mediated Cell Phenomena: Adhesion and Migration. *Annu. Rev. Biophys. Biophys. Chem.* **20**:387-414.
- Laurencin, C.T., El-Amin, S.F., Ibim, S.E., Willoughby, D.A., Attawia, M., Allcock, H.R. , Ambrosio, A.A. (1996): A Highly Porous 3-Dimensional Polyphosphazene Polymer Matrix for Skeletal Tissue Regeneration. *J. Biomed. Mater. Res.* **30**:133-138.
- Lee, S.C., et al. (1994): Healing of Large Segmental Defects in Rat Femurs is Aided by RhBMP-2 in PLGA Matrix. *J. Biomed. Materials Res.* **28**:1149-1156.

- Lee, Y., McIntire, L.V. , Zygourakis, K. (1994): Analysis of Endothelial Cell Locomotion: Differential Effects of Motility and Contact Inhibition. *Biotech. Bioeng.* **43**:622-634.
- Lian, J.B. , Stein, G.S. (1992): Concepts of Osteoblast Growth and Differentiation: Basis for Modulation of Bone Cell Development and Tissue Formation. *Crit. Rev. Oral Biol. Med.* **3**:269-305.
- Light, M. , Kanat, I.O. (1991): The Possible Use of Coralline Hydroxyapatite as a Bone Implant. *J. Foot Surg.* **30**:472-476.
- Lo, H., Kadiyala, S., Guggino, S.E. , Leong, K.W. (1994): Biodegradable Foams for Cell Transplantation. In: *Biomaterials for Drug and Cell Delivery*, Mikos AG, Murphy RM, Bernstein H Peppas NA, eds., **331**, Pittsburgh: Materials Research Society, 41-46.
- Luria, E.A., Owen, M.E., Friedenstein, A.J., Morris, J.F. , Kuznetsow, S.A. (1987): Bone Formation in Organ Cultures of Bone Marrow. *Cell Tissue Res.* **248**:449-454.
- Malik, M.A., Puleo, D.A., Bizios, R. , Doremus, R.H. (1992): Osteoblasts on Hydroxyapatite, Alumina and Bone Surfaces *in vitro*: Morphology During the First 2 hours of Attachment. *Biomaterials* **13**:123-128.
- Maniatopoulos, C., Sodek, J. , Melcher, A.H. (1988): Bone Formation in Vitro by Stromal Cells Obtained from Bone Marrow of Young Adult Rats. *Cell Tissue Res.* **254**:317-330.
- Marden, L.J., Reddi, A.H. , Hollinger, J.O. (1990): Growth and Differentiation Factors: Role in Bone Induction and Potential Application in Craniofacial Surgery. *J. Craniofac. Surg.* **1**:154-160.
- Mikos, A.G., Lyman, M.D., Freed, L.E. , Langer, R. (1994): Wetting of Poly(L-lactic acid) and Poly(DL-lactic-co-glycolic acid) Foams for Tissue Culture. *Biomaterials* **15**:55-58.

- Mikos, A.G., Sarakinos, G., Lyman, M.D., Ingber, D.E., Vacanti, J.P. , Langer, R. (1993): Prevascularization of Porous Biodegradable Polymers. *Biotech. Bioeng.* **42**:716-723.
- Mikos, A.G., Thorsen, A.J., Czerwonka, L.A., Bao, Y., Langer, R., Winslow, D.N. , Vacanti, J.P. (1994): Preparation and Characterization of Poly(L-lactic acid) Foams. *Polymer* **35**:1068-1077.
- Miller, M.J., Goldberg, D.P., Yasko, A.W., Lemon, J.C., Satterfield, W.C., Wake, M.C. , Mikos, A.G. (1996): Guided Bone Growth in Sheep: A Model for Tissue-Engineered Bone Flaps. *Tissue Engineering* **2**:51-59.
- Miller, R.A., Brady, J.M. , Cutright, D.E. (1977): Degradation Rates of Oral Resorbable Implants (Polylactates and Polyglycolates): Rate Modification with Changes in PLA/PGA Copolymer Ratios. *J. Biomed. Mater. Res.* **11**:711-719.
- Mooney, D., Hansen, L., Vacanti, J., Langer, R., Farmer, S. , Ingber, D. (1992): Switching From Differentiation to Growth in Hepatocytes: Control by Extracellular Matrix. *J. Cell. Phys.* **151**:497-505.
- Mooney, D.J., Park, S., Kaufmann, P.M., Sano, K., McNamara, K., Vacanti, J.P. , Langer, R. (1995): Biodegradable Sponges for Hepatocyte Transplantation. *J. Biomed. Mater. Res.* **29**:959-965.
- Morey-Holton, E.R., van der Meulen, M.C., Whalen, R.T. , Arnaud, S.B. (1993): Gravity and Skeletal Adaptation. In: *Handbook of Physiology, Section4: Adaption to the Environment*, eds., Oxford University Press,
- Nijweide, J.P. (1975): Embryonic Chicken Periosteum in Tissue Culture, Osteoid Formation and Calcium Uptake. *Proc. K. Ned. Akad. Wet.* **C78**:410-417.
- Nijweide, P.J., van der Plas, A. , Scherft, J.P. (1981): Biochemical and Histological Studies on Various Bone Cell Preparations. *Calcif. Tissue Int.* **33**:529-540.

- Oonishi, H. (1991): Orthopaedic Applications of Hydroxyapatite. *Biomaterials* 12:171-178.
- Organ, G.M., Mooney, D.J., Hansen, L.K., Schloo, B. , Vacanti, J.P. (1992): Transplantation of Enterocytes Utilizing Polymer-Cell Constructs to Produce a Neointestine. *Transpl. Proceed.* 24:3009-3011.
- Owen, T.A., Aronow, M., Shalhoub, V., Barone, L.M., Wilming, L., Tassinari, M.S., Kennedy, M.B., Pockwinse, S., Lian, J.B. , Stein, G.S. (1990): Progressive Development of the Rat Osteoblast Phenotype In Vitro: Reciprocal Relationships in Expression of Genes Associated With Osteoblast Proliferation and Differentiation During Formation of the Bone Extracellular Matrix. *J. Cell. Phys.* 143:420-430.
- Peck, W.A., Birge, S.J. , Fedak, S.A. (1964): Bone Cells: Biochemical and Biological Studies After Enzymatic Isolation. *Science* 146:1476-1477.
- Petty, W., Spanier, S. , Shuster, J.J. (1988): Prevention of Infection after Total Joint Replacement. *J. Bone Joint Surg.* 70A:536-539.
- Petty, W., Spanier, S., Shuster, J.J. , Silverthorne, C. (1985): The Influence of Skeletal Implants on the Incidence of Infection. *J. Bone Joint Surg.* 67A:1236-1244.
- Pfeilschifter, J., Wolf, O., Naumann, A., Minne, H.W., Mundy, G.R. , Ziegler, R. (1990): Chemotactic Response of Osteoblastlike Cells to Transforming Growth Factor β . *J. Bone Miner. Res.* 5:825-830.
- Pistner, H., Bendix, D.R., Muehling, J. , Reuther, J.F. (1993): Poly(L-Lactide): A Long-Term Degradation Study *In Vivo*. *Biomaterials* 14:291-298.
- Pockwinse, S.M., Stein, J.L., Lian, J.B. , Stein, G.S. (1995): Developmental Stage-Specific Cellular Responses to Vitamin D and Glucocorticoids during Differentiation of the Osteoblast Phenotype: Interrelationship of Morphology and Gene Expression by *in Situ* Hybridization. *Exper. Cell Res.* 216:244-260.

- Pockwinse, S.M., Wilming, L.G., Conlon, D.M., Stein, G.S. , Lian, J.B. (1992): Expression of Cell Growth and Bone Specific Genes at Single Cell Resolution During Development of Bone Tissue-Like Organization in Primary Osteoblast Cultures. *J. Cell. Biochem.* **49**:310-323.
- Pratt, B.M., Harris, A.S., Morrow, J.S. , Madri, J.A. (1984): Mechanisms of Cytoskeletal Regulation. *Ann. J. Pathol.* **117**:349-354.
- Puleo, D.A., *Interaction of Osteoblasts with Orthopedic Biomaterials In Vitro*, Ph.D. Thesis, Rensselaer Polytechnic Institute, 1991.
- Puleo, D.A., Holleran, L.A., Doremus, R.H. , Bizios, R. (1991): Osteoblast Responses to Orthopedic Implant Materials *in vitro*. *J. Biomed. Mater. Res.* **25**:711-723.
- Quarles, L.D., Yohay, D.A., Lever, L.W., Caton, R. , Wenstrup, R. (1992): Distinct Proliferative and Differentiated Stages of Murine MC3T3-E1 Cells in Culture: An *In Vitro* Model of Osteoblast Development. *J. Bone Miner. Res.* **7**:683-692.
- Rao, L.G., Ng, B., Brunette, D.M. , Heersche, J.N.M. (1977): Parathyroid Hormone and Prostaglandin E₁ Response in a Selected Population of Bone Cells After Repeated Subculture and Storage at -80 °C. *Endo.* **100**:1233-1241.
- Recker, R.R. (1992): Embryology, Anatomy, and Microstructure of Bone. In: *Disorders of Bone and Mineral Metabolism*, Coe FL Favus MJ, eds., New York: Raven Press, 219-240.
- Reddi, A.H. (1981): Cell Biology and Biochemistry of Endochondral Bone Development. *Collagen Rel. Res.* **1**:209-226.
- Reddi, A.H., Ma, S. , Cunningham, N.S. (1988): Induction and Maintenance of New Bone Formation by Growth and Differentiation Factors. *Ann. Chir. Gynaecol.* **77**:189-192.

- Reed, A.M. , Gilding, D.K. (1981): Biodegradable Polymers for Use in Surgery - Poly(Glycolic)/Poly(Lactic Acid) Homo and Copolymers: 2. *In Vitro* Degradation. *Polymer* **22**:342-346.
- Rickard, D.J., Sullivan, T.A., Shenker, B.J., Leboy, P.S. , Kazhdan, I. (1994): Induction of Rapid Osteoblast Differentiation in Rat Bone Marrow Stromal Cell Cultures by Dexamethasone and BMP-2. *Develop. Biol.* **161**:218-228.
- Rifas, L., Cheng, S.L., Shen, V. , Peck, W.A. (1989): Monokines Produced by Macrophages Stimulate the Growth of Osteoblasts. *Connect. Tissue Res.* **23**:163-178.
- Roux, F.X., Brasnu, D., Loty, B., George, B. , Guillemin, G. (1988): Madreporic Coral: A New Bone Graft Substitute for Cranial Surgery. *J. Neurosurg.* **69**:510-513.
- Russ, J.C. (1986): *Practical Stereology*. New York: Plenum Press.
- Sandberg, M.M., Aro, H.T. , Vuorio, E.I. (1993): Gene Expression During Bone Repair. *Clin. Orthop. Rel. Res.* **289**:292-312.
- Schoeters, G., Leppens, H., Van Gorp, U. , Van Den Heuvel, R. (1992): Haemopoietic Long-Term Bone Marrow Cultures from Adult Mice Show Osteogenic Capacity *In Vitro* on 3-Dimensional Collagen Sponges. *Cell Prolif.* **25**:587-603.
- Shaffer, J.W., Field, G.A., Goldberg, V.M. , Davy, D.D. (1985): Fate of Vascularized and Nonvascularized Autografts. *Clin. Orthop. Rel. Res.* **197**:32-43.
- Shalhoub, V., Conlon, D., Tassinari, M., Quinn, C., Partridge, N., Stein, G. , Lian, J. (1992): Glucocorticoids Promote Development of the Osteoblast Phenotype by Selectively Modulating Expression of Cell Growth and Differentiation Associated Genes. *J. Cell. Biochem.* **50**:425-440.

- Stokes, C.L. , Lauffenburger, D.A. (1991): Analysis of the Roles of Microvessel Endothelial Cell Random Motility and Chemotaxis in Angiogenesis. *J. Theor. Biol.* **152**:377-403.
- Sudo, H., Kodama, H.A., Amagai, Y., Itakura, Y. , Yamamoto, S. (1986): Mineralized Tissue Formation by MC3T3-E1 Osteogenic Cells Embedded in Three-dimensional Gel Matrix. In: *Cell Mediated Calcification and Matrix Vesicles*, Ali SY, eds., Oxford, U.K.: Elsevier Science, 291-296.
- Suganuma, J. , Alexander, H. (1993): Biological Response of Intramedullary Bone to Poly-L-Lactic Acid. *J. Appl. Biomater.* **4**:13-27.
- Tamada, J.A. , Langer, R. (1993): Erosion Kinetics of Hydrolytically Degradable Polymers. *Proc. Natl. Acad. Sci.* **90**:552-556.
- Tenenbaum, H.C. (1992): Cellular Origins and Theories of Differentiation of Bone-forming Cells. In: *Bone, Volume 1, The Osteoblast and Osteocyte*, Hall BK, eds., 1, Boca Raton, FL: CRC Press, 41-69.
- Tenenbaum, H.C. , Heersche, J.N.M. (1982): Differentiation of Osteoblasts and Formation of Mineralized Bone *In Vitro*. *Calcif. Tissue Int.* **34**:76-79.
- Thomson, R.C., Ishaug, S.L., Mikos, A.G. , Langer, R. (1995): Polymers for Biological Systems. In: *Molecular Biology and Biotechnology: A Comprehensive Desk Reference*, Meyers RA, eds., New York: VCH Publishers, 717-724.
- Thomson, R.C., Yaszemski, M.J., Powers, J.M. , Mikos, A.G. (1995): Fabrication of Biodegradable Polymer Scaffolds to Engineer Trabecular Bone. *J. Biomater. Sci. Polym. Edn.* **7**:23-38.
- Tibone, K.W. , Bernard, G.W. (1982): A New In Vitro Model of Intramembranous Osteogenesis from Adult Bone Marrow Stem Cells. In: *Factors and Mechanisms Influencing Bone Growth*, Dixon AD Sarnat BG, eds., 101, New York: Alan R. Liss, Inc., 107-123.

- Triffit, J.T. (1980): The Organic Matrix of Bone Tissue. In: *Fundamental and Clinical Bone Physiology*, Urist MR, eds., Philadelphia: J.B. Lippincott, 45-82.
- Vacanti, C.A., Kim, W., Upton, J., Vacanti, M.P., Mooney, D., Schloo, B., Vacanti, J.P. (1993): Tissue-Engineered Growth of Bone and Cartilage. *Transplant. Proceed.* **25**:1019-1021.
- Vainiopää, S., Kilpikari, J., Laiho, J., Helevirta, P., Rokkanen, P., Törmälä, P. (1987): Strength and Strength Retention *in vitro*, of Absorbable, Self-Reinforced Polyglycolide (PGA) Rods for Fracture Fixation. *Biomaterials* **8**:46-48.
- Vert, M., Chabot, F., Leray, J., Christel, P. (1981): Steroregular Bioresorbable Polyesters for Bone Surgery. *Makromol. Chem., Suppl.* **5**:30-41.
- Vert, M., Christel, F., Chabot, F., Leray, J. (1984): Bioresorbable Plastic Materials for Bone Surgery. In: *Macromolecular Biomaterials*, Hastings GW Ducheyne P, eds., Boca Raton: CRC Press, 120-142.
- von Recum, H.A., Cleek, R.L., Eskin, S.G., Mikos, A.G. (1995): Degradation of Polydispersed Poly(L-lactic acid) to Modulate Lactic Acid Release. *Biomaterials* **16**:441-447.
- Vrouwenvelder, W.C.A., Groot, C.G., de Groot, K. (1992): Behaviour of Fetal Rat Osteoblasts Cultured In Vitro on Bioactive Glass and Nonreactive Glasses. *Biomaterials* **13**:382-392.
- Wake, M.C., Patrick, C.W., Mikos, A.G. (1994): Pore Morphology Effects on the Fibrovascular Tissue Growth in Porous Polymer Substrates. *Cell Transplantation* **3**:339-343.
- Wolff, J. (1892): *Das gesetz der Transformation der knochen*. Berlin: Hirschwald.
- Wong, G. (1990): Isolation and Behavior of Isolated Bone-Forming Cells. In: *Bone: The Osteoblast and Osteocyte*, Hall BK, eds., 1, Caldwell, NJ: Telford Press, 171-192.

- Wong, G.L. , Cohn, D.V. (1975): Target Cells in Bone for Parathormone and Calitonin are Different: Enrichment for Each Cell Type by Sequential Digestion of Mouse Calvaria and Selective Adhesion to Polymeric Surfaces. *Proc. Natl. Acad. Sci.* **72**:3167-3171.
- Yagiela, J.A. , Woodbury, D.M. (1977): Enzymatic Isolation of Osteoblasts from Fetal Rat Calvaria. *Anat. Rec.* **188**:287-306.
- Yasko, A.W., Lane, J.M., Fellinger, E.J., Rosen, V., Wozey, J.M. , Wang, E.A. (1992): The Healing of Segmental Bone Defects Induced by Recombinant Human Bone Morphogenetic Protein (rhBMP-2). *J. Bone Joint Surg.* **74-A**:659-670.
- Yaszemski, M.J., Payne, R.G., Hayes, W.C., Langer, R.S., Aufdemorte, T.B. , Mikos, A.G. (1995): The Ingrowth of New Bone Tissue and Initial Mechanical Properties of a Degradable Polymeric Composite Scaffold. *Tissue Engineering* **1**:41-52.
- Yaszemski, M.J., Payne, R.G., Hayes, W.C., Langer, R.S. , Mikos, A.G. (1996): The Evolution of Bone Transplantation: Molecular, Cellular, and Tissue Strategies to Engineer Human Bone. *Biomaterials* **17**:175-185.
- Yee, J.A., Yan, L., Dominguez, J.C., Allan, E.H. , Martin, T.J. (1993): Plasminogen-Dependent Activation of Latent Transforming Growth Factor Beta (TGF β) by Growing Cultures of Osteoblast-Like Cells. *J. Cell. Physiol.* **157**:528-534.
- Zygourakis, K., Bizios, R. , Markenscoff, P. (1991): Proliferation of Anchorage-Dependent Contact-Inhibited Cells: I. Development of Theoretical Models Based on Cellular Automata. *Biotechnol. Bioeng.* **38**:459-470.

APPENDIX

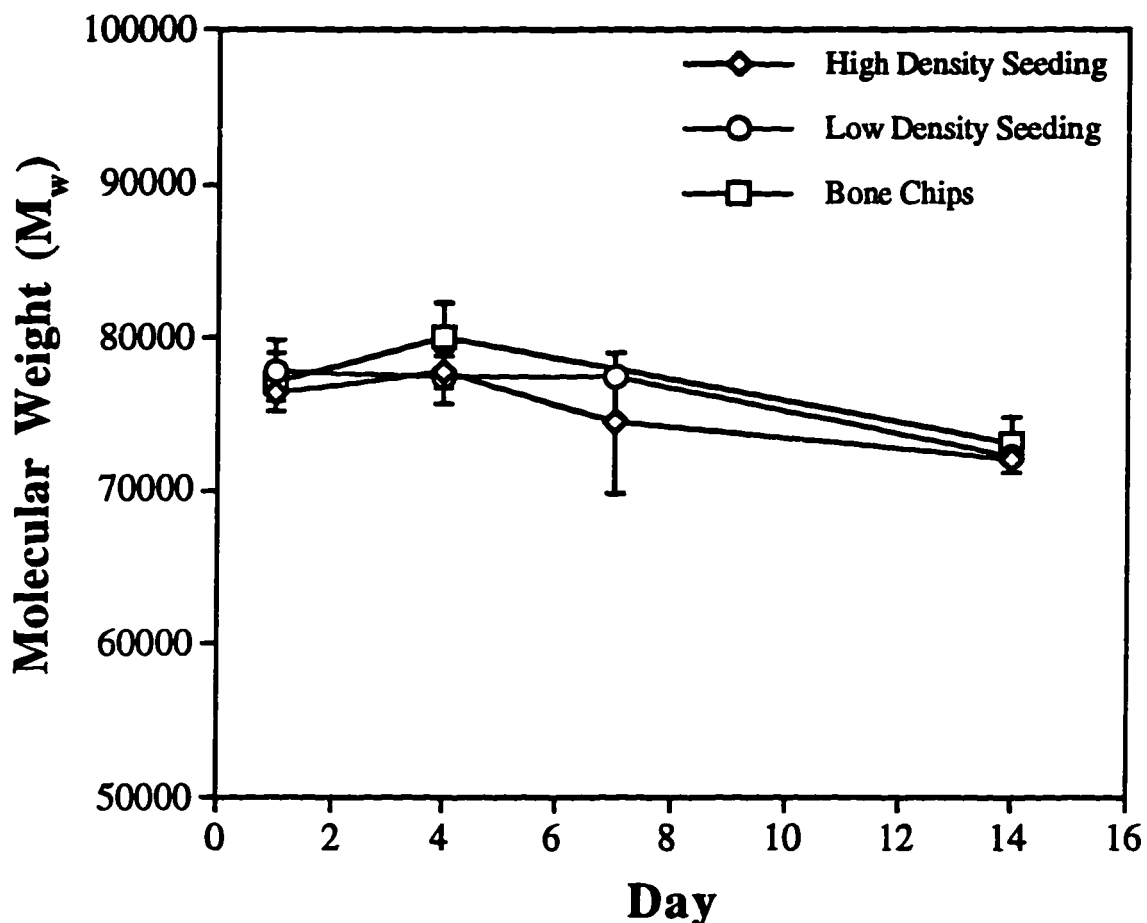


Figure 5-11. Weight average molecular weight of the 75:25 PLGA films used in the osteoblast migration study (chapter 5) over time. A high osteoblast density ($84,000 \text{ cells/cm}^2$) culture, low osteoblast density ($42,000 \text{ cells/cm}^2$) culture, or bone chips were cultured on the polymer films. The area of the polymer films that were in contact with the cells or bone chips was cut out and measured for molecular weight. Error bars designate means \pm s.d. for $n=3$.

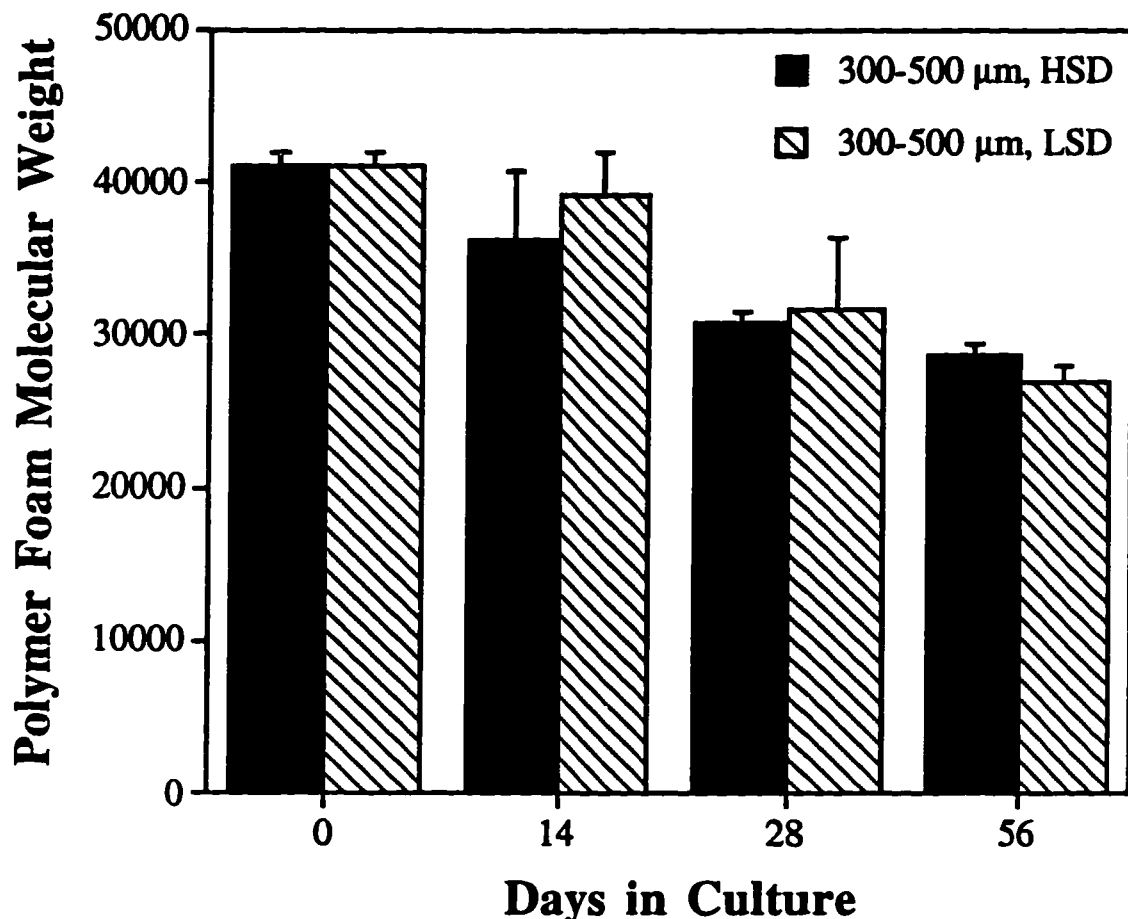


Figure 6-9. Weight average molecular weight of 75:25 PLGA foams (used in the study described in chapter 6) over time. Polymer foams having pores in the range of 300-500 μm in diameter were seeded with either a high seeding density (HSD) (22.1×10^5 cells/cm 2) or low seeding density (LSD) (6.83×10^5 cells/cm 2) of rat stromal osteoblasts. No significant differences in molecular weight were observed between the foams seeded with a high or low density of osteoblasts. Error bars designate means \pm s.d. for n=3.

VITAE

Susan L. Ishaug was born in Minneapolis, Minnesota, daughter of Joan and Virgil Ishaug. She has one older sister, Patty Pieper, and a younger brother, Brian Ishaug. Suzie (as she prefers to be called) grew up in the suburbs of Minneapolis and attended Spring Lake Park High school. She received her Bachelor of Science degree in Chemical Engineering from the University of Minnesota in 1991 before moving to Houston to attend Rice University.

To date, she is the author of 15 publications, her work has been presented in over 20 meetings, and she has supervised six undergraduate students in the lab. She was the first recipient of the Dr. William B. Walsh Award for Excellence in Bioengineering in 1996, and won first place for the Departmental Poster Award and Graduate Research Presentation Award that same year. She also won a poster award at the 1996 Houston Society for Engineering in Medicine and Biology and another Graduate Research Award in 1994.

Suzie has many hobbies, but most people would say her favorite hobby is talking. She definitely enjoys verbal exercise because she genuinely likes to be around people. Most of her other hobbies are some type of sport, such as volleyball, softball, skiing, scuba diving, sky diving, and mountain biking, to just name a few. She also loves to travel. During high school, she stayed with a Spanish family in Madrid and Denia, Spain for a summer month; lived in Costa Rica for 5 months through an undergraduate exchange program with some travel through other Central American countries; worked in Piteå, Sweden for 2 summer months before her graduating year at the University of Minnesota, taking a month long tour of Europe that same summer; and finally traveled throughout the eastern half of Australia for a month, scuba diving in the Great Barrier Reef, with her good friend Colleen Lynch and her sister, Patty.

Her real love in life, however, is her husband, Pete Riley. Like Suzie, he loves to take risks and do things on a whim. They met on a ski trip organized by a classmate of Suzie's. After graduation, Suzie and Pete (and her cats Nemo and Norman) will be living in Los Alamos, New Mexico, where Suzie will be working as a postdoctoral fellow at the Los Alamos National Laboratory.

She has great friends at Rice that she's going to miss very much when she leaves. They are all welcome to come visit her in Los Alamos and she hopes that they all will.